UNIVERSITY OF SOUTHAMPTON

FACULTY OF ENGINEERING, SCIENCE & MATHEMATICS

School of Engineering Sciences

Genetic Algorithm based Optimisation of FRP Composite Plates in Ship Structures

by

Komsan Maneepan

Thesis for the degree of Doctor of Philosophy

August 2007

Acknowledgements

I would like to express my sincere gratitude to Professor Ajit Shenoi, Dr. Han Koo Jeong and Dr. James Blake for their academic supervision, support and kind encouragement throughout the work period.

I also express my thanks to Prof. W.G. Price, the head of the School of Engineering Sciences, Prof. P.A. Wilson and all members of Fluid Interaction Research group for their kind support. Special thanks to Dr. Ming-Yi Tan for his technical support. I also would like to thank Dr. A.K. Nayak, Dr. N. Samphathkumar, Dr S.W. Boyd and Dr. K. Djidjeli for the useful discussions.

I wish to thank my mother, my sisters and my wife for their never ending support in my life. I also dedicate this work to my father. Finally, thanks to the Royal Thai Navy for providing me with financial support throughout the research program.

Abstract

Composite materials (herein means Fibre Reinforced Plastic, FRP) are increasingly used in the construction of marine vehicles because of their outstanding strength, stiffness and light weight properties. However, the use of FRP comes with difficulties in the design process as a result of the large number of design variables involved: composite material design, topologies and laminate schemes. All variables are related to each other leading to a high dimensional and flexible design space. It is hard to use traditional design methods in order to gain solutions for an initial design stage in a short time. Hence, this thesis deals with the presentation of a structural synthesis (optimisation framework) for plate components of composite ship structures. The framework broadly consists of an optimisation technique and structural analytical methods.

To make the framework compatible with the nature of composite ship structural design problems, the Genetic Algorithm (GA) is selected as the optimisation tool because of its robustness, its ability in dealing with both continuous and discrete variables and its excellent searching for a global optimum. The typical plate types in a ship structure are the stiffened and unstiffened plates. For a stiffened plate, the combination of the grillage analysis of energy method based on Navier solution and an equivalent elastic properties approach are introduced. Using this, it is possible to produce layer by layer optimisation results for the base plate, web and crown of the stiffened plate. Unfortunately, solutions of the adopted grillage analysis do not cover the mechanical behaviour of the plate between stiffeners so the Higher-Order Shear Deformation Theory (HSDT) must be employed.

This method provides accurate solutions for thin to moderately thick plates with a compromised computational time. Then stiffness, strength and stability can be considered in the design problem.

In addition, to achieve the program of the structural synthesis, various computational modules are implemented according to the evaluation of composite micromechanics properties, maximum stress failure criteria and structural weight function. Then the main modules are validated with available resources. The usefulness of the program has been proved by comparing it with the optimal solutions from finite element software. Finally, many application examples of secondary and tertiary composite ship structures are presented. The optimal results prove the success of the optimisation framework. This could be evidence for further improvement to obtain a valuable structural optimisation tool.

List of Publications produced from this thesis

1. Maneepan K., Jeong H.K. and Shenoi R.A. (2005) Optimisation of FRP tophat stiffened single skin and monocoque sandwich plates using genetic algorithm, Proceeding of 15^{th} international offshore and polar engineering conference, June 19-24, Seoul, Korea, pp. 513-518

2. Maneepan K., Shenoi R.A., Jeong H.K. and Blake J.I.R. (2006) Multi-objective optimisation of orthogonally tophat-stiffened composite laminates plates, Proceedings of 25^{th} international conference on offshore mechanics and arctic engineering, June 4-9, 2006, Hamburg, Germany, OMAE2006-92442

3. Maneepan K., Shenoi R.A., Blake J.I.R. and Jeong H.K. (2007) Genetic Algorithms (GAs) based optimisation of FRP composite plated grillages in ship structures, International Journal of Maritime Engineering, (accepted for publication)

Contents

Acknowledgements **i**

Abstract **ii**

List of Figures **ix**

List of Tables **xii**

Nomenclature **xiv**

1 Introduction **1**

1.1 General introduction 1

1.2 Motivation and research aim 3

2 Review of optimisation techniques for structural design **4**

2.1 Introduction 4

2.2 Background to FRP composites 4

2.3 Marine applications of FRP composites 10

2.4 Design methods 12

2.5 Development of optimisation techniques 16

2.6 Applications of optimisation techniques to composite structures 23

2.7 Summary 27

3 Review of structural solutions for FRP composite plates **29**

3.1 Introduction 29

3.2 Background to FRP composite mechanics 29
3.3 Analytical methods for stiffened plates 33
3.3.1 Grillage analysis 33
3.3.2 Orthotropic plate theory methods 36
3.3.3 Folded plate methods 38
3.4 Analytical methods of unstiffened plate 40
3.5 Numerical methods for composite structures 44
3.6 Summary 47

4 Methodology **50**
4.1 Introduction 50
4.2 Methodology adopted 50
4.3 Description of the optimisation framework 51

5 Structural analysis and Optimisation procedure **54**
5.1 Introduction 54
5.2 Grillage analysis 54
5.3 Higher order shear deformation theory (HSDT) 59
5.4 Genetic Algorithm 64
5.4.1 Introduction 64
5.4.2 Initial population 64
5.4.3 Evaluation 67
5.4.4 Exploiting operator 68
5.4.5 Exploring operators 70
5.5 Design variable representation 72
5.6 Weight function 73

6 Validation and testing **75**
6.1 Introduction 75
6.2 Grillage analysis 75
6.3 Higher order shear deformation theory 79

6.4 Optimisation procedure 83
6.4.1 Varying GA operators 83
6.4.2 Varying starting points 84
6.5 Comparison with ANSYS optimisation 86

7 Applications to stiffened plates **91**
7.1 Introduction 91
7.2 Parametric study of grillage structures 94
7.3 Unidirectional stiffened plate 98
7.3.1 Maximise stiffness 98
7.3.2 Maximise strength 99
7.3.3 Weight minimisation 101
7.4 Tophat cross stiffened plate 103
7.4.1 Maximise stiffness 103
7.4.2 Maximise strength 105
7.4.3 Weight minimisation 106

8 Applications to unstiffened plates **110**
8.1 Introduction 110
8.2 Parametric study 110
8.3 Laminated plate 112
8.3.1 Maximise stiffness 112
8.3.2 Maximise strength 114
8.3.3 Maximisation of critical buckling load 116

9 Conclusion and further work **119**
9.1 Conclusion 119
9.2 Further work 121

A Composite properties **123**

B Composite failure criteria **126**

References **128**

List of Figures

1.1 Stiffened single skin structure 2

2.1 The comparative fibre cost 6
2.2 HMS Sandown 11
2.3 Design decision process 17
2.4 Classification of optimisation techniques 18
2.5 Global and local minimum of the multiple-peak function 22

3.1 Stress components 30
3.2 An orthotropic lamina with its principal material axes arbitrary orientated with respect to reference co-ordinate axes 32
3.3 General derivation procedures of equivalent single layer theories 41

4.1 Optimisation framework 53

5.1 (a) Tophat cross stiffened plate and (b) Grillage representation for the stiffened plate 55
5.2 (a) Tophat cross section of girders and beams with the local coordinate for fibre layup (b) Geometric parameters of girders and (c) Geometric parameters of beams 56
5.3 The co-ordinate system of a rectangular laminated plate of thickness (t) subjected to in-plane compressive edge forces ($\hat{N}_{xx} = -N^0_{xx}, \hat{N}_{yy} = -N^0_{yy}$) 60
5.4 The diagram of Genetic Algorithms 65
5.5 Binary representation of a laminate element 72

6.1 GA run by varying a couple of operators with GA parameters set-1 83
6.2 GA run by varying a couple of operators with GA parameters set-2 84
6.3 GA run for different starting point 85
6.4 Convergence time of each starting point 86
6.5 The 1×1 blade stiffened plate with its dimensions 87
6.6 The convergence of GA run for 1×1 grillage 88
6.7 The iteration history of ANSYS optimisation 90

7.1 Positions at which failure index is considered for unidirectional stiffened plate 93
7.2 Positions at which failure index is considered for cross stiffened plate . . . 94
7.3 Normalised maximum deflection vs. number of girders by fixing number of beams at five for three length-to-width ratio cases 95
7.4 Normalised values of direct- and shear- stresses on the crown element of the middle girder and the middle beam vs. number of girders by fixed number of beams at five 96
7.5 The influence of fibre angle on Failure Index (FI) from maximum stress criterion 97
7.6 Convergence of GA run for maximisation of strength: unidirectional stiffened plates 100
7.7 Convergence of GA run for weight minimisation: unidirectional stiffened plates 101
7.8 Convergence of GA run for maximisation of stiffness: cross stiffened plates 103
7.9 Convergence of GA run for maximisation of strength: cross stiffened plates 105
7.10 Convergence of GA run for weight minimisation: cross stiffened plates . . . 107

8.1 The effect of Young's modulus of fibre and layer thickness on central deflection 111
8.2 The effect of Young's modulus of fibre and layer thickness on critical uniaxial compressive buckling load 112

8.3 Convergence of GA run for maximisation of stiffness: laminated plate . . . 113
8.4 Convergence of GA run for maximisation of strength: laminated plate . . . 115
8.5 Convergence of GA run for maximisation of critical buckling load for uniaxial compression: laminated plate . . . 117
8.6 Convergence of GA run for maximisation of critical buckling load for biaxial compression: laminated plate . . . 118

List of Tables

2.1 Marine composite construction productivity rates from Eric Greene Associates Inc. (2001) 9

2.2 Characteristics of optimisation techniques 28

3.1 The contracted notation 31

6.1 Comparison between the results of the developed programs from energy method based Navier solution (EM), Orthrotropic Plate Method (OPM), Force Method (FM) and the results of Clarkson (1965) for the maximum deflection δ_{max} (mm) and maximum stress of girder σ^{g}_{max} (MPa) and beam σ^{b}_{max} (MPa). 77

6.2 Comparison between the results of the developed program of equivalent elastic properties and those of Datoo (1991) 78

6.3 Comparison of the developed program shear stress calculation with Datoo (1991) 79

6.4 Comparison between nondimensionalised maximum deflections $(\bar{w})$ of the developed TSDT program and those of TSDT,FSDT,CLPT and 3-D elasticity solution (3-D) from Reddy (1997) 80

6.5 Nondimensionalised stresses in a three layer [0/90/0] simply supported square laminate under sinusoidal transverse load 81

6.6 Comparison of nondimensionalised uniaxial buckling loads (N) of the developed TSDT program with those of TSDT, FSDT and CLPT of Reddy (1997) 82

6.7 Comparison between nondimensionalised biaxial buckling loads (N) of the developed TSDT program and those of FSDT with shear correction factor (K) = 5/6 of Reddy (1997) 82
6.8 The optimal results of 1 × 1 blade stiffened plate 89

7.1 Material properties of a resin and fibres from Smith [105] 92
7.2 Minimisation of the central deflection for the unidirectional stiffened laminated plate 99
7.3 Minimisation of Failure Index (FI) at three positions on the unidirectional stiffened laminated plate 99
7.4 Weight minimisation of unidirectional stiffened laminated plate subjected to stiffness and strength constraints 102
7.5 Minimisation of central deflection of cross stiffened laminated plate 104
7.6 Minimisation of Failure Index (FI) at five positions on the cross stiffened laminated plate 106
7.7 Weight minimisation of cross stiffened laminated plate under stiffness and strength constraints 109

8.1 Minimisation of central deflection for the unstiffened laminated plate . . . 114
8.2 Maximise strength of the unstiffened laminated plate 114
8.3 Maximisation of buckling load for the unstiffened laminated plate 117

Nomenclature

A_w	Areal weight
a	Area of i^{th} element
a_b, a_g	Crown width of beams and girders
b, g	Number of beams and girders
B, L	Width and length of a plate
D_b, D_g	Flexural rigidity of beam and girder
$d_{na(i)}$	Vertical distance from neutral axis of the girder or beam's cross section
E_1, E_2	Elasti moduli in fibre direction and direction normal to fibre
$E_{b(i)}, E_{g(i)}$	Membrane equivalent moduli of i^{th} element of beam and girder
E_f	Elasti moduli of fibre
E_x^m	Membrane equivalent moduli of laminate in x-direction
E_y^b	Bending equivalent moduli of laminate in y-direction
f	Design variable of fibre type
$FI1, FI2$	Failure index in 1-2 axis on lamina of longitudinal and transverse fibre direction
$FI12$	Failure index in 1-2 axis on lamina of in-plane direction

G_{12}	In-plane shear modulus
h_b, h_g	Web height of beams and girders
$I_{b(i)}, I_{g(i)}$	Moment of inertia of i^{th} element related to neutral axis of beam and girder
$I_{(i)}$	General form of moment of inertia
$I_{cx(i)}$	Moment of inertia of i^{th} element about its horizontal axis through its own centroid
m, n	Wave numbers
M_g, Q_g	Moment and shear force of girder
n_{bp}, n_{cg}, n_{wg}	Number of layers of base plate, crown and web of girders
n_{cb}, n_{wb}	Number of layers of crown and web of beams
N_b, N_g	Number of element of beam and girder
N_{cr}	Critical buckling load
P	Uniform pressure load
s	Distance around stiffener's cross section from the middle of crown element
SF_1, τ_1	Shear flow and shear stress at the corner of the crown element
SF_2, τ_2	Shear flow and shear stress at the neutral axis of the crown element
t, t_k	Total thickness and layer thickness and of stiffener's element
t_{bp}, t_{cg}, t_{wg}	Layer thickness of base plate, crown and web of girder
t_{cb}, t_{wb}	Layer thickness of crown and web of beam
T_{cg}, T_{cb}	Total thickness of crown of girder and beam
T_{wg}, T_{wb}	Total thickness of web of girder and beam
u, v, w	In-plane and transverse displacements

v_{12}, v_{21}	In-plane Poisson's ratio
Z_g	Vertical distance from the neutral axis of the girder
δ_{max}	Maximum deflection of plate
$\rho_{bp}, \rho_{cg}, \rho_{wg}$	Composite density of lamina of base plate,crown and web of girder
σ_b, σ_g	Direct stress of beam and girder
σ_{bt}, σ_{gt}	Direct stress at crown element of beam and girder
θ	Fibre angle in each ply
τ_b, τ_g	Shear stress of beam and girder

GA glossary:[∓]

Genes	A subsection of a chromosome which (usually) encodes the value of a single parameter.
Chromosome	A datastructure which holds a 'string' of task parameters, or genes. This may be stored, for example, as a binary bit-string, or an array of integers.
Genotype	The genetic composition of an organism: the information contained in the the entire collection of genes.
Individual	A single member of a population.

[∓] Internet, $http://surf.de.uu.net/hhg2ec/Q99\_1.htm$, retrieved August 7, 2007

Population	A group of individuals which may interact together.
Phenotype	The expressed traits of an individual.
Reproduction	The creation of a new individual from two parents.
Genetic operator	A search operator acting on a coding structure that is analogous to a genotype of an organism .
Parent	An individual which takes part in reproduction to generate one or more other individuals, known as offspring.
Offspring	An individual generated by any process of reproduction.
Crossover	A operator which forms a new chromosome by combining parts of each of two parent chromosomes.
Mutation	A operator which forms a new chromosome by making (usually small) alterations to the values of genes in a copy of a single, parent chromosome.
Fitness	A value assigned to an individual which reflects how well the individual solves the task in hand.
Pool	The whole set of genes in a breeding population.
Selection	The process by which some individuals in a population are chosen for reproduction, typically on the basis of favoring individuals with higher fitness.

Chapter 1

Introduction

1.1 General introduction

The use of FRP in various industries has been expanding for the few last decades due to their attractive strength to weight ratio and unique manufacturing techniques, tailoring the strength of materials for certain design specifications.

In the ship building industry, FRP has been used for many types of ship, such as passenger ferries, lifeboats, minecountermeasure vessels and yachts. Typically the structural styles of these FRP ships can be classified into four types:

- (type-1) Tophat stiffened single skin structure
- (type-2) Monocoque structure
- (type-3) Sandwich structure
- (type-4) Corrugated structure

Although each type has its own advantages and disadvantages which designers have to consider, for all of these structural types un-/stiffened plates are the main components of the hulls leading to a similarity in the initial design stage. Out of these structural styles, type-1 should be an excellent design example. It is intensively used in ship construction

(Figure 1.1) because of the ease of fitting equipment, cost reductions with increasing number of hulls and ease of quality control. In the design of unstiffened plates, for example

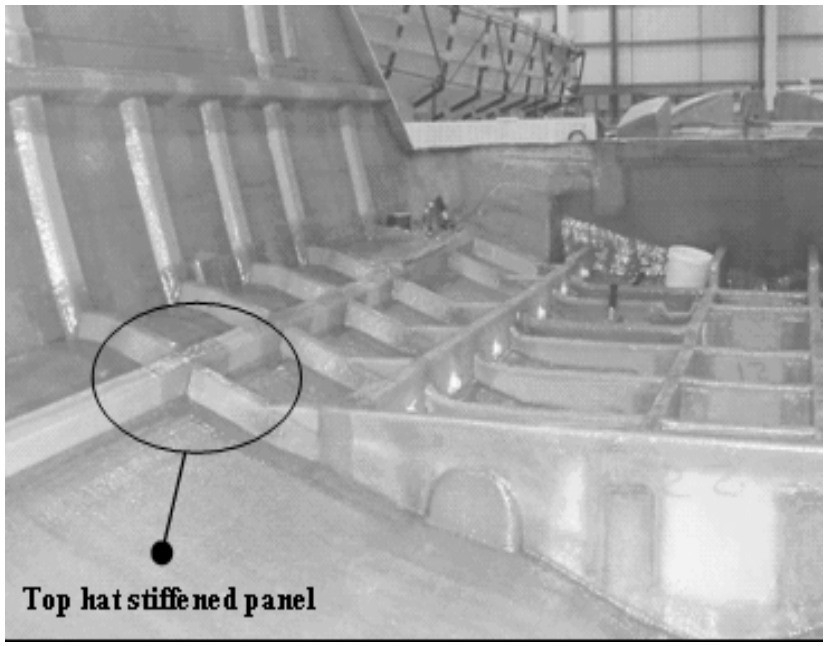

Figure 1.1: Stiffened single skin structure

a laminate single skin, many design variables have to be considered, such as fibre orientation, layer thickness, fibre types and so on. Furthermore, their failure modes, such as strength degradation, buckling and delamination, also need to be taken into account.

Looking at stiffened plates, the number of design variables is higher so that a large design space is inevitable. Examples of additional variables are section height, section width, web angle and flange width, as well as web and crown layup. Moreover, the failure modes of the plates are more complicated because of their complex geometry. For instance, column buckling of stiffener/plate combination, shear buckling of webs and interlaminar shear failure of the flange to base plate bond are considered.

1.2 Motivation and research aim

As mentioned above, it is noticed that if the ship structure is designed to be for example the strongest, lightest and cheapest, the design scheme is complicated due to issues such as composite material design, production process, alternative lamination schemes and alternative topologies. Hence, the design of composite ship structures can be considered to be challenging research.

The aim of this work can be stated as follows: the optimisation methodology for minimising the weight of un-/stiffened laminated plates is introduced, implemented and proved for its use in the initial design stage. The main advantage of the proposed methodology is providing quick solutions of structural dimensions and composite material design.

Chapter 2

Review of optimisation techniques for structural design

2.1 Introduction

Since there are many aspects that must be considered in the design process of composite structures, at the beginning of this chapter the definition of constituents, production processes and manufacturing cost classifications are briefly described to remind the reader of these fundamental concepts. Next, the marine applications of FRP are reviewed in order to gain an understanding of how it is used in practice. Then ship design methods and their limitations are explained. A literature review on ship design is also presented. As the nature of the design problem is repeatable, optimisation techniques are commonly used as a tool in the design process. Those optimisation techniques and their applications to composite structures are reviewed and this could be a guideline in finding the appropriate techniques for this work.

2.2 Background to FRP composites

A composite is a combination of one or more reinforcements with resin to produce a new material having different material properties from their constituents. Therefore, one main

factor having influence on the composite properties is the selection of component materials whose characteristics are illustrated as follows [111].

Resin is a material used to fasten reinforcements together. To ensure compatibility with the fibre reinforcement, the resin should have the following properties:

1. The resin should be able to deform at least to the same extent as fibre when a composite is loaded in tension.

2. The resin should transfer loads efficiently to prevent cracking or debonding,

3. The resin should have a high strain to failure property so that the composite is likely to have a toughness property leading to high resistance in cracking propagation

4. The resin should be able to resist water or other aggressive substances in a marine environment (e.g. fire conditions) and to withstand a constant stress cycling.

In the marine industry, there are three main types of resins, namely polyesters, vinyl-esters and epoxies.

Polyesters are the most commonly used for marine structural applications because of their low cost and ease of use in manufacturing processes. However, they provide only moderate mechanical properties and in the open mould, styrene emissions are high during the curing process. High resin shrinkage between 5 to 8 % occurs during cure. The working life (shelf-life) is limited to typically 6 to 12 months while pot life may be anything from a few minutes to several hours depending on the room temperature and the quantity of catalyst.

Vinyl-esters have been used to a limited extent since they are expensive. Similar to polyesters, high cure shrinkage and styrene emissions have been found during curing process. Nevertheless, they provide a very high chemical/ environmental resistance and high mechanical properties.

Epoxies offer various superior properties compared to other resin types such as high mechanical and thermal properties, high water resistance, high temperature resistance and long working times. However, they are the most expensive of the three types described.

The reinforcement is typically in the form of fibres with significantly higher mechanical properties than the resins. In marine application, the common fibres are E-glass, S-glass, carbon and aramids. Because the characteristics of E-glass are high electrical resistance, high strength and lowest cost related to the price of other fibre types (see Figure 2.1), it is widely used in marine FRP construction. S-glass offers higher tensile strength

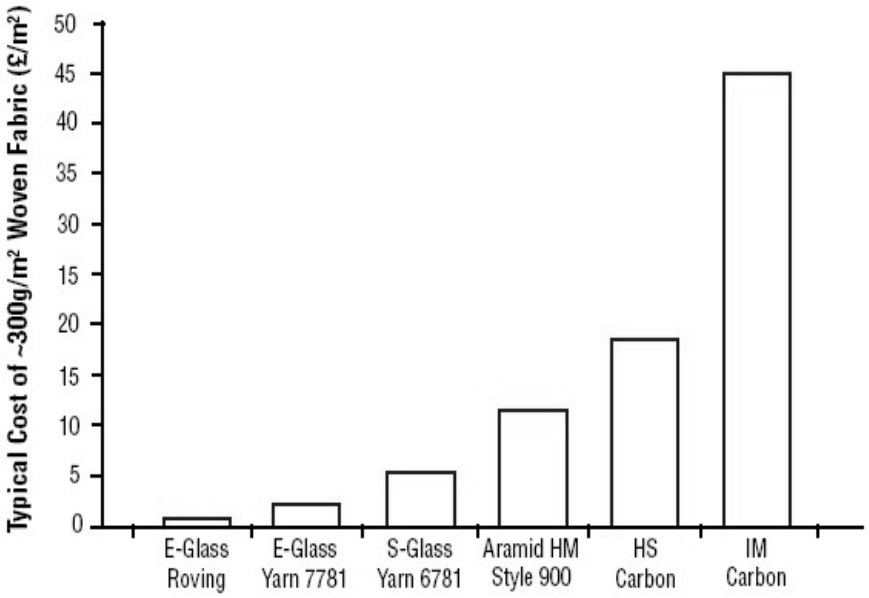

Figure 2.1: The comparative fibre cost

and better fatigue resistance than E-glass but S-glass is more expensive. Its application is often found more in aerospace structure where high-performance composites are required.

Carbon fibres are available in a variety of strength-modulus characteristics. Two typical carbon fibres are high strength carbon (HS) and high modulus carbon (HM). HS is more widely used than HM because HM is more expensive than HS due to a requirement

of a higher production temperature. Since all carbon fibre types have relatively low density compared to E-glass, their application is found in the structures where weight saving is a major design requirement.

The composite properties depend on not only the selected constituents but also composite structural forms which can be expressed as follows:

Unidirectional lamina, where all fibres run in one direction only, is a basic form of continuous fibre composite. Its stiffness and strength along the fibre direction are much greater than those in the transverse direction. This composite form is rarely found in real applications but in the basic design stage of a large structure, generally it can be used as the simplified model for complex composite forms.

Woven fabrics are produced by the interlacing of warp (0) fibre and weft (90) fibre in a regular pattern or weave style (e.g. twill, plain weave, basket weave and satin). Hence, a flexible fibre is suitable for this composite form. This composite form gives better in-plane transverse properties than the unidirectional lamina.

The laminate forms are comprised of more than one unidirectional or woven lamina arranged with different fibre angles. The mechanical behaviours of this form strongly rely on its stacking sequence. The applications example of this composite form can be found in the structures of small crafts such as lifeboats.

A hybrid composite is a composite having more than one fibre type or a composite combined with metal. This composite form gains benefits from the best combination of different fibre types or from other material types.

Chopped strand mat (CSM) consists of randomly oriented chopped fibres which are held together by resin. The advantages of CSM are very fast wet out time (an impregnated

reinforcement time) and excellent drape properties. However, it can be attacked by passage of moisture through the membrane (or osmosis).

Another factor affecting the quality of a composite is the production method, such as hand layup, spray layup, filament winding, pultrusion and so on. Out of these methods, hand layup, the oldest method, is widely used because it is flexible, it requires little capital investment and prior knowledge, as well as being highly economical for prototypes and short production series. Briefly the procedures of this method are that the fibre mat is simply laid into an open mould by hand and resin is then applied with a brush. After that, the laminate is rolled and allowed to cure under standard atmospheric pressure.

Spray layup was developed as an alternative to hand layup in order to raise the productivity. Generally, chopped fibre and resin are simultaneously sprayed by spray gun into the mould and the laminate is rolled. Although the cost of this method is lower than hand layup, a lower composite quality is obtained.

Resin transfer moulding (RTM) is used to obtain a higher quality laminate and high fibre volume fraction. RTM is the most common liquid moulding method and it is capable of producing large, complex and highly integrated components. Moreover, it combines low capital cost, low mould cost with a quality work. In this process, the closed mould is used with dry reinforcement and the mould can be closed in various ways. The low viscosity liquid resin is injected into the mould by vacuum pressure.

Although the use of composites leads to many benefits, high manufacturing cost will be faced for some applications. Therefore, this cost aspect is the major issue that the designer must consider. Generally, the total cost consists of two parts: direct and indirect cost. Direct cost is defined as the cost which directly attributes to the manufacture of a specific product. These are the costs of materials and labour. For composite marine construction, material and production costs are closely related. The high cost material

needs high skilled labour and more complicated production facilities. Production cost depends on many factors such as type of vessel constructed, production quantities and shipyard efficiency. Table 2.1 shows a source of rough estimating data as it applies to various types of construction. It can be seen that the type of construction and application of the ship can affect the work done and labour cost, for example the labour cost of single skin with frames is higher than that of sandwich construction for a Scott fibreglass boat construction.

Table 2.1: Marine composite construction productivity rates from Eric Greene Associates Inc. (2001)

Source	Type of Construction	Application	$kg/hour^{*}$ $(lbs/hour)$	$m^2/hour^{\odot}$ $(ft^2/hour)$	$hours/m^{2\otimes}$ $(hour/ft^2)$
Scott fibreglass boat construction	Single skin with frames	Recreational	9.07^{*} (20)	$3.7^{\odot}$ (33)	$0.27^{\otimes}$ (0.03)
		Military	5.44^{*} (12)	$1.86^{\odot}$ (20)	$0.54^{\otimes}$ (0.05)
	Sandwich Construction	Recreational	4.54^{*} (10)	$1.58^{\odot}$ (17)	$0.63^{\otimes}$ (0.6)
		Military	2.72^{*} (6)	$0.93^{\odot}$ (10)	$1.08^{\otimes}$ (10)
BLA combatant Feasibility Study	Single skin with frames	Flat panel (Hull)	5.90^{**} (13)	2.04^{**} (22)	0.49^{**} (0.05)
		Stiffeners & Frames	2.27^{**} (5)	0.84^{**} (9)	1.19^{**} (12)
	Core preparation for sandwich construction	Flat panel (Hull)	11.79^{**} (26)	3.99^{**} (43)	0.25^{**} (0.02)
		Stiffeners	11.79^{**} (26)	3.99^{**} (43)	0.25^{**} (0.02)
	Vacuum assisted resin Transfer molding (VARTM)	Flat panel (Hull)	4.54^{δ} (10)	3.99^{δ} (43)	0.25^{δ} (0.02)
		Stiffeners	3.18^{δ} (7)	1.30^{δ} (14)	0.77^{δ} (0.07)

* Based on mat/woven roving laminate
** Based on one woven roving(WR) or unidirectional (UD) layer
$^{\odot}$ Single ply of mat/woven roving laminate
$^{\otimes}$ Time to laminate one ply of mat/woven roving (reciprocal of $m^2/hour$ $(hour/ft^2)$)
$^{\delta}$ Finished single ply based on weight of moderately thick single-skin laminate

2.3 Marine applications of FRP composites

In the early 1940s, small boats, such as canoes, speedboats, coastal yachts and lifeboats, traditionally built of wood were firstly changed to use FRP as a result of their lower initial and maintenance cost and more freedom in design. For luxury yachts or high-speed boats, high cost carbon fibres are attractive because of their lightweight properties compared to other fibre types. To avoid a serious unexpected failure from misused carbon fibre in sailboats, Sponberge (1986) discussed the basic sailboat hull engineering and studied the results of flexural as well as impact tests conducted on five different sandwiches.

For larger ships (e.g. cargo vessels, fast ferries and hovercraft), Smith (1990) concluded that ships built of FRP are limited to ship lengths less than about 40 m since the smaller the hull size, the cheaper the construction cost by comparison to those built of steel. However, due to the advance of manufacturing technologies and the demand for composite ships at the present time, Mouritz *et al.* (2001) have predicted that ships up to 160 m may be built from FRP by the year 2020. This prediction is supported by the trend curve of the length of composite ships against the year of construction. To make this prediction possible, the fabrication technology needs to be developed. Horsmon and Bernhard (2003) for instance provided fabrication details with practical considerations for the production of large composite vessels in an efficient and cost effective manner.

Mouritz *et al.* (2001) presented a detailed review on naval ships and submarines. It has been mentioned that naval patrol boats are rarely built longer than about 20 m because of their low hull girder stiffness which is the main problem of building ships with composite. This is backed up by the deflection estimation of hull girders of a 50 m long composite vessel which is higher than that of steel vessels by about 240 % presented by Alm (1983). However, this stiffness problem can be solved by using a sandwich structure. For example, the Swedish Navy in the late 1980s built a 30 m long surface effect ship known as the Smyge MPC2000, from sandwich composite materials. With these materials, the ship had a light weight, excellent corrosion resistance, high damage resistance

against underwater shock loading, a number of stealth properties and good noise damping properties.

FRP is attractive to constructors of minecoutermeasure vessels (MCMV) because of the need to have a low magnetic signature. In the late 1960s, a pioneering decision of using FRP in place of wood was taken by the Royal Navy because the construction cost of wooden vessels was higher (based on UK labour rates and material prices), wood hulls require ongoing maintenance and FRP hull can resist explosive loads better than wooden hulls, Smith (1990). To increase the hull girder stiffness, the MCMV is commonly built of the framed single skin hull type. Example of MCMV is the Royal Navy's Hunt and Sandown shown in Figure 2.2.

Figure 2.2: HMS Sandown

Submarines are built of FRP because of the high pressure and corrosion resistance as well as the reduction of weight and magnetic signature. Tucker (1979) successfully built a civilian submarine from E-glass/polyester resin fabricated by the hand layup method.

The submarine can operate in moderate sea depth. Morisano (2003) built a human powered submarine from composite material to achieve the highest strength to weight ratio.

In the past, to reduce the topside weight of ships, aluminium alloy have been used as the building material for the superstructure while the ship hull is made of steel. However, aluminium alloy superstructures have poor fire resistance. Furthermore, due to the dissimilarity of building materials, there is a widespread cracking between hull and superstructure leading to expensive repairs. To overcome this, FRP has been recommended to replace the aluminium because their tensile and compressive strength is close to mild steel and FRP has a lower Young's modulus than mild steel. This is likely to eliminate fatigue failure induced by cyclic, wave-induced bending of the ship hull. An example of a ship with a composite superstructure section for instance is the Lafayette frigate.

Composites have also found use in other applications. Marsh (2001) reported that composite drive shafts are benefiting vessels ranging from lifeboats to cruise ships because of their lighter weight, saving on complexity, resistance to corrosion, absorbing torque and tolerating tensional shocks. Recently, a carbon fibre shaft, 23 m in length, was chosen for use in an auto express catamaran built for Minoan High Speed Ferries. Another example are propellers, traditionally made of high stiffness metal materials, which deform only slightly and are usually designed to work at a constant speed, operating at reduced efficiency at other speeds. To overcome this drawback, the composite propeller is introduced which can deform to operate more efficiently at a variety of speeds. Lee and Lin (2004) determined fibre orientation in a composite propeller to obtain the most efficient design.

2.4 Design methods

Ship design is usually described with the aid of the design spiral, which consists of three types of constraints: direct constraints on the design, constraints on the design process and constraints originating from the design environment. Typical steps in the spiral include

inputting ship parameters, selecting machinery, calculating weight balance, checking sea-keeping, calculating longitudinal strength and estimating cost, including life cycle costs. It can be seen that the design of the ship structure is a part of the spiral. Due to the scope of this work, the ship structural designs are described as follows.

Ship structural design can be achieved by: rule based design, first principle design or stochastic method.

Rule base design, the oldest approach, is related to load consideration, strength and design criteria from classification rules. It is easy to use when determining structural dimensions of a ship and it helps to save time in the design office and approval process. However, its simplified formulas cannot distinguish between structural adequacy and over-adequacy and they can only be used within certain limits. Furthermore, the available classification rules for ships built of FRP have their own standards and limitations. Lloyd's Register (LR) provides rules applying to ships less than 30 m length and the American Bureau of Shipping (ABS) rules are limited to ships upto 50 m. Hence, if ship length exceeds the scope of classification rules, first principle design (finding dimensions based on applying structural theory directly) or stochastic methods are required.

First principle design consists of three parts: design load, structural response analysis and strength assessment. The loads acting on a ship are such as still water global loads, wave loads, local loads, external pressure loads, internal loads (liquid tanks/dry cargo) and dynamic loads. For instance, the vertical load (q_{sv}) of still water global loads can be determined from the following equation:

$$q_{sv}(x) = b(x) - w(x) \tag{2.1}$$

where $b(x)$ is the buoyancy force, $w(x)$ is the weight of the ship and x is the distance along the ship length.

The structural responses of the hull girder and the associated members can be subdivided into three components: primary response (entire hull), secondary response (e.g. stiffened panels, main deck and double bottom) and tertiary response (unstiffened plate).

At the initial design stage, the primary response is analysed when the ship bends as a beam under the longitudinal distribution load. The formulas for this analysis are based on beam theory. For example, the bending moment (M) at a cross section of a composite beam can be found by Eq.3.16 in the next chapter.

To evaluate the secondary response, the theories reviewed in section 8.3.1 in Chapter 3 could be used, namely grillage analysis, equivalent orthotropic plate method (EOPM) and folded plate method (FPM). For tertiary response, the uses of equivalent single laminate theories (ESL) are possible. However, those theories are analytical methods which could have a difficulty for complex geometry or structures subjected to various boundary conditions. As a result of this, numerical methods such as the finite element method (FEM) are often used to analyse those structures.

For the strength assessment part, ultimate bending moment, ultimate strength, buckling, yielding, serviceability and ultimate limit states are considered. The occurance of yielding, for example can be assessed by using the Von Mises yield criterion for steel ship and composite failure criterion (e.g. Tsai-Wu, Tsai-Hill, Maximum stress criteria) for composite ships.

The stochastic method is a design procedure based on a probabilistic model for loads and strength. The output of this method is the required strength of the structure, which can be derived from safety factors related to the calculation of the probability of failure (P_f). P_f is calculated from a probability distribution function of all relevant quantities: loads, load effects (e.g. hull girder bending moment) and limit values. Since the probability distributions of loads and load effects are less known and the distributions of limit

values, arising from many separated variations (material properties, accuracy of analysis, etc.) are not easy to obtain, this design method is less favoured compared to other methods.

To study the development in ship design, the following papers have been reviewed. Optimisation of ship structures is not a new concept.

Within the Transaction of RINA, Moe (1968) designed the longitudinal strength members of tankers to gain their minimum cost and weight by the 'non-linear programming' optimisation procedure. Subsequently, Fisher (1972) presented economic optimisation procedures in preliminary design in which the "unconstrained minimisation" method of Nelder and Mead (1965) was employed. Smith (1973) used non-linear programming to minimise the weight of an oil tanker design. Watson (1976) considered how the relationship between dimensions, the coefficients and approximate formulae of traditional naval architecture had changed and their consequent improvement in ship design. With further advances in computational power, the consideration that the design success of a ship in operation is often based on more than one objective was applied by Sen (1992) who proposed the "multiple criteria decision making" (MCDM) method and applied the methodology to design various types of ship. From 1980's to the present day, whilst papers have been published on design philosophies and techniques and Andrews (1981), Chalmers (1982), Frieze (1987), Keane (1988), Loukakis (1988) and Andrews (2003), there have been few publications involved with design optimisation of ships and ship structures.

Furthermore, comprehensive reviews of ship design can be found in the proceedings of the International Ship and Offshore Structures Congress (ISSC). The recent relevant papers from ISSC reports are presented below.

Hughes (1997) presented a strategy for achieving a first principles optimum structural design of a ship using modern computer-based tools (MAESTRO program containing

safety factor from DNV (HSLC) Rules). The optimisation was done for minimum weight of aluminium and composite ships under the constraint of a strength criteria. The structural analysis depends on the Finite Element Method (FEM) which could lead to a high computational time. The design variables are the structural scantlings (e.g. plate thickness).

Rigo (2001) and Rigo and Fleury (2001) presented the development of LBR-5 (stiffened panels software) which includes a new design methodology consisting of three basic modules: cost, constraint and optimisation. LBR-5 can be used for complex floating structures generally comprising of stiffened cylindrical shells which are built of isotropic material only. Design variables that can be dealt with are plate thickness, stiffener dimension and stiffener spacing. Since the LBR-5 does not include a finite element analysis, it is fast in obtaining the optimal solution.

Karr *et. al.* (2002) introduced a combination of three existing computer applications: LBR-5, ISSMID-T (an integrated process/product model for the design of midship sections of tankers) and virtual reality simulations as a generic design methodology for simulation based ship design. The example application is performed on the midship section of a double hull cargo vessel.

Moreover based on the ISSC reports, it has been found that many papers present only the applications of ship structural design software and the improvement in capability of these software. It is therefore apparent that there is a lack of published research into frameworks for optimising composite ship structure.

2.5 Development of optimisation techniques

Optimisation is the act of obtaining the best results under given circumstances. Over one hundred years, optimisation has been of great interest to both theoreticians and engineers.

For engineering, it is very important because designers have to take many technical and managerial decisions in several stages. To help the designer, nowadays computers are commonly used as a design tool. Figure 2.3 shows a general example of how designers and computers work together.

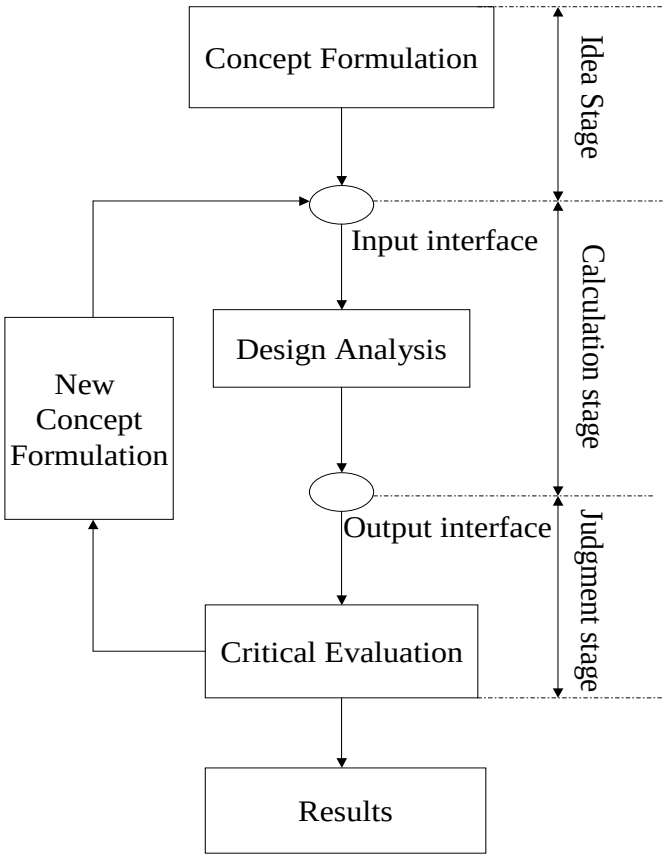

Figure 2.3: Design decision process

In the idea stage, designers consider concept formulations and construct optimisation functions. In the calculation stage, these functions are implemented in a program by which the computer calculates the results. The judgment stage is that if these results do not satisfy their requirements, a new design formulation process is started. From the design decision process, it can be seen that the nature of design procedure is iterative and it can be set as an optimisation problem whose components are generalised as:

Objective functions: minimise or maximise $f(x)$

Constraints: equality constraints $h_j(x) = 0$ and/or inequalities constraints $g_k(x) > 0$

Design variable: $x = [x_1, x_2, ..., x_n]^T$

To solve the optimisation problem, there are numerous optimisation techniques available, which can be classified based on the existence of constraints and the nature of the design variables as shown in Figure 2.4.

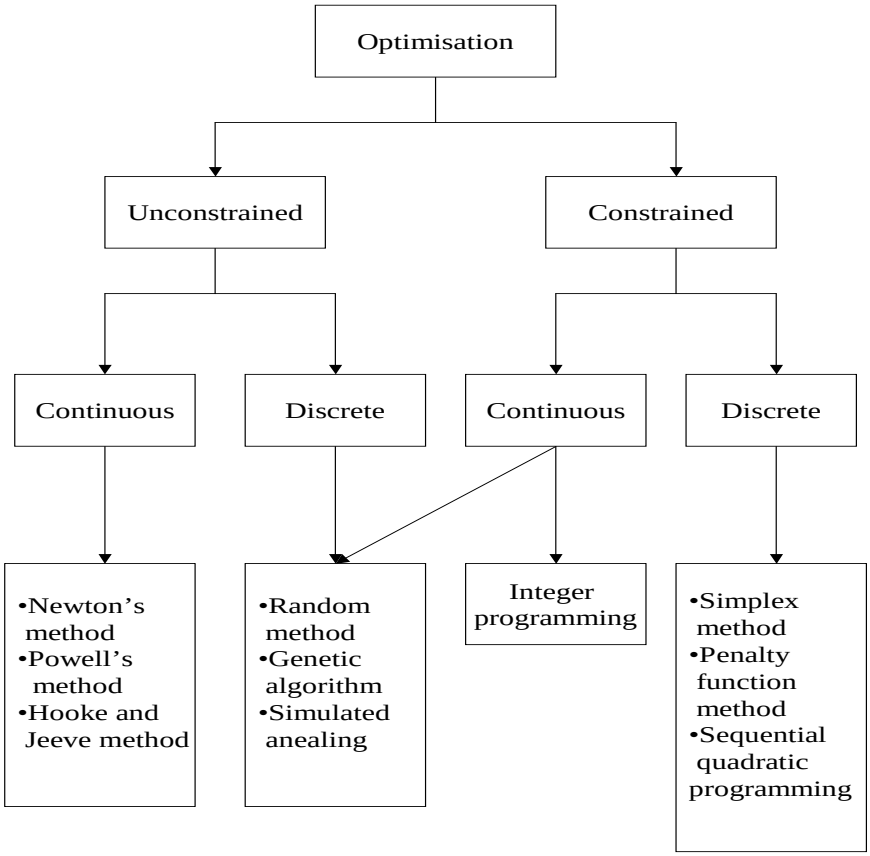

Figure 2.4: Classification of optimisation techniques

The developments of these techniques begin with unconstrained class. The oldest technique is based on differential calculus that was firstly introduced by Newton and/or Leibniz during the later part of the 17th century (Manoha (1993)). It is limited to only an unconstrained problem related to min-max condition of calculus. Similarly, Newton's method is introduced by using the first few terms of a series expansion of a function about a point (Taylor series expansion). The unconstrained optimisation methods could be also divided into two groups: methods involved with derivative (Steepest descent method, Fletcher-Reeves method, etc.) and methods without derivative (Powell's method, Hooke and Jeeves method, etc.).

To deal with constrained problems, the simplex technique is devised by George B. Dantzing in late 1940s for problems having linear objectives and constraints, which could be in forms of equalities and inequalities. If the number of design variables is small, the problem could be solved by drawing graphs. Otherwise, it can be solved in tableau form or by a computer program.

For non-linear constrained problems, the earliest development was the extension of simple min-max conditions by using the formulation of augmented Lagrangian multipliers, which are based on variational methods. This leads to numerous difficulties in practical applications as a result of non-linear differential equation.

Kelly (1961) presented the cutting plane technique which can solve a problem having linear objectives and nonlinear constraints. The algorithm of this technique involves solving a sequence of linear programming and nonlinear constraints, which are linearised by using a Taylor's series in the following form.

$$g_j(x) \approx g_j(t) + \nabla g_j(t)^T (x - t) \tag{2.2}$$

where t is an arbitrary point and x is a set of design variables. Then all functions are linear and can be solved by linear programming (LP) per iteration.

To solve the problem of nonlinear objectives with a variety of types of constraints, Rosen (1960) presented the gradient projection technique. Its main idea is choosing a feasible starting point and moving to a better point based on the modified gradient of the objective function in the iterative scheme. The modified gradient is implemented by the normalised search direction (S_i) as shown in the following equation:

$$S_i = \frac{-P_i \nabla f(x_i)}{\| -P_i \nabla f(x_i) \|} \tag{2.3}$$

where P_i is the projection matrix. The new approximated point for iteration is related to both S_i and the vector of the Lagrangian multiplier.

Box (1965) extended the simplex technique of unconstrained minimisation to solve constrained minimisation problems by comparing the values of the objective function at the (n+1) vertices (corners) of a general simplex and moving the simplex gradually towards the optimum point during the iterative process. This technique firstly generates points that individually satisfy the side constraints and then checks whether each point satisfies all other constraints. It is noted that this technique is simple in computation and does not require large computer storage as none of the derivatives are required. However, if the feasible region is non-convex, there is no guarantee of convergence.

From the benefit of using unconstrained optimisation techniques, which have simpler algorithms, the idea of transforming constrained problems to unconstrained ones has been proposed. For simple problems, the intervals of design variables can be substituted into objective functions to become unconstrained problems. For more complex problems, a formulation called a penalty function is another way to transform the constrained problem.

Carroll (1961) set up the interior penalty function by the following formulation,

$$\phi(x, r_k) = f(x) - r_k \sum_{j=1}^{m} \frac{1}{g_j(x)} \tag{2.4}$$

where (r_k) is the penalty parameter. This technique produces subsequent points lying inside the acceptable region of the design space.

Fiacco and McCormick (1967) presented a form of the exterior penalty function which is,

$$\phi(x, r_k, t) = f(x) - r_k^{-1} \sum_{j=1}^{m} [g_j(x) - t_i]^2 \tag{2.5}$$

where t is non-negative for a strictly decreasing penalty parameter (r_k). Unlike the interior penalty technique, this technique generates a non-feasible sequence of unconstrained minimum points that may yield a feasible solution. Its convergence starts from the infeasible region.

At the present, Sequential Quadratic Programming (SQP) techniques developed in the 1970s are probably the most effective optimisation technique for the nonlinear constrained problems since the principle of SQP is transforming the problems into an easier subproblem that can be solved by a basic iterative process.

All techniques mentioned above are based on mathematical programming, which require calculus or a relation between points in a design space. Because of this, some of them are limited to a continuous design space. Moreover, all of them are almost assured of locating the relative optimum closest to the starting points so that for a design space having multiple optima as shown in Figure 2.5, they may provide the local optimum if the starting point is far from the global one.

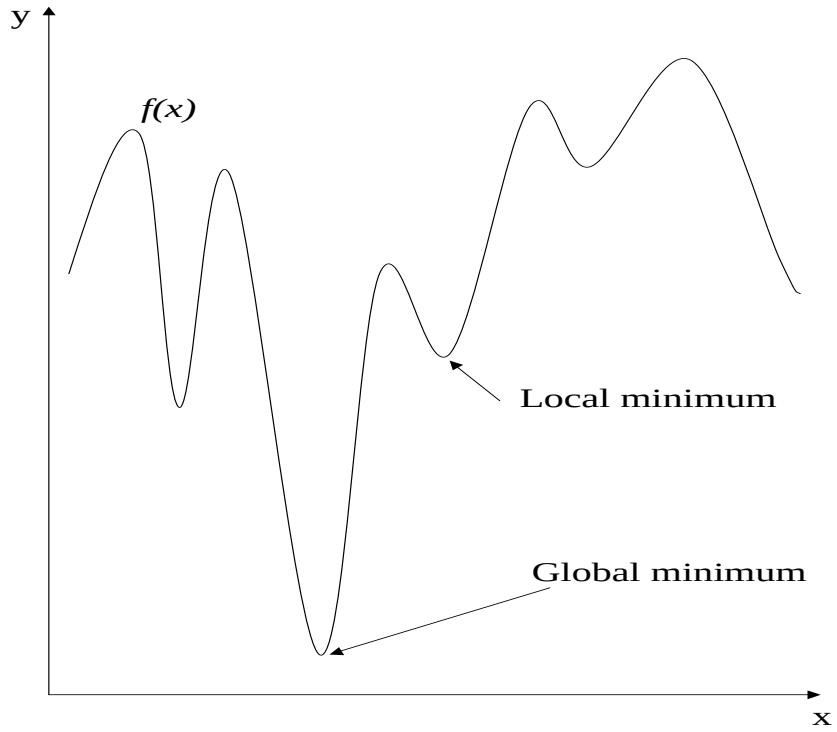

Figure 2.5: Global and local minimum of the multiple-peak function

The category of stochastic search techniques such as Simulated Annealing (SA) and Genetic Algorithm (GA) can overcome this drawback of mathematical programming techniques. They have been growing rapidly in popularity over the last one or two decade. SA proposed by Metropolise et al. (1953) is derived from a simulation of behaviour of particles in thermal equilibrium at a specific temperature. GA is more popular than SA in structural optimisation. GA was firstly developed by Holland (1975). Its search algorithm mimics the mechanics of natural selection and natural genetics. A general form of GA sexual reproduction consists of an initialisation of the populations, fitness evaluation, selecting members of population and genetic operators. Because GAs work with a coding solution set, searching from a population of solutions, using fitness functions and probabilistic transition rules, in searching for the global optimum, GA is better than

mathematical programming techniques. It is easily implemented because it is only necessary to change the chromosome to solve other problems using the same basic algorithm. However, it is difficult to encode design variables and to find the value of the fitness function.

2.6 Applications of optimisation techniques to composite structures

The optimisation formulations for the design of composite laminates lead to non-linear functions of the number of plies, lamina thickness and fibre orientation. Traditionally, these design variables are defined as real numbers, which can be solved by gradient-based techniques. Hirano (1979) used Powell's technique (conjugate direct technique) to find the optimum lamina fibre angle of laminated plates for maximum critical buckling stress, which is based on a closed form solution. Schmit and Mehrinfar (1982) proposed multi-level optimum design of structures with fibre-composite stiffened panel components, where weight minimisation is the objective and local buckling displacement and strength are the constraints. Inside the optimisation scheme, a sequence of unconstrained problems are solved by a modified Newton technique. Soares *et al.* (1995) presented the two level optimisation for thin shell composite structures. At the first level, which is defined as an unconstrained problem, the Davidon-Fletcher-Powell variable metric technique, that minimises the displacement of the structures, is used to find the fibre direction of each ply. At the second level where the problem is a constrained problem (minimising the volume of material subject to constraints of maximum displacement of nodal points in the FEA model, Tsai-Hill failure criterion and/or the natural frequency), the modified feasible directions technique is employed. Again, Powell's technique was used by Moh and Hwu (1997) to design composite sandwich plates. The highest critical buckling load is required which is controlled by the fibre orientations of the face laminas. Kim *et al.* (1997) employed a gradient projection algorithm to find the optimum stacking sequence

of laminated plates with the design sensitivity information based on Tsai-Wu failure criteria. Walker *et al.* (1997) designed symmetrically laminated plates to obtain the minimum deflection and weight by using the golden section technique based on the finite element formulation with the Tsai-Wu criterion as a constraint. Bruyneel and Fleury (2002) introduced the approximation concept to solve the optimisation of composite structures when both plies thickness and fibre orientations are considered as design variables to find the highest stiffness structure. The papers mentioned above provide similar conclusions; the classical optimisation techniques get trapped at local optima and the optimum fibre angle is a real number, which is not suitable for manufacturing processes.

Recently, the evolutionary optimisations (SA or GA) are more popular in the design of composite structures because they are based on random processes, which are used to set the direction of better searching and they can store and use information from previous results. Sciuva *et al.* (2003) used SA for multi-constrained optimisation of laminated and sandwich plates. The maximum buckling load and minimum mass are the objectives and transverse stiffness, mass and frequencies are the constraints. Fibre orientation is the design variable. Laminated plate theories are used for structural analysis. For this particular problem, it has been concluded that SA provides better results than GA. However, there is no other research to confirm that SA is better than GA or a test with both techniques in other optimisation problems of composite structures. Moreover, the application of SA on composite structural design is rare since GA is more popular than SA due to its simplicity.

Riche and Haftka (1993) presented the use of GA to optimise the stacking sequence of a composite laminate for maximum buckling load, which is calculated from a closed form solution subjected to strain failure constraints. Sivakumar *et al.* (1998) successfully applied GA and FEA related to FSDT to a laminate with an elliptical hole. Three examples of applications are presented and their objectives are such as maximising fundamental frequency, maximising first and second natural frequency, and weight minimisation. Constraints are a range of ply angle and major and minor axes of the ellipse. In the GA,

there is a possibility that the optimum point may not lie in the decoded values within the chosen string. Hence care should be taken for deciding the string length such that the variables are well distributed within the prescribed bounds. Park *et al.* (2001) used a GA to find the optimal stacking sequence of laminated composites under various loading and boundary conditions, optimised for maximum strength concerned with Tsai-Hill failure criterion. The plate stresses are calculated by FEA derived from FSDT. The design variable is ply orientation. Muc and Gurba (2001) emphasis the excellent feature of a GA in that it does not require any sensitivity analysis and therefore propose the use of GA incorporated into a FEA package for the optimisation of composite structures with regard to stacking sequence, shape and sizing. This could be applied to problems with unconstrained optimisation formulations. To find the optimum fibre orientation, maximum buckling load is set as the objective. To find the optimum shape and sizing, maximum strength of the structures in combination with an assumed failure criterion is the objective. Park *et al.* (2003) designed laminated plates to obtain the optimum fibre angle for weight minimisation under stiffness and mould filling time requirements by using a GA combined with a finite element calculation program (FEAD-LASP).

Only a few researchers have combined multi-objective design with GA. Walker and Smith (2003) introduced the use of GAs together with a multi-objective approach and the FEM for the design optimisation of symmetrically laminated plates to minimise both mass and deflection. Costa *et al.* (2004) used a multi-objective GA to tackle the differentiable and convex problem. The multiple-objectives were cost, mass, thickness and compliance of a laminate plate. Structural analysis formulations were based on FEA. Deka *et al.* (2005) firstly presented multi-objective optimisation of hybrid composite laminates by using GA and FEA. The objectives of the problem were weight and cost which were given equal importance. The design variable was the stacking sequence. Due to less research involving optimal design of laminated plates under various loads, Kim and Lee (2005) designed symmetrically laminated composite plates under uniaxial compression, shear, biaxial and a combination of shear and biaxial loading by GA to obtain the optimal stacking sequence,

which provided the maximum critical buckling load calculated from FEA based on CLPT.

Much research deals with the application of GAs to unstiffened laminate composites. On the other hand, GA based optimisation concerned with stiffened plates is less common in the literature. Bisagni and Lanzi (2002) used a combination of a GA and neural networks as optimisation tools and FEA for structural analysis to design composite plates stiffened in one direction for minimum weight subjected to buckling load, collapse load and the pre-buckling stiffness. Kang and Kim (2005) designed unstiffened and unidirectionally stiffened composite plates by using GA with COSAP (non-linear finite element code) to obtain minimum weight under constrained post buckling strength.

Several studies have concentrated on improving the reliability and efficiency of GAs in applications to optimise laminate structures. Nagendra *et al.* (1996) presented the investigations of the effect of various modifications (focus on GA operators) to basic GA for the minimum weight design of stiffened panels subjected to stability and strain constraints. The improved GA reduced the weight of the plates by about 4 %. Soremekun *et al.* (2001) suggested incorporating a generalised elitism selection into a standard GA. The improved GA is applied to two problems: buckling load maximisation of simply supported laminated plates and twist angle maximisation of cantilever-laminated plates. The fibre angle is set as the design variable. Gantovik *et al.* (2002) introduced a suitable algorithm for GAs with memory that can work with both discrete and continuous variables simultaneously and can be used for weight minimisation of laminated sandwich plates subjected to strength and buckling constraints based on closed form solutions. The use of the memory and spline approximation for a continuous variable avoids repeating analyses of previously encountered designs. Rahul *et al.* (2005) employed the combination of GA with a parallel computing environment (called IMPGA) and FEM for hybrid laminates under transverse impact loading. Three types of optimisation problem have been considered namely cost minimisation, weight minimisation and combined cost weight minimisation. The design variables are ply angle, ply material and ply thickness. The parallel computation causes

the optimisation scheme to have low communication with the GA.

2.7 Summary

According to the literature review of ship design in section 2.4, all optimisation methods have considered only traditional structural materials of steel and aluminium. Optimisation of FRP structures has not been applied explicitly to ship structural topologies.

Optimisation methods have been reviewed from classical to modern methods as well as their applications to composite structural design problems. The comparison of characteristics of some optimisation techniques is presented in Table 2.2. Moreover, the points below can be drawn:

- Classical methods such as Newton's method, Box method and so on are concerned with the differentiation or relation between points in a design space. Their applications to composite structural design problems show that the optimum fibre angles are real numbers which are unsuitable for manufacturing process because the typical fibre angle in layup process are such as 0°, 45° and 90°. Moreover, the global optimum could not be obtained because classical optimization methods provide the nearest point satisfying the optimum condition which is, for example, the slope at the point equal to zero.

- The composite structural design problem has a design space that may be non-linear, discontinuous and fluctuating. Hence, the use of stochastic optimisation methods is more appropriate than that of classical methods because they rely on probabilistic transition rules. Out of those, the most popular method is GA, which has been successfully used by many researchers.

- There are many papers involving the optimisation of unstiffened laminated plates using GAs but few papers involved with the use of GA with stiffened plates. Moreover, few researchers have combined multi-objective design with GA.

Table 2.2: Characteristics of optimisation techniques

Techniques	Objective	Constraint	Variables	Starting point	Convergence
Complex techniques	linear or nonlinear	linear or nonlinear inequality but cannot be equality	continuous	feasible	by searching. inefficient for large number of variables and no guarantee to converge for nonconvex problems
SUMT (interior)	linear or nonlinear	linear or nonlinear	continuous	feasible	using derivative
SQP	linear or nonlinear	linear or nonlinear	continuous	feasible or infeasible	using derivative
GA standard	linear or nonlinear	linear or nonlinear	continuous or discrete	feasible or infeasible	using stochastic searching
GA+ Based derivative method	linear or nonlinear	linear or nonlinear	continuous	feasible or infeasible	using stochastic searching. (conventional method help to guarantee global optimum)

Chapter 3

Review of structural solutions for FRP composite plates

3.1 Introduction

Before reviewing the structural analysis methods, the understanding of fundamental knowledge of laminate mechanics is vital and this is summarised in the first section. The literature review of these methods, is divided into two main parts: analytical and numerical methods. Their advantages and disadvantages will be presented in summary at the end of this chapter.

3.2 Background to FRP composite mechanics

The background of composite laminate theory is described as it is fundamental to the understanding of structural and failure analyses of composite structures. Firstly, the stress components (σ_{ij}) can be defined on three perpendicular planes as shown in Figure 3.1. These linear stress tensors σ_{ij} can be determined based on Hook's law and can be expressed as,

$$\sigma_{ij} = Q_{ijkl}\epsilon_{kl} \tag{3.1}$$

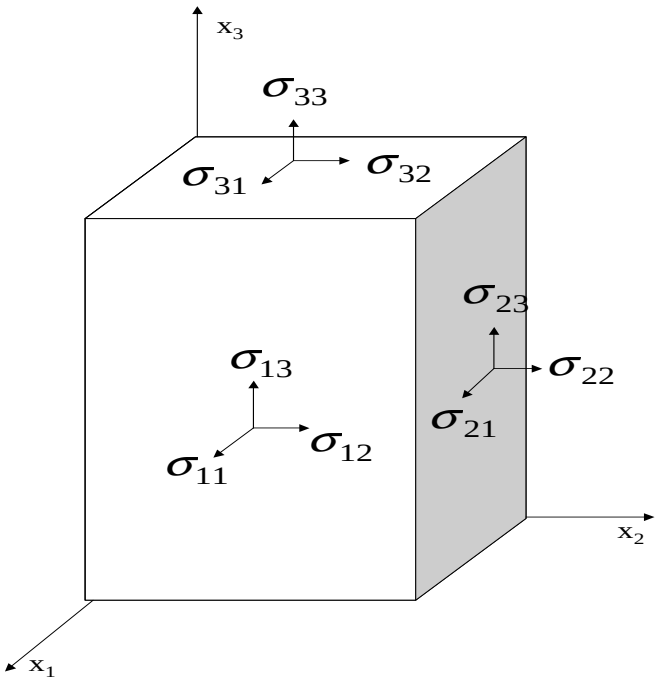

Figure 3.1: Stress components

where σ_{ij} and ϵ_{kl} are the second-order stress and strain tensors respectively, Q_{ijkl} are the fourth-order elasticity tensors and $(i, j, k, l = 1, 2, 3)$. To present Q_{ijkl} in compact form, it is convenient to introduce a contracted notation, shown in table 3.1.

By the symmetric properties of materials Eq. 3.1 can be written in the form of tensor notation as,

$$\begin{bmatrix} \sigma_1 \\ \sigma_2 \\ \sigma_3 \\ \sigma_4 \\ \sigma_5 \\ \sigma_6 \end{bmatrix} = \begin{bmatrix} Q_{11} & Q_{12} & Q_{13} & Q_{14} & Q_{15} & Q_{16} \\ & Q_{22} & Q_{23} & Q_{24} & Q_{25} & Q_{26} \\ & & Q_{33} & Q_{34} & Q_{35} & Q_{36} \\ & & & Q_{44} & Q_{45} & Q_{46} \\ & & & & Q_{55} & Q_{56} \\ Sym. & & & & & Q_{66} \end{bmatrix} \begin{bmatrix} \epsilon_1 \\ \epsilon_2 \\ \epsilon_3 \\ \epsilon_4 \\ \epsilon_5 \\ \epsilon_6 \end{bmatrix} \tag{3.2}$$

Table 3.1: The contracted notation

Strains		Stresses	
Tensor notations	New notations	Tensor notations	New notations
ϵ_{11}	ϵ_1	σ_{11}	σ_1
ϵ_{22}	ϵ_2	σ_{22}	σ_2
ϵ_{33}	ϵ_3	σ_{33}	σ_3
$2\epsilon_{23} = \gamma_{23}$	ϵ_4	$\sigma_{23} = \tau_{23}$	σ_4
$2\epsilon_{13} = \gamma_{13}$	ϵ_5	$\sigma_{13} = \tau_{13}$	σ_5
$2\epsilon_{12} = \gamma_{12}$	ϵ_6	$\sigma_{12} = \tau_{12}$	σ_6

In the case of a two-dimensional space (for example, this is the assumption for the analysis of thin plates) all the terms related to the x_3 axis in the previous equations can be neglected; the stress-strain relations can be simplified as follows:

$$\begin{bmatrix} \sigma_1 \\ \sigma_2 \\ \sigma_6 \end{bmatrix} = \begin{bmatrix} Q_{11} & Q_{12} & 0 \\ Q_{12} & Q_{22} & 0 \\ 0 & 0 & Q_{66} \end{bmatrix} \begin{bmatrix} \epsilon_1 \\ \epsilon_2 \\ \epsilon_6 \end{bmatrix} \tag{3.3}$$

For this 2D consideration, the constitutive relation is,

$$\begin{bmatrix} \epsilon_1 \\ \epsilon_2 \\ \epsilon_6 \end{bmatrix} = \begin{bmatrix} \frac{1}{E_{11}} & -\frac{v_{12}}{E_{11}} & 0 \\ -\frac{v_{12}}{E_{11}} & \frac{1}{E_{22}} & 0 \\ 0 & 0 & \frac{1}{G_{12}} \end{bmatrix} \begin{bmatrix} \sigma_1 \\ \sigma_2 \\ \sigma_6 \end{bmatrix} \tag{3.4}$$

where E_{ij} and v_{ij} are Young's modulus and Poisson's ratio respectively. Thus, by inverting Eq.3.4 and then comparing with Eq. 3.3, the compliance tensors can be expressed as,

$$Q_{11} = \frac{E_{11}}{(1 - v_{12}E_{22}/E_{11})}, \qquad Q_{12} = \frac{v_{12}E_{12}}{(1 - v_{12}E_{22}/E_{11})} \tag{3.5}$$

$$Q_{22} = \frac{E_{22}}{(1 - v_{12}E_{22}/E_{11})}, \qquad Q_{66} = G_{12} \tag{3.6}$$

To transform stresses from global axes (x-y plane) to local axes (L-T plane) Figure 3.2, the relations of stresses related to these axes can be explained as follows.

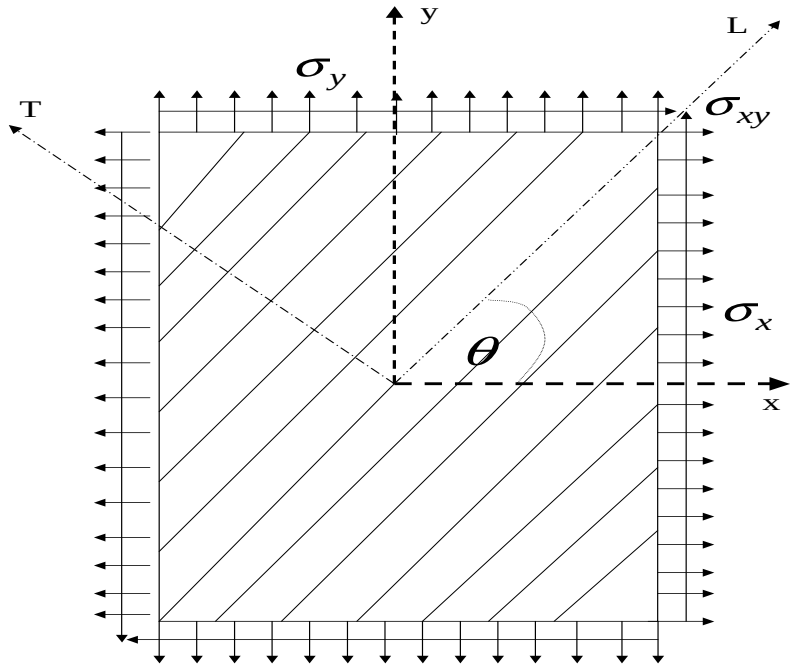

Figure 3.2: An orthotropic lamina with its principal material axes arbitrary orientated with respect to reference co-ordinate axes

The equilibrium equation for L-, T- and LT-directions are presented as,

$$\sigma_L = \sigma_x cos^2\theta + \sigma_y sin^2\theta + \sigma_{xy}(2sin\theta cos\theta) \tag{3.7}$$

$$\sigma_T = \sigma_x sin^2\theta + \sigma_y cos^2\theta - \sigma_{xy}(2sin\theta cos\theta) \tag{3.8}$$

$$\sigma_{LT} = -\sigma_x(sin\theta cos\theta) + \sigma_y(sin\theta cos\theta) + \sigma_{xy}(cos^2\theta - sin^2\theta) \tag{3.9}$$

These three equations can be represented in matrix form,

$$\begin{bmatrix} \sigma_L \\ \sigma_T \\ \sigma_{LT} \end{bmatrix} = [T] \begin{bmatrix} \sigma_x \\ \sigma_y \\ \sigma_{xy} \end{bmatrix}, \quad [T] = \begin{bmatrix} cos^2\theta & sin^2\theta & 2sin\theta cos\theta \\ sin^2\theta & cos^2\theta & -2sin\theta cos\theta \\ -sin\theta cos\theta & sin\theta cos\theta & (cos^2\theta - sin^2\theta) \end{bmatrix} \tag{3.10}$$

Similarly, the strain relation can be written as,

$$\begin{bmatrix} \epsilon_L \\ \epsilon_T \\ \frac{1}{2}\epsilon_{LT} \end{bmatrix} = [T] \begin{bmatrix} \epsilon_x \\ \epsilon_y \\ \frac{1}{2}\epsilon_{xy} \end{bmatrix} \tag{3.11}$$

Eq. 3.3 can now be modified as follows,

$$\begin{bmatrix} \sigma_x \\ \sigma_y \\ \sigma_{xy} \end{bmatrix} = [T]^{-1} \begin{bmatrix} Q_{11} & Q_{12} & 0 \\ Q_{12} & Q_{22} & 0 \\ 0 & 0 & 2Q_{66} \end{bmatrix} [T] \begin{bmatrix} \epsilon_x \\ \epsilon_y \\ \frac{1}{2}\epsilon_{xy} \end{bmatrix} = [\bar{Q}] \begin{bmatrix} \epsilon_x \\ \epsilon_y \\ \frac{1}{2}\epsilon_{xy} \end{bmatrix} \tag{3.12}$$

The $[\bar{Q}]$ is called the transform reduced stiffness matrix which plays an important role in the derivation of equivalent single layer theories. Finally it is noted that $[T]$ is important in assessing the failure of unidirectional lamina when the fibre orientation differs from the loading direction.

3.3 Analytical methods for stiffened plates

3.3.1 Grillage analysis

In ship structures, beams are the stiffening members for the plating which is required to provide watertight integrity. Those beams are usually placed longitudinally and transversely forming a mesh which intersects orthogonally. The network of these beams is called a grillage as defined by Clarkson (1965). Two methods exist, both based on beam theory, that can be used to find the mechanical response of the grillage. These are the displacement method (DM) and the force method (FM).

The displacement method, Clarkson (1965), is the most common method used for grillage analysis. It relies on straight segments of beams between the intersection points which are analysed in terms of deflections and slopes at the intersection points.

In the Force method, the pressure loads acting normal to the plates are represented by loads acting at the grillage intersection points. At each intersection point an equilibrium condition is applied and the deflection is calculated by using beam theory in terms of the reaction forces. Hence, it provides an exact solution for steel grillages. Lazarides (1952) introduced the calculation procedure of FM to a square grillage by ignoring torsion of beams. This calculation procedure, used by Clarkson (1963), provided solutions which agree well with experimental data.

Since the number of equations increases when the number of interactions increases, finding the mechanical solutions of a grillage having a large number of beams requires a computer based solution. Smith (1964) developed a computer program to analyse the grillages with up to 25 intersections or up to 100 intersections where two axes of symmetry are present. More recently, Jang *et al.* (1996) employed FM by ignoring torsional rigidity of beams within their optimisation process of a surface effect ship built from aluminum. The complex structures due to longitudinal girder and transverse web frames are represented as a number of grillages. To find the reaction force (F_k) at the i^{th} intersection, the following equation needs to be solved.

$$(e_{ik} + d_{ik})F_k = v_i \tag{3.13}$$

where v_i is the deflection of the web frame at the i^{th} intersection when only uniform load is applied and e_{ik} and d_{ik} are influence coefficients for the girder and beam respectively which are derived from Timoshenko beam theory.

Cheung *et al.* (1982) applied grillage analysis based on the displacement method to multi-spine box-girder bridges to find the longitudinal bending moment and transverse shear. The results of this method agree well with a 3D analysis using the finite strip method. The method is used by Evan *et al.* (1983) to take into account the effects of shear as well as bending upon the non-linear and collapse behaviour of multi-cellular structures under lateral loading. This method can be used not only for static analysis but also dynamic analysis. Balendra and Shanmugam (1985) analysed free vibration of

plate structures such as plates, stiffened plates and cellular structures using the grillage method. It is concluded that reasonably good results can be obtained by comparision with FEM results. Moreover, the grillage method could be applied for sandwich panels. For instance, Tan and Montage (1991) converted the panels into an analogous 2D grillage of orthogonally-orientated beams.

To avoid solving a large number of equations, Vedeler (1945) used the grillage analysis of the energy method based on Navier's solution in which the deflection of the grillage is determined by equating the total strain energy of all beams to work done by a normal load so that only one equation needs to be solved for deflection (w) at every intersection. For a grillage made of isotropic material, the deflection can be obtained as,

$$w = \sum_{m=1}^{\alpha} \sum_{n=1}^{\alpha} f_{mn} sin \frac{m\pi x}{L} sin \frac{n\pi y}{B} \tag{3.14}$$

in which f_{mn} can be defined as,

$$f_{mn} = \frac{16qLB}{\pi^6 mnE} \frac{1}{\left[m^4(g+1)\frac{I_g}{l^3} + n^4(b+1)\frac{I_b}{b^3}\right]} \tag{3.15}$$

where E is Young's Modulus of the building material, g and b are the number of girders and beams respectively, m and n are the wave number of a double sine series, I_g and I_b are the second moment of area of girder and beam respectively and L and B are the length and width of the grillage structure respectively.

For stiffened plates made of composite materials, Smith (1990) explained that composite beam theory is applicable to a plate stiffened in one direction only under the assumption that the plane section on the panel is to remain a plane section when subjected to bending moments and the Poisson's ratio effect is negligible. The cross section is divided up into a number of N elements related to the reference axes. When the cross section is symmetrical and bending (M_v) is confined to one plane, the bending stress at the i^{th}

element can be presented as,

$$\sigma_i = \frac{E_i M_v z_i}{D_v} \tag{3.16}$$

where D_v is the flexural rigidity of the section and z_i is the distance from neutral axis to the i^{th} element.

3.3.2 Orthotropic plate theory methods

The Classical Plate equation (see Eq.3.17) for unstiffened plates made of isotropic material subjected to a lateral load, explained by Timoshenko (1959), is derived from a combination of four distinct subsets of plate theory: the kinematic (strain-displacement relation), constitutive (Hooke's Law), force resultant, and equilibrium equations.

$$D\frac{\partial^4 w}{\partial x^4} + 2D\frac{\partial^4 w}{\partial x^2 \partial y^2} + D\frac{\partial^4 w}{\partial y^4} = q \tag{3.17}$$

where q is the distributed normal pressure load per area, w is the displacement along the z-axis, $D = Eh^3/12(1-v^2)$, h is the plate thickness and v is the Poisson's ratio of the plate material.

For a plate made of material which has three planes of symmetry with respect to its elastic properties, the plate equation in the case of plane stress known as the orthotropic plate equation is derived in the same fashion as in the case of a plate built of isotropic material and results in the following equation,

$$D_x\frac{\partial^4 w}{\partial x^4} + 2H\frac{\partial^4 w}{\partial x^2 \partial y^2} + D_y\frac{\partial^4 w}{\partial y^4} = q \tag{3.18}$$

Between Eq.3.17 and Eq.3.18, the clear differences are the flexural rigidity terms which in Eq.3.18, are $D_x = E_x h^3/12(1-v_x v_y)$, $D_y = E_y h^3/12(1-v_x v_y)$ and $H = v_x D_y + 2G_{xy}h^3/12$ where G_{xy} is the shear modulus in the xy-plane. For a stiffened plate made of isotropic material, after the stiffeners are smeared out by adding the equivalent stiffness into the base plate, the properties of the base plate become orthotropic so that the orthotropic

plate equation can be applied by adding the effect of the stiffener into the flexural rigidity terms. Huffington and Blacksburg (1956) presented a theoretical determination of rigidity properties of orthogonally stiffened plates in terms of the elastic constants and geometrical configuration of component parts of the structures. For instance, $D_x = D + EI/s$, where I is the moment of inertia of the stiffener and s is the stiffener spacing. The results of these evaluations did agree well with experimental data.

However, Bedair (1997) discussed this method for stiffened plates, called the orthotropic plate method (OPM), noting that it could be justified if the stiffeners are closely spaced but poses difficulties in derivation if the stiffeners are not equally spaced. Moreover, this method has been used by Cheung *at al.* (1982) to find the longitudinal moments and transverse shear of multi-spine box-girder bridges. A comparison with a 3D analysis using the finite-strip method concluded that the OPM provides accurate results if the number of spines is not less than three.

The application examples of this method are shown as follows. Mikami and Yonezawa (1983) regarded transversely stiffened web plates as an othotropic rectangular plate with variable rigidities for predicting the ultimate static strength of plate girders under bending. Krisek *et al.* (1990) used OPM based on harmonic analysis for shear lag analysis of a steel and composite single-cell box girder. Mikami and Niwa (1996) presented an approximate formulation based on OPM to predict ultimate strength for orthogonally stiffened steel plates subjected to uniaxial compression. The analysis of the results shows good agreement with many test results. Hosseini *et al.* (2005) proposed an approximate method which is related to the closed form solution of a rectangular orthotropic plate for blade-stiffened panels to estimate its critical buckling load in the preliminary design stage of structures.

In the case of the plate built of composite material, the effect of stiffeners is added into

the flexural rigidities of the base plate which are represented by Smith (1990) as follows:

$$D_{11} = D_x + (D_{sx} + A_{sx}e_x^2)/b, \qquad D_{12} = v_y D_x \tag{3.19}$$

$$D_{22} = D_y + (D_{sy} + A_{sy}e_y^2)/a, \qquad D_{66} = \frac{G_{xy}h^3}{12} + \frac{1}{2}\left(\frac{D_{Tx}}{b} + \frac{D_{Ty}}{a}\right) \tag{3.20}$$

where A_{sx} and A_{sy} are axial rigidities of longitudinal and transverse stiffeners, D_{sx} and D_{sy} are the flexural rigidities of the stiffeners about their centroids, D_{Tx} and D_{Ty} are the stiffener torsional rigidities, a and b are the spacings of transverse (y-direction) and longitudinal (x-direction) stiffeners respectively and e_x and e_y are the distances from the mid-plane of the plating to the centroids of the stiffeners.

The orthotropic equation used for the plate under lateral load (q) is written as:

$$D_{11}\frac{\partial^4 w}{\partial x^4} + 2(D_{12} + 2D_{66})\frac{\partial^4 w}{\partial x^2 \partial y^2} + D_{22}\frac{\partial^4 w}{\partial y^4} = q \tag{3.21}$$

Similarly, this method can be adapted and applied to corrugated panels made of composite materials as can be seen in Smith and Clarke (1986).

3.3.3 Folded plate methods

The analytical method of the stiffened plate, based on both beam and plate theory, is the Folded Plate Method (FPM). Without the grillage assumption, the method can provide a refined solution of the plate. Smith (1966) described the application of the FPM to the steel plate stiffened in one direction under lateral loading and subjected to a simply supported condition at one pair of opposite sides. The plate is represented by an array of beams and interconnected flat rectangular plates. As each beam is simply supported at its ends, the deflection shape can be represented by Fourier series and then forces and moments can be derived according to simple beam theory. Plate elements are assumed to satisfy the isotropic plate equation. Then continuity conditions are defined along the interconnecting boundaries between plates and beams, followed by applying an equilibrium condition on the beam element. From this, the matrix equation (Eq. 3.22)

can be established and can be solved to provide the displacement solution.

$$K_n \Delta_{Bn} = -R_n \tag{3.22}$$

where K_n is a square stiffness matrix of order $4n_B$, n_B is the number of beams, Δ_{Bn} is a column matrix of unknown beam displacements and rotations and R_n is a column matrix of forces and moments acting on the beams due to lateral loads and initial deformations.

It has been concluded that the FPM is limited to structures consisting of flat rectangular panels simply supported at one pair of opposite sides and stiffened in one direction only (for orthogonally stiffened plates, the transverse stiffeners are smeared out by adding the stiffness properties into the plate element), a direct solution of the plate equations may be obtained without difficulty. This conclusion is confirmed by bridge design code (CHBDC 2000) which restricts the use of this method to bridges with support conditions closely equivalent to line supports at both ends of the bridge.

The method is computationally expensive and complicated when the number of elements increases because one beam element contains four equilibrium equations so that for the whole plate, the beam displacement can be obtained by solving $4n_B$ equations where n_B is the number of longitudinal beams. Because of this, Smith C.S. (1972) developed approximate formulas and data curves for evaluating the instability of flat panels with top-hat frames and referred to the folded-plate method as the refinement structural analysis method for typical FRP structures. A computer program was developed based on the folded plate analysis by March and Taylor (1990) to analyse box girder bridges, which can be disassembled as orthotropic or isotropic plates.

In the case of a composite plate, Smith (1990) showed that the derivation procedures are the same as those of the plate built of isotropic materials. The difference is that rather than using simple beam theory for a beam element, composite beam theory is used instead. Similarly, orthotropic plate theory is applied for the plate element of the plate

stiffened in one direction. Orthogonally stiffened structures may be treated as transverse stiffeners together with equivalent orthotropic plate. The problem is solved in a similar manner to that of finite element analysis.

3.4 Analytical methods of unstiffened plate

The unstiffened plate in composite ship structures could be laminated plates or sandwich plates. The mechanical response of these plates can be solved by laminated plate theories which could be reviewed as follows. Laminated plate can be solved by 3-D elasticity theory, layer-wise theory or equivalent single-layer theories (ESL). 3-D elasticity theory (3DT) provides exact solutions because each layer is treated as a homogeneous anisotropic material. From the equations of motion which balance all forces existing on each layer as shown in Pagano (1969), the 3DT results in 3N governing differential equations, N being the number of layers. This leads to high computational expense when the number of layers increases. The complexity of the derivation increases due to continuity of the displacements and stresses at the interface of every layer. Therefore, solutions of this theory for an arbitrary laminate with various edge conditions are difficult to obtain.

Equivalent single layer theories (ESL) are derived from the 3-D elasticity theory by making suitable assumptions concerning the kinematics of deformation or the stress state through the thickness of the laminate, Reddy (1997). ESL theories treats a heterogeneous plate as a statically equivalent single layer having a complex constitutive behaviour. Examples of ESL are Classical laminated plate theory (CLPT), First order shear deformation theory (FSDT) and Higher-order shear deformation theory (HSDT). For all theories of ESL, generally the derivation procedure is the same and can be shown in the following diagram (see Figure 3.3),

CLPT is based on Kichhoff's hypothesis which assumes that a straight-line perpendicular to the mid-plane remains perpendicular after loading and there is no extension of the

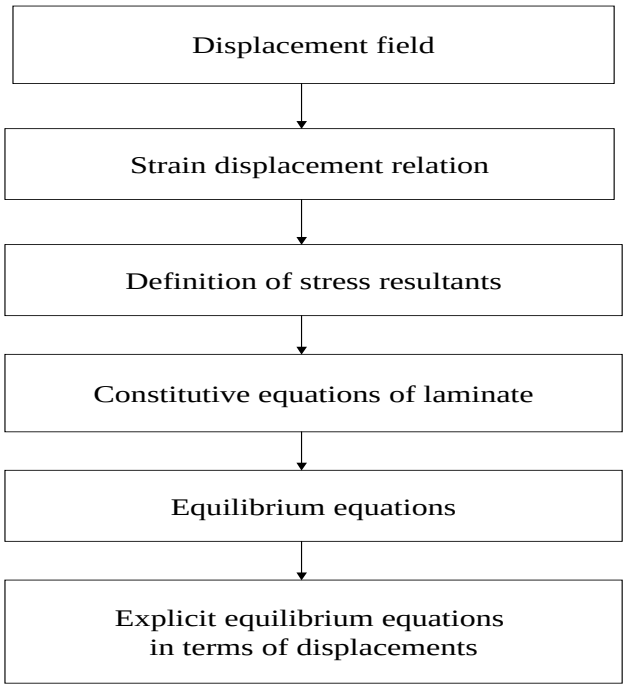

Figure 3.3: General derivation procedures of equivalent single layer theories

transverse normal. Therefore, the displacement field can be expressed as,

$$u = u_0(x, y) - z\frac{\partial w_0(x, y)}{\partial x} \tag{3.23}$$

$$v = v_0(x, y) - z\frac{\partial w_0(x, y)}{\partial y} \tag{3.24}$$

$$w = w_0(x, y) \tag{3.25}$$

According to this displacement field, CLPT is the simplest theory and is widely used for gross analysis of laminated structures. Pagano (1969) applied this theory to laminated plates and found that its solutions deteriorated when the span-to-depth ratio is reduced. This theory provides accurate solutions only for thin plates where small transverse shear effects occur. Moreover, Leung *et al.* (2003) stated that due to this assumption, CLPT is restricted to plates whose elastic to shear modulus ratios are not very large. This theory underestimates deflections and overestimates vibration frequencies and buckling loads.

To eliminate the drawback of CLPT, FSDT is introduced by relaxing Kirchoff's hypothesis so that the transverse normal does not remain perpendicular to the mid-surface after deformation in order to include transverse shear deformations. Due to the terms of rotations of the transverse normal, the displacement field of FSDT can be presented as,

$$u = u_0(x, y) + z\psi_x(x, y) \tag{3.26}$$

$$v = v_0(x, y) + z\psi_y(x, y) \tag{3.27}$$

$$w = w_0(x, y) \tag{3.28}$$

Within the derivation procedure, the shear resultant terms (Q_X and Q_Y), which do not exist in CLPT, appear and have an influence on the accuracy of this theory. These terms are presented by Whitney and Pagano (1970) as follows,

$$\begin{bmatrix} Q_X \\ Q_Y \end{bmatrix} = K \begin{bmatrix} A_{45} & A_{55} \\ A_{44} & A_{45} \end{bmatrix} \begin{bmatrix} w_{,y} + \psi_y \\ w_{,x} + \psi_x \end{bmatrix} \tag{3.29}$$

In a subsequent paper, Whitney and Pagano (1970) reformulated Eq. 3.29 as,

$$\begin{bmatrix} Q_X \\ Q_Y \end{bmatrix} = \begin{bmatrix} k_1^2 A_{45} & k_1 k_2 A_{55} \\ k_1 k_2 A_{44} & k_2^2 A_{45} \end{bmatrix} \begin{bmatrix} w_{,y} + \psi_y \\ w_{,x} + \psi_x \end{bmatrix} \tag{3.30}$$

The difference between the two is in the use of only one shear correction factor (K) in Eq 3.29 and two shear correction factors (k_1, k_2) in Eq. 3.30. However, both of these representations show good agreement with exact solutions. For composite laminates, the shear correction factors are difficult to determine because they rely on a number of different parameters such as the properties of each ply, stacking sequence and structural geometries. Generally, the evaluation of those shear factors are related to exact elasticity solutions or empirical data.

To overcome some of the disadvantages of linear theories (CLPT and FSDT), the Higher

order shear deformation theories (HSDT) were introduced that assume the through thickness distributions of the displacement functions to be higher order polynomials of the thickness co-ordinate. The HSDT having third-order is often found in the literature because single-layer theories of more than third-order are cumbersome and the increase in accuracy is outweighed by the increase in the number of unknowns as can been seen in Liu and Li (1996). Lo *et al.* (1977) introduce a third order shear deformation theory (TSDT) to account for transverse shear deformation effects, transverse normal strain and a non-linear distribution of in-plane displacements through the plate thickness. The displacement field of this theory is presented as,

$$u = u_0(x,y) + z\psi_x(x,y) + z^2\varsigma_x(x,y) + z^3\phi_x(x,y) \tag{3.31}$$

$$v = v_0(x,y) + z\psi_x(x,y) + z^2\varsigma_y(x,y) + z^3\phi_y(x,y) \tag{3.32}$$

$$w = w_0(x,y) + z\psi_z(x,y) + z^2\varsigma_z(x,y) \tag{3.33}$$

Compared to linear theories, it is noted that additional unknowns are introduced into the displacement field. However, this theory does not require shear correction factors. Reddy (1984) replaced the displacement in the z-axis in Eq. 3.33 by $w = w_0(x,y)$ or considering only direct extension in the z-axis. This results in the same number of dependent unknown variables as in the FSDT in Whitney and Pagano (1970). By applying the HSDT to many laminated plates, it can be concluded that HSDT are of considerable interest in the analysis of laminated composite plates because an accurate prediction of interlaminar shear stresses enables an accurate determination of strength and failure of a laminate.

For laminates made of dissimilar material layers, CLPT, FSDT and HSDT cannot present the zig-zag distribution of in-plane displacements through the laminate thickness and they provide erroneous double valued interlaminate stresses on the laminate interface because those theories represent in-plane displacement components by continuous functions. To overcome these drawbacks, the layer-wise theories (LWT) are introduced based on a layer

assembly system describing each composite laminate as an assembly of individual layers. For piecewise approximation of the in-plane deformation through individual lamina, Barbero *et al.* (1990) expressed the displacement field as,

$$u_i(x, y, z) = u_i(x, y) + \sum_{j=1}^{N_i} U_i^j(x, y)\phi_j^i(z) \tag{3.34}$$

$$u_3(x, y, z) = w(x, y, z) \tag{3.35}$$

To improve the accuracy of LWT, a combination of the ideas of LWT, FSDT and HSDT are presented such as Toledo and Murakami (1986) for first order zig-zag theory and Aitharaju and Averill (1999) for higher-order zig-zag theory. Although LWT provide a solution which is very close to the exact solution, they suffer from a numerical crisis if the layer number becomes too large because, as can be noted from their displacement field, the number of layers are related to the number of unknown variables.

3.5 Numerical methods for composite structures

The analytical solution is difficult to calculate for some structural problems for complex structures so numerical methods providing approximate solutions are more appropriate. The well known numerical methods for structural problems are the Finite Strip Method (FSM), the Finite Difference Method (FDM) and the Finite Element Method (FEM).

Finite Strip Method (FSM) is regarded as a special form of the displacement formulation of FEM. FSM uses the minimum total potential energy theorem to develop the relationship between unknown nodal displacement parameters and the applied load. Yoda and Atluri (1992) investigated the post buckling of stiffened laminated composite panels by using FSM based on higher order shear deformation theory. Its results are validated with some typical experimental results. Dawe *et al.* (1993) described the use of FSM for the analysis of the geometrically non-linear elastic response of composite laminated, orthotropic prismatic plate structures subjected to progressive uniformed shortening. Loughlan and

Delaunoy (1993) studied the buckling characteristics of composite stiffened plates under in-plane shear load using the method. Two bead stiffened panels under combined compressive and shear load were also analysed by Dawe and Peshkam (1996) using this method. As the FSM is a popular method for analysing thin-walled prismatic plates, it is used by Loughlan (1996) to investigate the buckling characteristics of some carbon fibre composite stiffened box sections subjected to compressive and bending loading action. Wang and Dawe (1996) developed the FSM in the contexts of both first-order shear deformation and classical plate theories for an analysis of the overall, geometrically non-linear, elastic behaviour of diaphragm supported prismatic plate structures which may be made of composite laminated material and may have initial geometric imperfections. Yuan and Dawe (2004) described the development of a B-spline finite strip method for predicting the natural frequencies of vibration and the buckling stresses of rectangular sandwich panels. Razzaq and EI-Zafrany (2005) reduced the dimensionality of FEM by applying a new concept to FSM. Mindlin's plate-bending theory, Mindlin (1951), has been employed for the derivation of an efficient element. The developed program is applied for trapezoidal and stiffened plate and cylindrical shells made of isotropic or composite layered materials.

Finite Difference Method (FDM) finds solutions based on a system of difference equations. Within this method, finite difference plays an important role, they are one of the simplest ways of approximating a differential operator and they are extensively used in solving differential equations. At the present time, the FDM is rarely found in the literature concerned with structural analysis. Aksu and Ali (1976) employed the FDM to analyse the free vibration of rectangular stiffened plates having a single stiffener. Turvey and Der Avanessian (1985) presented the governing equations for the axisysmmetric elastic large defection analysis of ring stiffened plates and a graded finite difference implementation of dynamic relaxation was used for their numerical solutions. Mukhopadhyay (1989a,b) used a semi-analytic FDM on a stiffened plate with various boundary conditions for vibration and stability analysis. The results of this method indicated good agreement with previously published results.

To overcome the disadvantages of the Finite Difference Method (FDM) such as the difficulty in applying boundary conditions and the fact that they are not suitable for complex structures, the use of the Finite Element Method (FEM) is proposed. The FEM is a numerical method for the solution of boundary-value problems. This method can be regarded as an extension of earlier established analytical techniques in which a structure is represented as an assemblage of discrete elements interconnected at a finite number of nodal points. There are plenty of papers dealing with this method as much commercial software based on the FEM is available and it is known as the universal tool for structural analysis. Herein, the papers involved with the application and development of this method is presented. Chattopadhyay *et al.* (1992) used the FEM with an isoparametric quadratic plate bending element for free vibration of composite stiffened plates. In the present formulation, stiffeners can be placed anywhere within the plate element and they need not necessarily follow nodal lines. Chattopadhyay *et al.* (1993) employed the FEM with the eight-node isoparametric quadratic plate-bending element, which includes transverse shear deformation for the analysis of bead-stiffened composite plates under transverse loads. Again, the developed FEM is used by Chattopadhyay *et al.* (1995) for the large deflection analysis of the plates. The free vibration of stiffened composite laminates using the FEM is presented by Guo and Harik (1996). Harik *et al.* (1997) developed a finite element model for the problem of stiffened laminates in bending problem. The element layer and the stiffeners are modelled using degenerated shell elements and 3D beam elements respectively. This model can be used for both thin and thick plates. The response of multidegree linear elastic structures subjected to stationary random stochastic loading obtained from the FEM is described by Goswami (1997). Rao (2000) used the method to capture the behaviour of plain/stiffened plates and shell structures, which are typical structures used in the aerospace industry. Concentrically and eccentrically stiffened laminated plates have been analysed by Sadek *et al.* (2000) using a FEM based on a refined higher order displacement model. The plate element used is a nine-node isoparametric one with seven degrees of freedom at each node. The stiffener element

is a three-node isoparametric beam element with four degrees of freedom at each node. Hosseini-Toudeshky *et al.* (2005) used the FEM for buckling analyses of bead stiffened composite panels with different bead spacing, bead depth, bead radii and panel lengths. Wang *et al.* (2005) also used this method to examine the influence of manufacturing induced thermal residual stress on the optimal shape of stiffeners in stiffened symmetrically laminated plates.

3.6 Summary

In the earlier sections, the reviews on structural analytical methods of plates and numerical methods have been undertaken to build the methodology for the design of composite ship structures.

According to the review of structural analytical methods for stiffened plate, the following points could be concluded:

- If a plate is represented as a plated grillage, in the case of isotropic material the Force Method (FM) can provide exact solutions. However, a high computational time is inevitable when the number of beam intersection is high. This does not cause any problem when using the Energy Method (EM) because it is necessary to solve only one equation within the solver stage. Moreover, the Energy Method (EM) has the benefit of the simplicity of one-dimensional calculation. For instance, the stresses are calculated from simple beam theory.

- For stiffened plates made of isotropic material, Orthotropic Plate Method (OPM) is popular due to its simplicity. Nevertheless, it is not easy to obtain stress results because stiffeners are smeared out. Orthotropic Plate Method (OPM) is justified only when stiffeners are closely spaced.

- The Folded Plate Method (FPM) is a further refinement that requires less assumptions about the stiffened plate. However, its application is limited to plates stiffened

in only one direction and subjected to simply supported conditions at one pair of opposite sides.

For unstiffened plates (laminate), the review of analytical methods can be summarised as follows.

- 3-D elasticity theory provides the exact solutions but it is complicated to apply for laminates having a large number of layers, which leads to a large number of unknown parameters. Layer-wise theory, which provides the solution closest to the exact solution, has the same problem as 3-D elasticity theory.

- Out of the Equivalent single layer (ESL) theories, Classical Laminated Plate Theory (CLPT) is the simplest due to Kirchhoff's hypothesis. It is widely used for gross analysis of laminated structures and provides an accurate solution for thin plates where small transverse shear effects can be neglected. CLPT is unique but the First Order Shear Deformation Theory (FSDT) and Higher Order Shear Deformation Theory (HSDT) are not because FSDT can be presented in a different form of shear correction factors and HSDT can be presented in a different form of truncation terms.

- As a result of introducing first-order shear deformation terms in the displacement field, First Order Shear Deformation Theory (FSDT) provides a better solution than Classical Laminated Plate Theory (CLPT). However, the shear correction factor (K) is not easily determined.

Based on the literature review of numerical methods, the following conclusions can be drawn.

- Since the Finite Strip Method (FSM) is the direct application of the theory of elasticity to determine the stiffness matrix of folded plate elements, FSM requires the least computational time among numerical methods. FSM can provide detailed models that can capture interactions between the shell and stiffeners. The model can be varied in geometry. However, although the Finite Strip Method (FSM)

allows different segments to have different properties, it cannot permit a variation of thickness or properties in each segment. This restricts the models to having lengthwise or breadthwise uniform properties.

- The Finite Element Method (FEM) is considered to be the universal method for the solution of mechanics problems and there are numerous commercial FEM software packages available. For stiffened shell design, FEM can capture the behaviour of a shell beyond its initial stability point. Nevertheless, choosing an appropriate meshing scheme is difficult. This method is computationally expensive and the numerical noise introduced by the discretisation interferes with the performance of a gradient-based optimisation algorithm.

- Among those methods, the Finite Difference Method (FDM)is the simplest to study and understand but it is not convenient to define the boundary conditions and it is difficult to apply to complex structures. This is the reason why there are less published papers concerned with the structural application of this method at the present time.

Chapter 4

Methodology

4.1 Introduction

In accordance with the aim of this work (to introduce a methodology for the initial design of a composite ship structure), the former chapters have presented a review of optimisation techniques and ship structural analysis. The outcome of this review has resulted in the development of the methodology presented below.

4.2 Methodology adopted

The methodology (herein referring to the optimisation framework) adopted for a composite ship structural design is a combination of GA and structural analytical methods of composite plates. The framework is used for the initial composite ship structural design stage where the optimum results of scantlings should be obtained as quickly as possible. Hence, rather than using a numerical method for finding structural analysis solutions, simplified methods are employed.

In the Energy method (EM) based on Navier solutions, the grillage is represented by a stiffened plate because this way only one governing equation needs to be solved although the design variables are varied. The EM was originally developed for a steel grillage so

that the equivalent elastic properties of symmetric unidirectional laminate are included into its derivation. In the case of an unstiffened plate (laminate plate), higher order shear deformation theory (HSDT) is chosen because it can provide accurate solutions to problems ranging from thin to moderately thick plate.

Since the design problem of a composite ship may be characterized as non-linear of high order, discrete and fluctuant, the GA is selected as the optimization tool. It will be proved in a later section that the GA works on problems of this nature.

4.3 Description of the optimisation framework

As described in Figure 4.1, the framework is divided into two parts: GA searching procedure (label 1-5) and evaluation part (label 6-19). Remembering that GA follows the principles of natural evolution and selection in the context of engineering. Each design is different from each other in some subtle but quantified way (for example, different number of layers in the plates, different fibre orientation etc.). These design variants are then "bred" together to produce "offspring" which are compared against each other in terms of the most suitable at fulfilling some design criteria. To this end and refering the reader to Figure 4.1, the following description is presented.

Firstly, the input data, such as GA parameters, the maximum generation, types of GA operators and so on (the processes and terminology associated with natural evolution in the context of engineering are described in Chapter 5), are supplied by the designer in stage 1. The binary representation of design variables is decoded in stage 6 and the design variables of the composite compounds are transferred to the composite properties evaluation module where E_1, E_2, v_{12}, G_{12} and strength properties are calculated.

The material properties and geometric information (e.g. stiffener spacing, plate dimension and so on) are used for the evaluation of objectives and constraints in stages 8 and 9. The objective and constraints are then converted into objective functions in stages

11-14. This work deals only with single objective functions, however multiple objective functions could be dealt with in this framework. Any of the four parameters, weight, stiffness, strength or stability could be either an objective or a constraint.

The structural analysis modules are divided into two paths: stiffened plates (Grillage Analysis) and unstiffened plate (HSDT). The fitness of each individual is then the fitness evaluated in stage 10. If an individual satisfies all the constraints its fitness value is set equal to the normalized value of its objective function. If not, its fitness value is set to zero and it is thereby eliminated from the population. The results are then fed back to the GA searching stage which runs exploiting and exploring operators. This terminates when a maximum is achieved.

Since the aim of this section is to present a general description of the optimization framework following Figure 4.1, it has been seen that there are many aspects which may be new for readers. Hence, more explanations will be given in Chapter 5, which is concerned with the grillage analysis, HSDT, optimization procedure (GA) and weight function. The individual module of this framework is validated and tested in Chapter 6. Finally, the applications of this framework to stiffened and unstiffened plates are performed in Chapter 7 and 8 respectively.

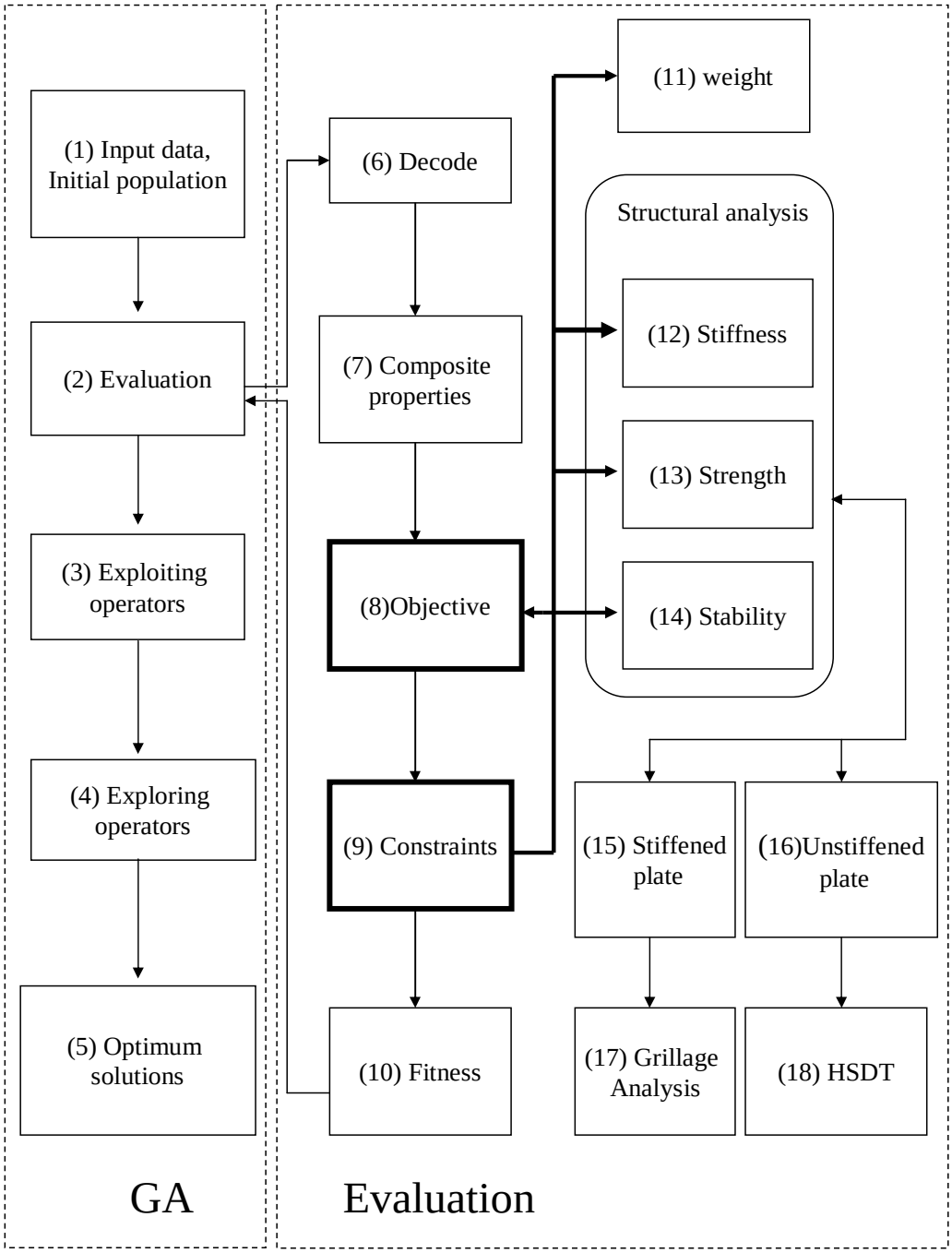

Figure 4.1: Optimisation framework

Chapter 5

Structural analysis and Optimisation procedure

5.1 Introduction

In the previous chapter, the optimisation framework for composite ship structures was proposed. This broadly consists of a structural analysis and an optimisation procedure. In this chapter, firstly the grillage analysis method adopted for composite plate grillages is introduced and the Higher Order Shear Deformation Theory (HSDT) used for unstiffened plates is described. Next, Genetic Algorithm (GA), one of the stochastic search methods which mimics the laws of natural evolution, is explained. Finally, an example of binary representation and objective formulation is given.

5.2 Grillage analysis

The analysis of grillages based on Navier's Method and found in Vedeler (1945), originally developed for a structure built of isotropic material, is adapted for composite plated grillages by substituting equivalent elastic properties of a symmetric laminate into the grillage analysis. Consider the grillage (see Figure. 5.1) consisting of b equally spaced beams in the length (L) direction and g equally spaced girders in the width (B) direction.

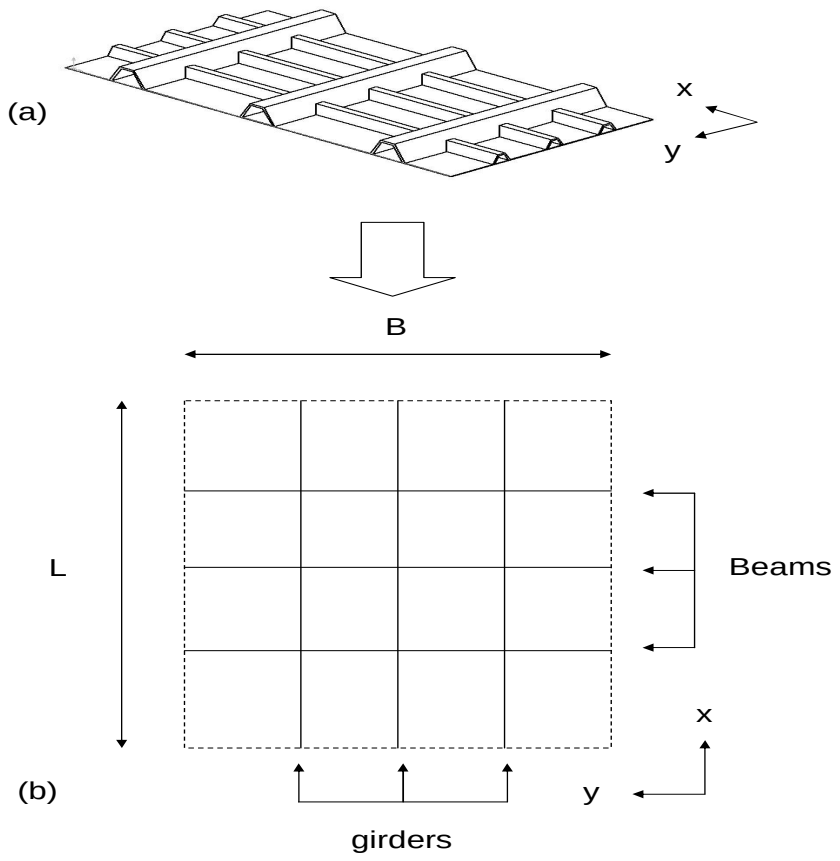

Figure 5.1: (a) Tophat cross stiffened plate and (b) Grillage representation for the stiffened plate

Since the structures are made of laminated composite, the tophat cross section could be comprised of many elements having different elastic properties. For example, the web, crown, base plate and core are elements of the tophat section. To represent the tophat cross stiffened plates, girders and beams of the grillage have tophat shape including base plate (See Figure 5.2). The width of base plate element is represented by the effective width. The effective width is introduced to make the calculated maximum stress from the simple beam formula to be the same as that obtained from an elastic solution in which

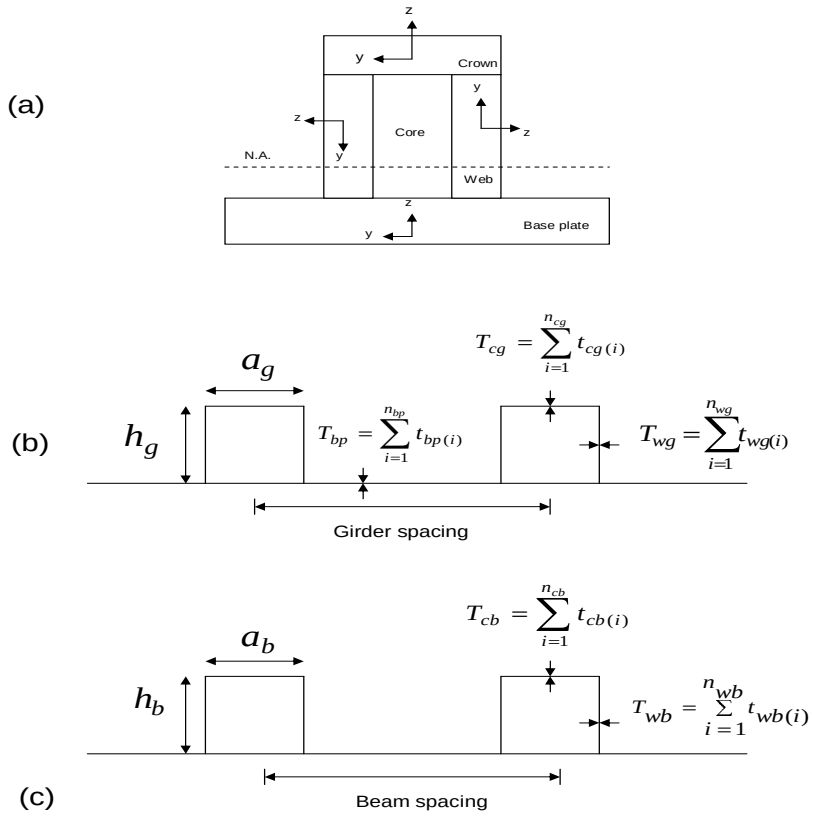

Figure 5.2: (a) Tophat cross section of girders and beams with the local coordinate for fibre layup (b) Geometric parameters of girders and (c) Geometric parameters of beams

the plate action of the flange is recognized. For a stiffened plate built of steel, the effective width is about 20% of girder or beam spacing. This is determined by the experiment.

To avoid the section coupling problem (bending is caused by an axial load), the geometry of the cross section must be symmetric. Each laminated element is assumed to be symmetric about its own plane and specially orthotropic in the membrane mode to eliminate the effect of the coupling terms $[B]$ and shear coupling A_{16}, A_{26}. From Datoo (1991), the membrane equivalent Young's modulus value of a laminate in the axial direction of the

i^{th} element (E_i) can be found by,

$$E_i = \frac{(A_{11}A_{22} - A_{12}^2)}{A_{22}t} \tag{5.1}$$

The extension stiffness $[A]$ of the element is expressed as:

$$A_{ij} = \sum_{k=1}^{N} t_k(\bar{Q}_{ij})_k \tag{5.2}$$

For $ij = 11, 12$ and 22, the expressions for $\bar{Q}_{ij}$, the transformed reduced stiffness of the k^{th} layer are as follows:

$$\bar{Q}_{11} = c^4Q_{11} + s^4Q_{22} + 2c^2s^2Q_{12} + 4c^4s^2Q_{66} \tag{5.3}$$

$$\bar{Q}_{12} = c^2s^2Q_{11} + c^2s^2Q_{22} + (c^4 + s^4)Q_{12} - 4c^2s^2Q_{66} \tag{5.4}$$

$$\bar{Q}_{22} = s^4Q_{11} + c^4Q_{22} + 2c^2s^2Q_{12} + 4c^4s^2Q_{66} \tag{5.5}$$

c and s are abbreviations for $cos\ \theta$ and $sin\ \theta$ and θ is the fibre angle in each ply. The reduced stiffness terms (Q_{ij}) where $i, j = 1, 2, 6$ are expressed as:

$$Q_{11} = \frac{E_1}{(1 - v_{12}v_{21})},\ Q_{22} = \frac{E_2}{(1 - v_{12}v_{21})}\ ,\ Q_{12} = \frac{v_{21}E_1}{(1 - v_{12}v_{21})},\ Q_{66} = G_{12} \tag{5.6}$$

If the cross section of girders and beams is N_g and N_b elements respectively, the combined flexural rigidity of girders (D_g) and beams (D_b) can be written as:

$$D_g = \sum_{i=1}^{N_g} E_{g(i)}I_{g(i)}, \quad D_b = \sum_{i=1}^{N_b} E_{b(i)}I_{b(i)} \tag{5.7}$$

$E_{g(i)}$ and $E_{b(i)}$ are the membrane equivalent Young's moduli in axial direction of the i^{th} element of girders and beams respectively. $I_{g(i)}$ and $I_{b(i)}$ are the second moments of area of the i^{th} element relative to Neutral Axis $(N.A.)$ of the girder and beam's cross sections respectively. The general form of $I_{g(i)}, I_{b(i)}$ can be presented by $I_{(i)}$ as follows:

$$I_{(i)} = I_{cx(i)} + a_{(i)}(d_{na(i)})^2 \tag{5.8}$$

The deflection (w) at any point on the grillage is expressed by the following double summation of trigonometric series called the Navier solution.

$$w(x,y) = \sum_{m=1}^{\infty}\sum_{n=1}^{\infty} a_{mn} sin\frac{m\pi x}{L} sin\frac{n\pi y}{B} \tag{5.9}$$

m and n are wave numbers and a_{mn} are coefficients which can be determined by the condition that the change in potential energy due to the assumed deflections is a minimum. The deflection curve of the q^{th} beam is obtained by giving x the constant value $x_q = \frac{qL}{(b+1)}$.

$$\begin{aligned}(w)_{x=x_q} &= \sum_{n=1}^{\infty} b_{qn} sin\frac{n\pi y}{B}, \\ b_{qn} &= \sum_{m=1}^{\infty} a_{mn} sin\frac{m\pi q}{(b+1)}\end{aligned} \tag{5.10}$$

Similarly, the deflection curve of the p^{th} girder is obtained by giving y the constant value $y_p = \frac{pB}{(g+1)}$.

$$\begin{aligned}(w)_{y=y_p} &= \sum_{m=1}^{\infty} c_{pn} sin\frac{m\pi x}{L}, \\ c_{pn} &= \sum_{n=1}^{\infty} a_{mn} sin\frac{n\pi p}{(g+1)}\end{aligned} \tag{5.11}$$

The total strain energy for all girders and beams can be represented as:

$$\begin{aligned}V = &\int_0^L \frac{D_g}{2}\left(\frac{\partial^2 w}{\partial x^2}\right)^2_{y=y_p} dx \\ &+ \int_0^B \frac{D_b}{2}\left(\frac{\partial^2 w}{\partial y^2}\right)^2_{x=x_q} dy\end{aligned} \tag{5.12}$$

The work done by a uniform pressure load (P) can be expressed as:

$$\int_0^L \int_0^B P \sum_{m=1}^{\infty}\sum_{n=1}^{\infty} a_{mn} sin\frac{m\pi x}{L} sin\frac{n\pi y}{B} dxdy \tag{5.13}$$

Equalising the minimum potential energy ($\partial V/\partial a_{mn}$) to Eq. 5.13, we get

$$\frac{\pi^4 D_b}{2B^3}\sum_{q=1}^{b} n^4 b_{qn} sin\frac{m\pi q}{(b+1)} + \frac{\pi^4 D_g}{2L^3}\sum_{p=1}^{g} m^4 c_{pn} sin\frac{n\pi p}{(g+1)} = \frac{4PLB}{\pi^2 mn} \tag{5.14}$$

where m and n are odd numbers. Now, the coefficient a_{mn} can be obtained as,

$$a_{mn} = \frac{16PLB}{\pi^6 mn\left\{m^4(g+1)\frac{D_g}{L^3} + n^4(b+1)\frac{D_b}{B^3}\right\}} \tag{5.15}$$

Hence, the complete expression for the deflection of the tophat stiffened plate can be found by substituting Eq. 5.15 into the double sine series in Eq. 5.9. The bending moment and shear force of the p^{th} girder can be obtained by,

$$M_g = -D_g\frac{\partial^2 w}{\partial x^2}, \quad Q_g = \frac{\partial M_g}{\partial x} \tag{5.16}$$

The direct stress in the axial direction and shear stress at each element on the girder cross section are given by the following expressions,

$$\sigma_g = \frac{E_{g(i)} M_g Z_g}{D_g}, \quad \tau_g = -\frac{E_{g(i)} Q_g}{D_g}\int_0^s Z_g ds \tag{5.17}$$

Where Z_g is the distance from the neutral axis of the girder to the i^{th} element and s is the distance around the cross section from the middle of the crown element to a point at which we wish to know the shear. Similar to Eq. 5.16 and Eq. 5.17, the direct stress (σ_b) and shear stress (τ_b) of the beam can be obtained.

5.3 Higher order shear deformation theory (HSDT)

The HSDT used in this work is based on the third-order shear deformation plate theories (TSDT) which were developed by Reddy (1997). It is a good compromise between accuracy and computational efficiency. The assumptions of this theory are almost the same

as the CLPT and FSDT except that the assumption on the straightness and normality of a transverse normal after deformation is relaxed by expanding the displacements as cubic functions of the thickness coordinate.

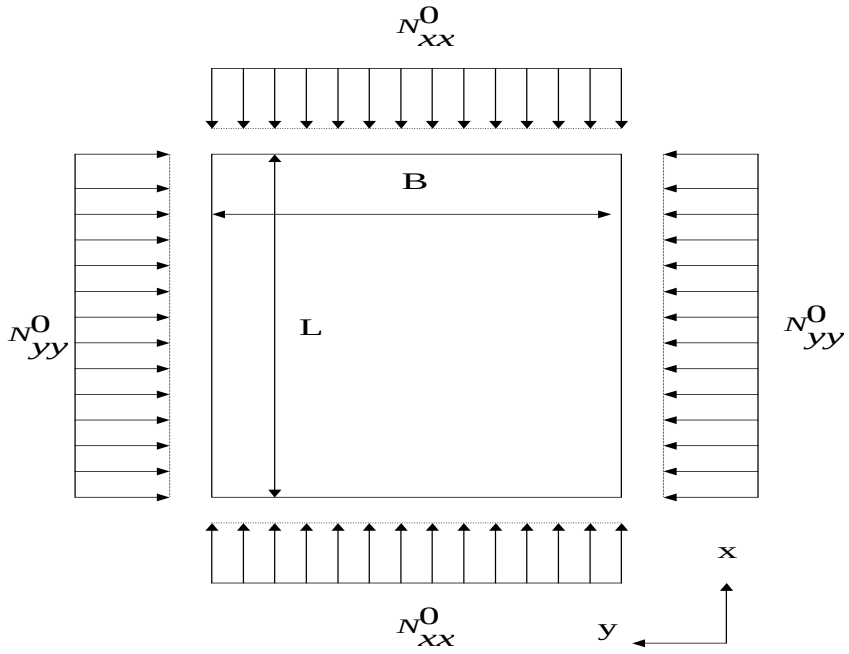

Figure 5.3: The co-ordinate system of a rectangular laminated plate of thickness (t) subjected to in-plane compressive edge forces ($\hat{N}_{xx} = -N^0_{xx}, \hat{N}_{yy} = -N^0_{yy}$)

Related to Figure 5.3, the displacement field of TSDT can be presented as,

$$u(x, y, z) = u_0(x, y) + z\phi_x(x, y) - c_1 z^3 \left(\phi_x + c_0 \frac{\partial w_0}{\partial x} \right) \tag{5.18}$$

$$v(x, y, z) = v_0(x, y) + z\phi_y(x, y) - c_1 z^3 \left(\phi_y + c_0 \frac{\partial w_0}{\partial y} \right) \tag{5.19}$$

$$w(x, y) = w_o(x, y) \tag{5.20}$$

where c_1 and c_0 are parameters introduced for the HSDT assumption. ϕ_x and ϕ_y denote rotations about the x and y axes.

By substituting the above displacement field into the nonlinear strain displacement relations, the following strain-displacements are obtained,

$$\begin{pmatrix} \epsilon_{xx} \\ \epsilon_{yy} \\ \epsilon_{xy} \end{pmatrix} = \begin{pmatrix} \frac{\partial u_0}{\partial x} + \frac{1}{2}\left(\frac{\partial w_0}{\partial x}\right)^2 \\ \frac{\partial v_0}{\partial y} + \frac{1}{2}\left(\frac{\partial w_0}{\partial x}\right)^2 \\ \frac{\partial u_0}{\partial y} + \frac{\partial v_0}{\partial x} + \frac{\partial w_0}{\partial x}\frac{\partial w_0}{\partial y} \end{pmatrix} + z \begin{pmatrix} \frac{\partial \phi_x}{\partial x} \\ \frac{\partial \phi_y}{\partial y} \\ \frac{\partial \phi_x}{\partial y} + \frac{\partial \phi_y}{\partial x} \end{pmatrix} + z^3 \begin{pmatrix} -c_1\left(\frac{\partial \phi_x}{\partial x} + \frac{\partial^2 w_0}{\partial x^2}\right) \\ -c_1\left(\frac{\partial \phi_y}{\partial y} + \frac{\partial^2 w_0}{\partial y^2}\right) \\ -c_1\left(\frac{\partial \phi_x}{\partial y} + \frac{\partial \phi_y}{\partial x} + 2\frac{\partial^2 w_0}{\partial x \partial y}\right) \end{pmatrix} \tag{5.21}$$

$$\begin{pmatrix} \epsilon_{yz} \\ \epsilon_{xz} \end{pmatrix} = \begin{pmatrix} \phi_y + \frac{\partial w_0}{\partial y} \\ \phi_x + \frac{\partial w_0}{\partial x} \end{pmatrix} + z^2 \begin{pmatrix} -c_2\left(\phi_y + \frac{\partial w_0}{\partial y}\right) \\ -c_2\left(\phi_x + \frac{\partial w_0}{\partial x}\right) \end{pmatrix} \tag{5.22}$$

where $c_2 = 3c_1$ and it is assumed that $c_0 = 1$. Since the transverse stresses are assumed to vanish at the bottom and top of the laminate, it can be known that $c_2 = 4/h^2$.

The equations of stresses for any ply, obtained by substituting the strain-displacement relation into the general elasticity equation, are put into the resultant terms. The stress resultants related to strains are as follows,

$$\begin{pmatrix} \{N\} \\ \{M\} \\ \{P\} \end{pmatrix} = \begin{bmatrix} [A] & [B] & [E] \\ [B] & [D] & [F] \\ [E] & [F] & [H] \end{bmatrix} \begin{pmatrix} \left\{\epsilon^{(0)}\right\} \\ \left\{\epsilon^{(1)}\right\} \\ \left\{\epsilon^{(3)}\right\} \end{pmatrix} \tag{5.23}$$

$$\begin{pmatrix} \{Q\} \\ \{R\} \end{pmatrix} = \begin{bmatrix} [A] & [D] \\ [D] & [F] \end{bmatrix} \begin{pmatrix} \left\{\gamma^{(0)}\right\} \\ \left\{\gamma^{(2)}\right\} \end{pmatrix} \tag{5.24}$$

$$(A_{mn}, B_{ij}, D_{mn}, E_{ij}, F_{mn}, H_{ij}) = \int_{-h/2}^{h/2} \left(\bar{Q}_{ij}, \bar{Q}_{mn}\right) \left(1, z, z^2, z^3, z,^4, z^6\right) dz \qquad (5.25)$$
$$(i, j = 1, 2, 6),\ (m, n = 1, 2, 4, 6)$$

where $\left\{\epsilon^{(0)}\right\}$, $\left\{\epsilon^{(1)}\right\}$ and $\left\{\epsilon^{(3)}\right\}$ are defined as the first, second and third matrix terms respectively on the right hand side of Eq. 5.21 and $\left\{\gamma^{(0)}\right\}$ and $\left\{\gamma^{(2)}\right\}$ are defined as the first and the second matrix terms respectively on the right hand side of Eq. 5.22.

The equations of motion of this theory can be derived from the virtual work stated as,

$$0 = \delta U + \delta V \qquad (5.26)$$

where δU, δV are strain and work done respectively.

Exact analytical solutions for specific boundary conditions can be obtained when using either Navier, Levy or Rayleigh-Ritz type solutions. Navier solutions are the most widely used and feasible when considering a simply supported cross-ply and have therefore been selected for this work. The laminate plates have to be restricted to specific simply supported boundary conditions.

For cross-ply, the boundary conditions are satisfied by the following expansion:

$$u_0(x, y) = \sum_{n=1}^{\infty} \sum_{m=1}^{\infty} U_{mn} cos\alpha x sin\beta y \qquad (5.27)$$

$$v_0(x, y) = \sum_{n=1}^{\infty} \sum_{m=1}^{\infty} V_{mn} sin\alpha x cos\beta y \qquad (5.28)$$

$$w_0(x, y) = \sum_{n=1}^{\infty} \sum_{m=1}^{\infty} W_{mn} sin\alpha x sin\beta y \qquad (5.29)$$

$$\phi_x(x, y) = \sum_{n=1}^{\infty} \sum_{m=1}^{\infty} X_{mn} cos\alpha x sin\beta y \qquad (5.30)$$

$$\phi_y(x,y) = \sum_{n=1}^{\infty}\sum_{m=1}^{\infty} Y_{mn} sin\alpha x cos\beta y \tag{5.31}$$

The transverse load $q(x,y)$ is also expanded in a Fourier series when employing the Navier procedure presented as,

$$q(x,y) = \sum_{n=1}^{\infty}\sum_{m=1}^{\infty} Q_{mn} sin\alpha x sin\beta y \tag{5.32}$$

$$Q_{mn}(z) = \frac{4}{LB}\int_0^L\int_0^B q(x,y) sin\frac{m\pi x}{L} sin\frac{n\pi y}{B} dxdy \tag{5.33}$$

Substituting Eqs. 5.27 to 5.33 into the equation of motion, for static purposes the coefficients $(U_{mn}, V_{mn}, W_{mn}\ ,\ X_{mn}, Y_{mn})$ can be found from the following equations,

$$[C]\ [\Delta] = \begin{Bmatrix} 0 \\ 0 \\ Q_{mn} \\ 0 \\ 0 \end{Bmatrix},\ [\Delta] = \begin{Bmatrix} U_{mn} \\ V_{mn} \\ W_{mn} \\ X_{mn} \\ Y_{mn} \end{Bmatrix} \tag{5.34}$$

where $[C]$ is the stiffness matrix. For a uniformly distributed load, $Q_{mn} = -\frac{16q_0}{\pi^2 mn}$ where q_0 is the magnitude of the load.

The stresses for the k^{th} layer can be obtained from the constitutive equations written as:

$$\begin{pmatrix} \sigma_{xx} \\ \sigma_{yy} \\ \sigma_{xy} \end{pmatrix}^{(k)} = \begin{pmatrix} \bar{Q}_{11} & \bar{Q}_{12} & 0 \\ \bar{Q}_{12} & \bar{Q}_{22} & 0 \\ 0 & 0 & \bar{Q}_{66} \end{pmatrix}^{(k)} \begin{pmatrix} \epsilon_{xx} \\ \epsilon_{yy} \\ \epsilon_{xy} \end{pmatrix}^{(k)} \tag{5.35}$$

$$\begin{pmatrix} \sigma_{yz} \\ \sigma_{xz} \end{pmatrix}^{(k)} = \begin{pmatrix} \bar{Q}_{44} & 0 \\ 0 & \bar{Q}_{55} \end{pmatrix}^{(k)} \begin{pmatrix} \epsilon_{yz} \\ \epsilon_{xz} \end{pmatrix}^{(k)} \tag{5.36}$$

For the case of buckling, the critical buckling load can be found by solving the following equation.

$$([C] - \lambda[G])[\Delta] = [0] \tag{5.37}$$

where [G] is the stiffness matrix due to the in-plane forces and λ is the buckling parameter.

$$G_{33} = \alpha^2 + \left(\frac{\hat{N}_{yy}}{\hat{N}_{xx}}\right)\beta^2, \quad G_{ij} = 0 \;\; i, j = 1, 2, ..., 5 \; (i \neq 3, j \neq 3) \tag{5.38}$$

In this work, critical buckling load (N_{cr}) is equal to λ at $(m, n = 1)$. For a uniaxial buckling load, $\hat{N}_{yy}/\hat{N}_{xx} = 0.0$ and for a biaxial buckling load $\hat{N}_{yy}/\hat{N}_{xx} = 1.0$.

5.4 Genetic Algorithm

5.4.1 Introduction

The Genetic Algorithms (GAs) are stochastic search methods which mimic the laws of natural evolution. As mentioned in section 4.3, natural evolution in the context of engineering requires "parent" designs "breeding" together to form "offspring" which are then ranked or selected for their ability to "breed" against some criteria or constraint. GAs can be applied to solving a variety of optimisation problems that are not well suited to standard optimisation algorithms, including problems in which the objective function is discontinuous, nondifferentiable, stochastic or highly nonlinear. The general structure of GAs (see Figure 5.4) is described by the following sections.

5.4.2 Initial population

In the first step of GA searching, the initial population is randomly generated. The population is represented as a group of organisms, each of which consists of a fixed number of chromosomes. Each chromosome is comprised of many genes that could be encoded by binary number, finite string digit, alphabet (letter) or real numbers.

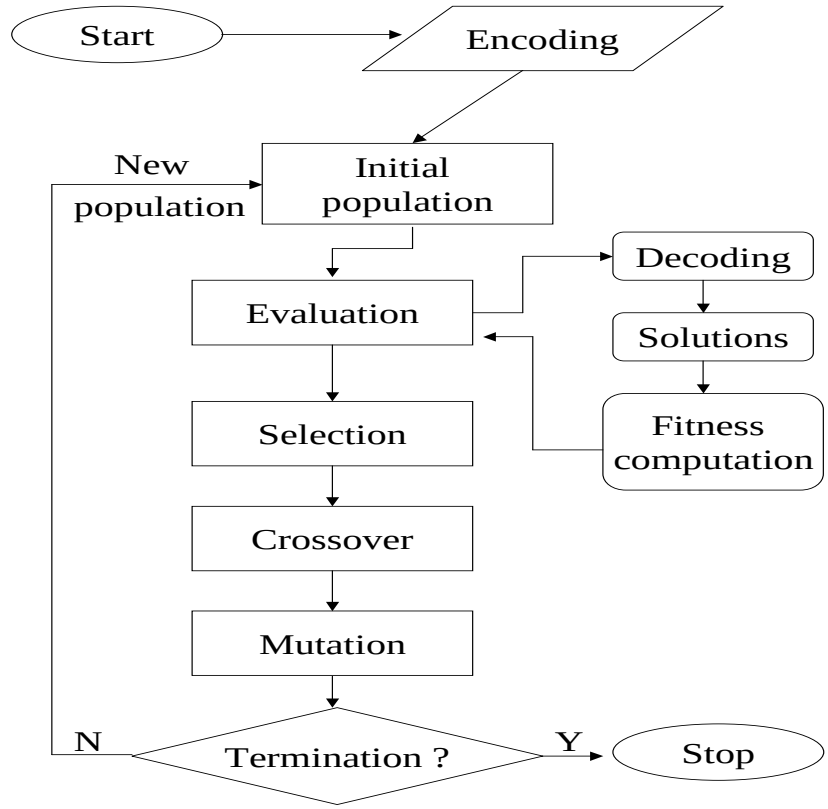

Figure 5.4: The diagram of Genetic Algorithms

Typically, the gene of a chromosome is encoded by using a binary number. Maneepan *et al.* (2006) designed a tophat stiffened plate by using a GA. The problem consists of many discrete design variables. For instance, the number of stiffeners (n_f) is one of the discrete variables and n_f could be 1,2,3,..8. This can be encoded by 3 binary bits from 000=1 to 111=8.

For continuous variables such as real numbers, the method of encoding is explained by Gen and Cheng (1997). Firstly the chromosome length is defined by the required precision. If the required precision is two places for instance, the range of domain of each variable could be divided into at least $(x^u - x^l)10^2$ size ranges where x^u and x^l are upper

and lower bounds of each variable respectively. The required bits denoted by (m) for a variable are calculated based on the following equation.

$$2^{m-1} < (x^u - x^l) \leq 2^m - 1 \tag{5.39}$$

The mapping from a binary string to a real number for a variable is completed by,

$$x = x^l + decimal(bi)\frac{(x^u - x^l)}{(2^m - 1)} \tag{5.40}$$

where $decimal(bi)$ is the decimal value of binary number (b) of the design variable (x).

To be clear, the following example is described. The optimisation problem has one design variable x_1 which has the range, $-3.0 < x_1 < 12.1$. Suppose that the precision is set as five places after the decimal point. Then between the range, there are 151,000 divisions from $(12.1-(-3.0)\times 10^5)$. The chromosome length (m) can be determined from Eq.5.39. It has been found that 151,000 is between 2^{17} and 2^{18}, so the chromosome length is equal to 18. If the chromosome is 000001010100101001, the decimal value of binary number $(decimal(bi))$ is equal to $(1 \times 2^{12}) + (1 \times 2^{10}) + (1 \times 2^8) + (1 \times 2^5) + (1 \times 2^3) + (1 \times 2^0) = 5417$. Finally, the corresponding value (phenotype) of this chromosome is evaluated from Eq. 5.40.

In some problems, a finite string digit is used for encoding. Lee and Lin (2004) use a GA to design a composite propeller, in the stacking sequence of the propeller, the $[-45]_2$ stack is assigned the digit 1, the $[0]_2$ stack is assigned the digit 2, the $[45]_2$ stack is assigned the digit 3 and the $[90]_2$ is assigned the digit 4. Hence, for instance, $[0_2/90_2/0_2/-45_2]$ is encoded as [2 4 2 1].

To increase the robustness of GAs, a feasible initial population is required. This can be implemented by adding the algorithm to eliminate every chromosome giving the solution which fails to satisfy all constraints.

5.4.3 Evaluation

This is the process of evaluating the fitness of a chromosome. The chromosome's genotype (binary code of all design variables) is transformed to its phenotype (a single characteristic of one design e.g. plate thickness). Generally, the fitness is directly related to the value of the objective function, $f(x)$, of the phenotype. For the minimisation problem, the fitness is equal to $1/f(x)$. Otherwise, the fitness is equal to $f(x)$.

According to the fitness calculation of the constrained problem, the use of a penalty function is necessary in order to transform the problem to an unconstrained problem. The principle of the penalty function is whenever the constraints are violated a penalty is added to the objective function. Therefore, the evaluation function ($eval(x)$) with a penalty term as used by Maneepan *et al.* (2005) to calculate the fitness can be expressed as,

$$eval(x) = f(x) + P(x) \tag{5.41}$$

where x represents the decoded values of a chromosome, $f(x)$ is the objective function and $P(x)$ is the penalty term which can be written as,

$$P(x) = \sum_{i=1}^{m} R g_i^2(x) \tag{5.42}$$

where $g(x),\ (i = 1, ..., m)$ are design constraints. R is the penalty parameter which is a constant value.

The rejection strategy is one form of the penalty method. Its principle is to discard all infeasible individuals created throughout the evolution process. This means at a time if the constraints are satisfied, $f(x)$ keeps its own value. Otherwise, $f(x)$ is assigned equal to zero.

To maintain a reasonable differential between the relative fitness rating of chromosomes and to prevent a too-rapid takeover by some super chromosomes, scaling mechanics are

introduced to the fitness calculation. Generally, the scaled fitness ($f_k^{'}$) is calculated from the raw fitness f_k for chromosome (k) by $f_k^{'} = scal(f_k)$ where $scal(.)$ is the function used to transform the raw fitness into scaled fitness. Different scaling methods have different scaling functions. An example of scaling methods is normalisation which can be defined for the maximisation problem as,

$$f_k^{'} = \frac{f_k - f_{min} + r}{f_{max} - f_{min} + r} \tag{5.43}$$

where f_{max} and f_{min} are the best and the worst raw fitnesses in the current population respectively. r is a small positive real number in the range from 0 to 1.

To find the fitness of a problem having more than one objective function, the weight sum strategy is employed as can be seen in Walker and Smith (2003) who presented multi-objective optimisation of laminated composite structures by GA. For the minimisation problem, the fitness is equal to one over the value of the combined objective functions (m_f) which can be determined from,

$$m_f = \mu_1 * \bar{f}_1 + \mu_2 * \bar{f}_2 + ... + \mu_n * \bar{f}_n \tag{5.44}$$

where $\bar{f}_1, \bar{f}_2, ..., \bar{f}_n$ are the normalised values of the objective functions. Weight factors $(\mu_1, \mu_2, ..., \mu_n)$ are greater than or equal to zero and $(\mu_1 + \mu_2 + ... + \mu_n) = 1$.

5.4.4 Exploiting operator

The exploiting operator or selection operator is used to exploit the design space by a randomised procedure to create a new population. The chromosomes with a large fitness are copied with a high probability into the mating pool whereas those with low fitness are copied with a low probability or are even removed from the population. Selection schemes include roulette wheel, tournament, elitism and ranking selection.

- Roulette wheel selection: at the time of spinning the roulette wheel, chromosomes are selected from the pool by determining their survival probability (p_k), that can

be expressed as,

$$p_k = eval(v_k) / \sum_{k=1}^{n} eval(v_k) \tag{5.45}$$

where $eval(v_k)$ is the fitness value of the individual (v_k), n is population size and $k = 1, 2, 3, ..., n$. If the individual has a relatively high fitness value, it has a high chance of being selected. Spinning is repeated until the selected chromosome population is equal to the population size.

- Tournament selection: the best chromosome is picked out among a few individuals (tournament size), which are randomly chosen. Selection procedure can be easily adjusted by changing the tournament size. If the tournament size is larger, the weak individuals have a smaller chance of being selected.

- Ranking selection: this method not only selects the best chromosomes but also increases the chance that every chromosome will be selected. The individuals in the population are ranked related to their fitness values. The selection is based on the following probability distribution (p_k).

$$p_k = \frac{2k}{(m(m+1))} \tag{5.46}$$

where k is the k^{th} chromosome in ascending order and m is the fittest chromosome.

- Elitism selection: it is an additional selection process that can co-operate with every selection method. Elitism forces the GA to collect at least one of the best chromosomes of a generation without change and then put it into the new population. Because of this, it can prevent the GA from losing the best chromsomes, which can be lost since they may not be selected to reproduce or they may be destroyed by the exploring operator.

5.4.5 Exploring operators

Crossover

The crossover, reproductive operator, performs a widespread search of the exploring solution space. At a time, it operates on parents (two chromosomes randomly selected from the population after performing the selection). The offspring are created by combining parent features.

- Single point crossover: there is one crossover point that is randomly selected from bits positioned on one chromosome. The two parent strings $x = [x_1, x_2, ..., x_n]$ and $y = [y_1, y_1, ..., y_n]$ are cut at the same point and the cut off strings are swapped across to produce offspring of the form.
  $x^{'} = [x_1, x_2, ..., x_k, y_{k+1}, y_{k+2}, ..., y_n]$ and $y^{'} = [y_1, y_2, ..., y_k, x_{k+1}, ..., x_n]$

- Two point crossover: it is used to produce offspring by exchanging binary genes between two points. Two individuals in the parent population are divided into three parts by two crossover points which are randomly selected. The middle parts of the parents are swapped to produce the offspring.

- Uniform crossover: this method mixes the parent chromosome at segment level. Hence, the genes of the parent chromosomes have a chance to be exchanged at every locus. The chance is controlled by the mixing ratio (m_r) whose range is typically between 0.5 to 0.8. The two offspring generated by uniform crossover are $x^{'} = x_k$ if $r \geq m_r$, otherwise $x^{'} = y_k$ and $y^{'} = y_k$ if $r \geq m_r$, otherwise $y^{'} = x_k$.

- Direction-based crossover: this uses the values of the objective function in determining the direction of the genetic search. The operator used by Lu and Tzang (2000) generates a single offspring ($B^{'}$) from two parents B_1 and B_2 according to the following rule,

$$B^{'} = r(B_2 - B_1) + B_2 \tag{5.47}$$

  where r is a random number between 0 and 1. It also assumes that the parent B_2 is not worse than B_1. When considering the minimisation problem, $fitness(B_2) \leq$

$fitness(B_1)$.

- Arithmetical crossover: it is defined by Bazarra (1990) as the combination of two chromosomes x_1 and x_2 as follows,

$$\lambda_1 x_1 + \lambda_2 x_2 \tag{5.48}$$

The multipliers are restricted by $\lambda_1 + \lambda_2 = 1$ and $\lambda_1 > 0, \lambda_2 > 0$.

Mutation

Mutation helps the GA search to increase population diversity by introducing new genetic material. This can be achieved by a random change to one or more randomly chosen genes in an individual. The following are the examples of mutation operator.

- Static mutation: the mutated gene is assigned a completely random value. With mutation probability, every gene in a population has an equal chance to be changed. In the case of a binary representation, it will be changed from 0 to 1 or 1 to 0.

- Gaussian mutation: an example of this method can be found in Dang and Li (2006). For a gene on the real-valued chromosome of an individual, a variation subject to Gaussian distribution is added to the original if a random real number is less than the mutation probability (p_m). For instance, if $\alpha \leq p_m$ then the offspring ($x_k^{'}$) is defined by $x_k^{'} = x_k + \beta_G \xi$, otherwise, $x_k^{'} = x_k$. ξ is generated independently for each gene and standard deviation of Gaussian distribution function and β_G is scaling parameter for adjusting the mutation steps.

- Dynamic mutation: explained by Gen and Cheng (1997) is designed for fine-tuning capabilities aimed at achieving high precision controlled by a parameter determining the degree of non-uniformity. This can cause the operator to produce a feasible offspring. For a given parent B (real-value chromosome), its gene x_k is selected to mutate, the offspring $B^{'} = [x_1, x_2, ..., x_k^{'}, ..., x_n]$. The position of $x_k^{'}$ is found from two possible choices. $x_k^{'} = x_k + \Delta(t, x_k^u - x_k)$ or $x_k^{'} = x_k - \Delta(t, x_k - x_k^l)$ where

x_k^u and x_k^l are the upper and lower bounds of x_k respectively. $\Delta(t, y)$ is a function which returns a value in the range $[0, y]$.

5.5 Design variable representation

The laminate is the fundamental element of all plate types. The binary representation of the design variables of the laminate scheme which is used for every application in this thesis is expressed and shown in Figure 5.5. Each laminate consists of eight plies but the coding is only for half of the laminate. Each ply is represented by seven bits except the first ply which always exists.

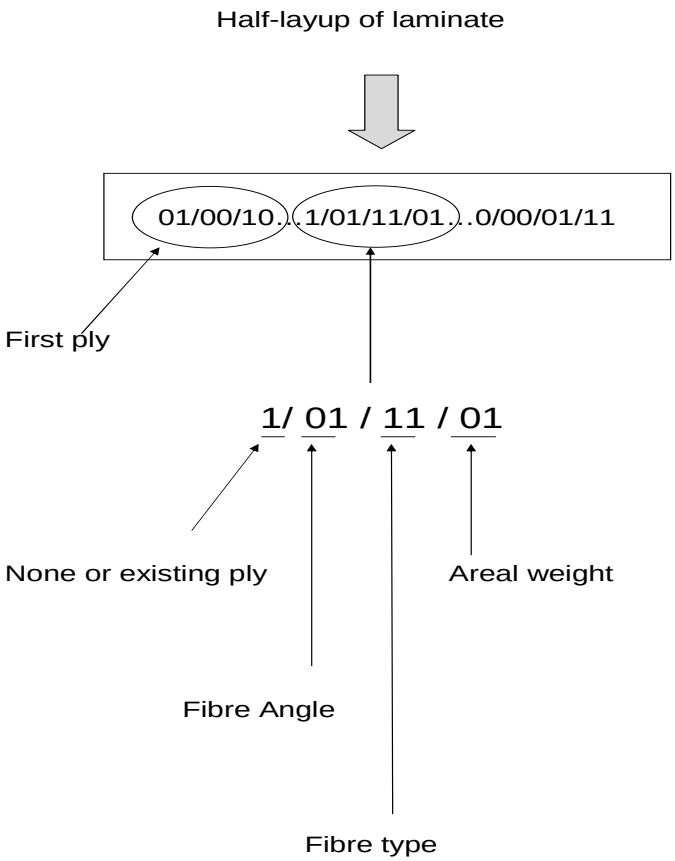

Figure 5.5: Binary representation of a laminate element

5.6 Weight function

The objective function can be changed following the purpose of the design. The main interest of this work is in weight minimisation. The following expression is the weight evaluation function of tophat cross stiffened plate.

Weight of base plate is a product of the volume of composite material with the density of the material. Weight of the individual ply of base plate is,

$$(LBt_{bp})\,\rho_{bp} \tag{5.49}$$

where L and B is length and width of base plate respectively. t_{bp} is the thickness of the individual ply and ρ_{bp} is the density of composite material of the individual ply.

As the base plate consists of n_{bp} layers, the total weight of base plate (W_{bp}) can be expressed as,

$$W_{bp} = LB \sum_{k=1}^{n_{bp}} t_{bp(k)} \rho_{bp(k)} \tag{5.50}$$

Similarly, the weight of the crown element of a girder (W_{cg}) which consists of n_{cg} layers can be written as,

$$W_{cg} = B \sum_{k=1}^{n_{cg}} t_{cg(k)} a_g \rho_{cg(k)} \tag{5.51}$$

where t_{cg} is the ply thickness of the crown element, a_g is the width of the crown element and ρ_{cg} is the density of composite material of the individual ply of the crown element.

For the web element of a girder which is comprised of n_{wg} layers, its weight (W_{wg}) can be presented as,

$$W_{wg} = B \sum_{k=1}^{n_{wg}} t_{wg(k)} h_g \rho_{wg(k)} \tag{5.52}$$

where t_{wg} is the ply thickness of web element, h_g is the height of web element and ρ_{cg} is the density of composite material of the individual ply of web element.

As one girder has two web elements, the total weight of girder W_g is,

$$W_g = W_{cg} + 2W_{wg} \tag{5.53}$$

The weight of the beam is defined by the same method as the weight of girder W_g. The total weight of the plate is,

$$W_T = W_{bp} + gW_g + bW_b \tag{5.54}$$

where g and b are the number of girders and beams respectively. Moreover, the weight function in Eq. 5.54 can be used for other types of plates. For a unidirectional stiffened plate, $b = 0$. For an unstiffened plate, $g = 0$ and $b = 0$.

Chapter 6

Validation and testing

6.1 Introduction

The accuracy of the optimisation framework is primarily related to the structural analysis module and the genetic algorithm module. The analysis method of a stiffened composite plate is validated with a displacement method on the steel grillage and the results of equivalent elastic properties of symmetric laminate. For the unstiffened case, HSDT is implemented and validated with the results of Reddy (1997). The GA based optimisation procedure is tested for its convergence with different starting points and different operators. Finally, the ability of the framework is demonstrated by comparing with ANSYS optimisation.

6.2 Grillage analysis

As the adapted grillage analysis is a combination of an analysis of steel grillage with equivalent elastic properties, each part is individually validated.

(a) Steel grillage:

The following steel grillage examples are used for validation and study purposes.

- 4×4 grillage: the grillage measures 3810 mm square and is acted on by an uniform pressure of 137.900 kPa.

- 4×5 grillage: the grillage measures 6096 mm $\times$ 2540 mm and is acted on by an uniform pressure of 34.475 kPa.

Each example from Clarkson (1965) has been tested by two cases (I-beams and box-beams). The dimension of the longitudinal I-beam is 254 mm deep by 127 mm wide with 18.288 mm thick flange and 9.144 mm thick web. This gives a second moment of area $I = 72465891.2\ mm^4$. The dimension of the transverse I-beam is 69.85 mm deep by 44.45 mm wide with 9.525 mm thick flanges, 5.08 mm thick web and this gives a second moment of area $I = 832462.85\ mm^4$. The dimension of the longitudinal box-beam is 254.0 mm deep 127.0 mm wide with 18.288 mm thick flanges and 9.144 mm thick webs. This gives a second moment of area $I = 80332665.14\ mm^4$. Transverse box-beams 69.85 mm deep by 44.45 mm wide with 9.525 mm thick flanges and 5.08 mm thick webs. This gives a second moment of area $I = 886572.94\ mm^4$. We use a Young's modulus for steel of 206.87 GPa.

To analyse the steel grillage, the following methods are implemented: the Force Method (FM) shown in Eq.3.13 presented by Jang *et al.* (1996), the Othotropic Plate Method (OPM) shown in Eq.3.18 presented by Timosheko (1959) and the Energy Method (EM), shown in Chapter 5 which is developed by the author for composite materials has been adjusted in this example to account for steel.

From Table 6.1, the following points can be made:

- The authors Force Method program provides exactly the same solution as Clarkson. This confirms that all the program coding is correct.

- The Energy Method (EM) and Orthotropic Plate Method (OPM) solutions provide higher values than the exact solutions of the Force method (FM) but they have a

Table 6.1: Comparison between the results of the developed programs from energy method based Navier solution (EM), Orthrotropic Plate Method (OPM), Force Method (FM) and the results of Clarkson (1965) for the maximum deflection δ_{max} (mm) and maximum stress of girder σ^g_{max} (MPa) and beam σ^b_{max} (MPa).

Grillage	Beam type	Solution	Clarkson (1965)	Present		
				FM	OPM	EM
4×4	I	$\delta_{max}(mm)$	10.95	10.95	11.01	11.01
		$\sigma_{max}(MPa)$	183.27	183.27	-	189.76
	box	$\delta_{max}(mm)$	9.63	9.63	9.93	9.93
		$\sigma_{max}(MPa)$	165.52	165.52	-	171.19
4×5	I	$\delta_{max}(mm)$	20.41	20.41	21.05	21.05
		$\sigma^g_{max}(MPa)$	137.88	137.88	-	142.79
		$\sigma^b_{max}(MPa)$	205.35	205.35	-	206.82
	box	$\delta_{max}(mm)$	18.34	18.34	19.10	19.10
		$\sigma^g_{max}(MPa)$	125.37	125.37	-	129.59
		$\sigma^b_{max}(MPa)$	184.66	184.66	-	186.87

much lower computational time. It is not easy to obtain the stress solution from the Othotropic Plate Method (OPM).

(b) Equivalent elastic properties:

In the case of the unidirectional stiffened plate, the base plate element is under membrane mode in the x-direction and under bending mode in y-direction if stiffeners lay along x-direction. Therefore, this section shows the validation of the developed program for the membrane equivalent Young's modulus in x-direction E^m_x which can be evaluated from Eq.5.1 and the bending equivalent Young's modulus in y-direction (E^b_y) which can be evaluated by the following equation.

$$E^b_y = \frac{12(D_{11}D_{22} - D^2_{12})}{t^3 D_{11}} \tag{6.1}$$

The bending stiffness $[D]$ is expressed as,

$$D_{ij} = \sum_k^n (t_k \bar{z}^2_k + \frac{t^3_k}{12})(\bar{Q}_{ij})_k \tag{6.2}$$

where $\bar{z}_k$ is the distance from mid-plane to centroid of k^{th} layer, n is the number of layer in laminate and Q_{ij} is the transformed stiffness which is presented in Eq.5.4, Eq.5.5 and Eq.5.5.

The equivalent Young's modulus is evaluated from five laminates: [0/0/0/0], [0/90/90/0], [90/0/0/90], [45/-45/-45/45] and [0/45/-45/90]s. The lamina properties are $E_1 = 140\,GPa$, $E_2 = 10\ GPa$, $G_{12} = 5\ GPa$ and $v_{12} = 0.3$. Ply thickness (t_k)=0.125 mm, all equal through laminate.

Table 6.2: Comparison between the results of the developed program of equivalent elastic properties and those of Datoo (1991)

Laminate	Equivalent elastic constants	Datoo (1991) GPa	Present GPa
[0/0/0/0]	E_x^m (membrane mode)	140	140
	E_y^b (bending mode)	10	10
[0/90/90/0]	E_x^m (membrane mode)	75.5	75.36
	E_y^b (bending mode)	26.4	26.35
[90/0/0/90]	E_x^m (membrane mode)	75.5	75.36
	E_y^b (bending mode)	124.7	124.21
[45/-45/-45/45]	E_x^m (membrane mode)	17.7	17.74
[0/45/-45/90]s	E_x^m (membrane mode)	54.1	54.07

From Table 6.2, it can be concluded that

- The author's results are almost identical to Datoo's results to the one decimal place precision presented by Datoo. The author is therefore confident with the validation.
- The highest E_x^m is obtained by laying all the fibres along the x-axis (zero fibre angle). The lower the number of zero angle lamina, the lower the magnitude of E_x^m.

(c) Shear stress calculation:

The symmetric rectangular box section consists of webs, crown and base plate. Web

height is 50 mm. Crown and base plate width is 200 mm. The Young's modulus of the crown and base plate elements is 54.1 GPa. The Young's modulus of web (E_w) is 17.7 GPa. The section is subjected to shear force $Q = 10\ kN$. The thickness of the crown and base plate elements is 1.0 mm. The thickness of the web is 0.5 mm. SF_1 and τ_1 are shear flow and shear stress at the corner of the crown element respectively. SF_2 and τ_2 are the shear flow and the shear stress at the neutral axis (N.A.) of the cross section respectively.

Table 6.3: Comparison of the developed program shear stress calculation with Datoo (1991)

	Datoo (1991)	Present
$SF_1\ (N/mm)$	99	98.7226
$\tau_1\ (N/mm^2)$	-	98.7226
$SF_2\ (N/mm)$	101	100.7413
$\tau_2\ (N/mm^2)$	-	102.7600

From Table 6.3, it can be noticed that the developed program agrees well with the results by Datoo who ignored the accuracy after the decimal.

6.3 Higher order shear deformation theory

The Higher order Shear Deformation Theory (HSDT) are implemented and tested in finding responses of laminated plates which are maximum deflection, stresses and critical buckling load for uniaxial and biaxial compression .

(a) Maximum deflection of laminated plate:

Laminate is [0/90/90/0]. Length to width ratio (L/B) of the plate is equal to 1.0. Material properties are $E_1 = 175\ GPa$, $E_2 = 7\ GPa$, $G_{12} = G_{13} = 3.5\ GPa$, $G_{23} = 1.4\ GPa$, and $v_{12} = v_{13} = 0.25$. The load acting on the plate is a sinusoidally distributed load (q_0). The normalised deflection is $\bar{w} = w_0(\frac{a}{2}, \frac{b}{2})(\frac{E_2 t^3}{L^4 q_0})$.

Table 6.4: Comparison between nondimensionalised maximum deflections ($\bar{w}$) of the developed TSDT program and those of TSDT,FSDT,CLPT and 3-D elasticity solution (3-D) from Reddy (1997)

L/t	$\bar{w} \times 10^2$				
	Present	TSDT	FSDT	CLPT	3-D
4	1.894	1.894	1.710	-	1.954
10	0.715	0.715	0.663	-	0.743
20	0.506	0.506	0.491	-	0.517
100	0.434	0.434	0.434	0.431	0.438

From Table 6.4, the present result is exactly the same as that of Reddy (1997) as expected. In addition, the third order shear deformation theory (TSDT) provides the best solution when compared to First order shear deformation theory (FSDT) and Classical laminated plate theory (CLPT) because its solution is closest to the 3-D's solution. As CLPT gives error results if the ratio of L/t less than 20, the deflection results are not shown at that range of L/t.

(b) Stresses on laminated plate:

Square laminated plate has [0/90/0] fibre orientation. Material properties are the same as in (a). The load acting on the plate is a sinusoidal transverse load. The normalised terms of stresses are,

$$\bar{\sigma}_x = \sigma_x(t^2/(q_0 L^2)) \quad \text{at } (L/2.0, B/2.0, t/2.0)$$
$$\bar{\sigma}_y = \sigma_y(t^2/(q_0 L^2)) \quad \text{at } (L/2.0, B/2.0, t/6.0)$$
$$\bar{\tau}_{xy} = \tau_{xy}(t^2/(q_0 L^2)) \quad \text{at } (0.0, 0.0, t/2.0)$$
$$\bar{\tau}_{yz} = \tau_{yz}(t/(q_0 L)) \quad \text{at } (L/2.0, 0.0, 0.0)$$
$$\bar{\sigma}_{xz} = \sigma_{xz}(t/(q_0 L)) \quad \text{at } (0.0, B/2.0, 0.0)$$

The validation of the program subroutine is validated in Table 6.5. From the table, it can be seen that the results of the presented program provide exactly the same as TSDT

which agree well with the 3-D exact solutions.

Table 6.5: Nondimensionalised stresses in a three layer [0/90/0] simply supported square laminate under sinusoidal transverse load

(L/t)	Theory	$\bar{\sigma}_x$	$\bar{\sigma}_y$	$\bar{\tau}_{xz}$	$\bar{\tau}_{yz}$	$\bar{\sigma}_{xy}$
2	$3D^a$	0.938	0.669	0.164	0.2591	0.0859
	$TSDT^b$	1.3112	0.5876	-	-	0.0889
	Present	1.3112	0.5876	0.1543	0.2411	0.0889
20	$3D^a$	0.552	0.210	0.385	0.0938	0.0234
	$TSDT^b$	0.5460	0.2043	-	-	0.0230
	Present	0.5460	0.2043	0.2549	0.0825	0.0230
50	$3D^a$	0.541	0.185	0.393	0.0842	0.0216
	$TSDT^b$	0.5399	0.1836	-	-	0.0216
	Present	0.5399	0.1836	0.2580	0.0760	0.0216
100	$3D^a$	0.539	0.181	0.395	0.0828	0.0213
	$TSDT^b$	0.539	0.1806	-	-	0.0214
	Present	0.539	0.1806	0.2586	0.0750	0.0214
a: Pagano (1970) and b: Kant and Swaminathan (2002)						

(c) Critical buckling load of laminated plate for uniaxial compression:

Laminate is [0/90/90/0]. Layer thickness is the same throughout the laminate. L/B of the plate is equal to 1.0. Material properties are $\frac{E_1}{E_2} = 40$, $\frac{G_{12}}{E_2} = \frac{G_{13}}{E_2} = 0.6$, $\frac{G_{23}}{E_2} = 0.5$ and $v_{12} = v_{13} = 0.25$. The normalised buckling load is $N = N_{cr}\frac{L^2}{E_2 t^3}$.

Table 6.6 shows that the developed program is correct and CLPT provides incorrect solutions for thick plates.

(d) Critical buckling load of laminated plate for biaxial compression:

Laminates are [0/90/90/0], [0/90/0/90/0] and [0/90/0/90/0/90/0]. Layer thickness is the same throughout the laminate. L/B of the plate is equal to 1.0. Material properties

Table 6.6: Comparison of nondimensionalised uniaxial buckling loads (N) of the developed TSDT program with those of TSDT, FSDT and CLPT of Reddy (1997)

L/t	$N \times 10^2$			
	Present	TSDT	FSDT	CLPT
5	11.997	11.997	11.575	36.160
10	23.340	23.340	23.453	36.160
20	31.660	31.660	31.707	36.160
50	35.347	35.347	35.356	36.160
100	35.953	35.953	35.955	36.160

are $\frac{E_1}{E_2} = 25$, $\frac{G_{12}}{E_2} = \frac{G_{13}}{E_2} = 0.5$, $\frac{G_{23}}{E_2} = 0.2$ and $v_{12} = v_{13} = 0.25$. The normalised buckling load is $N = N_{cr}\frac{L^2}{E_2 t^3}$.

Table 6.7: Comparison between nondimensionalised biaxial buckling loads (N) of the developed TSDT program and those of FSDT with shear correction factor (K) = 5/6 of Reddy (1997)

L/t	[0/90/0]		[0/90/0/90/0]		[0/90/0/90/0/90/0]	
	FSDT	Present	FSDT	Present	FSDT	Present
10	7.644	7.110	8.154	7.984	8.267	8.192
20	10.314	10.049	10.564	10.486	10.619	10.584
25	10.784	10.596	10.958	10.905	10.998	10.974
50	11.489	11.435	11.539	11.524	11.550	11.543
100	11.682	11.668	11.695	11.691	11.698	11.696
CLPT	11.747	11.668	11.747	11.691	11.747	11.696

Table 6.7 shows that the results of the developed program agree well with that of the FSDT and the larger the number of layers, the higher the critical buckling load.

6.4 Optimisation procedure

6.4.1 Varying GA operators

To confirm the correctness of the optimisation procedure, a case is chosen for which an optimum solution is already known: the minimisation of the central deflection of a rectangular plate with fibre alignment parallel to the shortest side. This is Case MD1 from Chapter 8, section 8.3.1.

To study the effect of GA operators on GA convergence, the case of minimisation of central deflection of a unidirectional stiffened plate is considered. The design variables of the case are represented by 29 binary bits. The following two sets of GA parameters are used for this study.

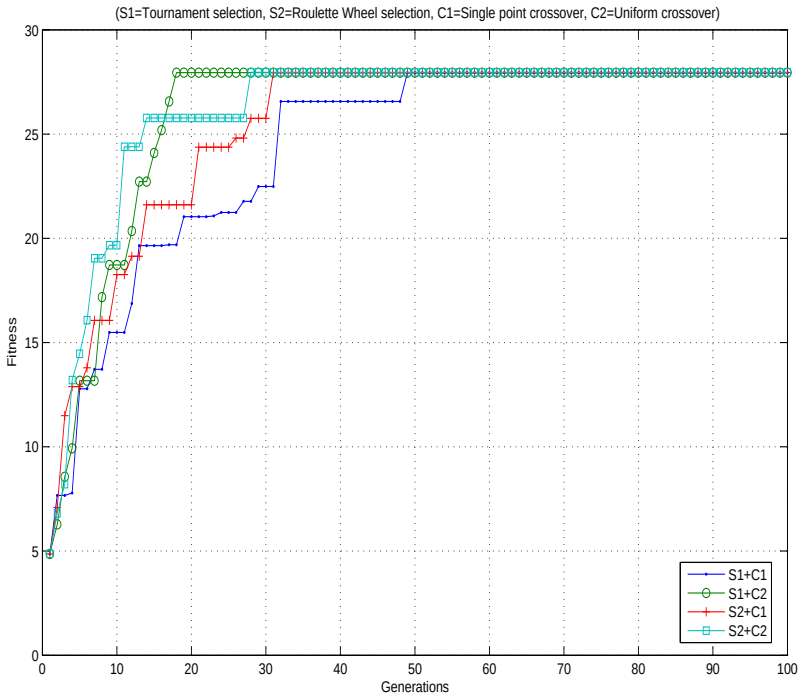

Figure 6.1: GA run by varying a couple of operators with GA parameters set-1

- Set-1: Population size is 50. Crossover probability is 0.5. Mutation probability is 0.02.

- Set-2: Population size is 100. Crossover probability is 0.8. Mutation probability is 0.01.

The graphs of GA convergence for various couple of operators in Figure 6.1 and Figure 6.2 where $s1$=Tournament selection, $s2$=Roulette wheel selection, $c1$=Single point crossover and $c2$=Uniform crossover show that a different pair has its own convergence characteristics for a different set of GA parameters. Therefore, it could not be decided which pair of operators is the most appropriate for this kind of optimisation problem. Hence, to find the optimum solution, many operators should be tried.

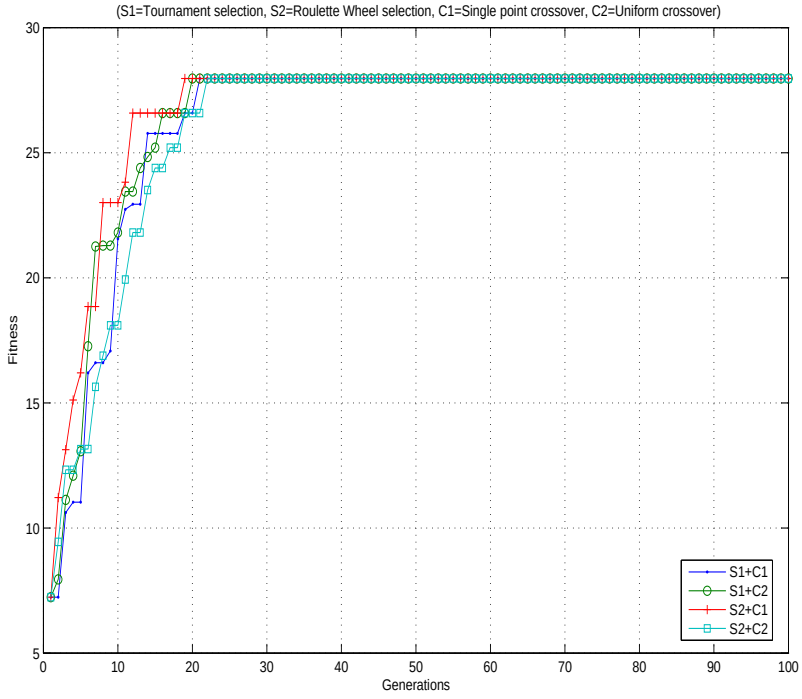

Figure 6.2: GA run by varying a couple of operators with GA parameters set-2

6.4.2 Varying starting points

This subsection presents the testing of the starting point from far to exact solution. The test problem is the same as the former section. The GA parameters for every starting point are Chromosome length = 4 bits, Population size = 4, Crossover Probability = 0.9,

and Mutation Probability = 0.01.

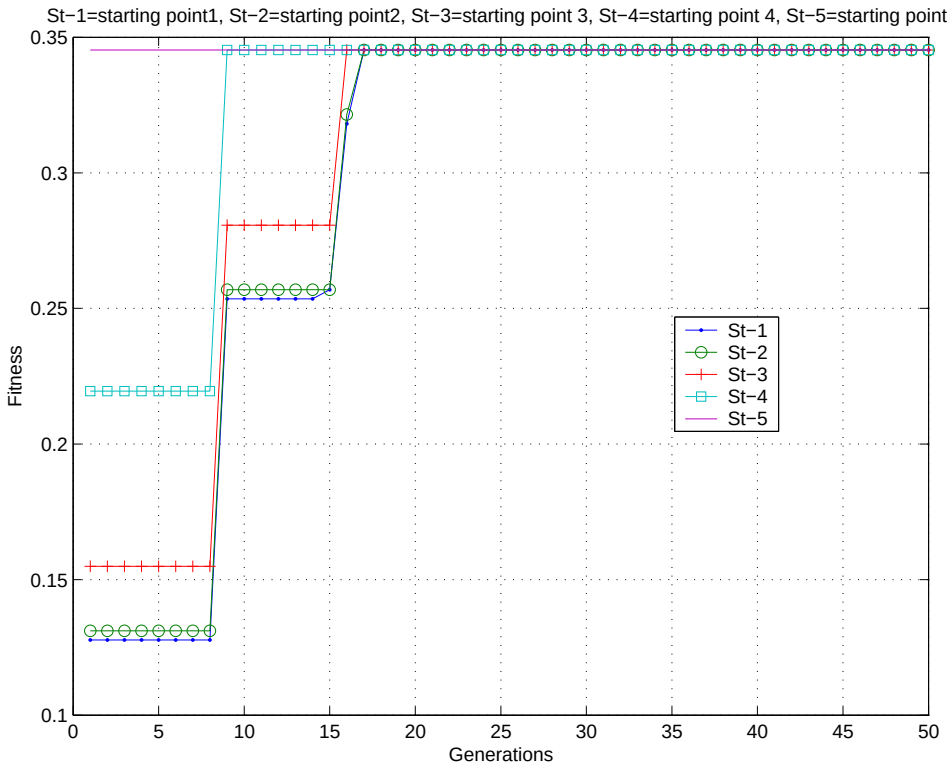

Figure 6.3: GA run for different starting point

As we know the exact solution of this problem is [1/1/1/1] = [90/90/90/90]. The following starting point is tested.

Starting point st-1 : Binary [0/0/0/0] : Fibre orientation [0/0/0/0]
Starting point st-2 : Binary [0/0/0/1] : Fibre orientation [0/0/0/90]
Starting point st-3 : Binary [0/0/1/1] : Fibre orientation [0/0/90/90]
Starting point st-4 : Binary [0/1/1/1] : Fibre orientation [0/90/90/90]
Starting point st-5 : Binary [1/1/1/1] : Fibre orientation [90/90/90/90]

From the Figure 6.3 and 6.4, it can be seen that,

- The graphs of st-1, st-2, st-3 and st-4 converge at 17^{th}, 17^{th}, 16^{th} and 9^{th} generation respectively. As the st-5 is the same point as the exact solution, its graph converges

at the first generation.

- From Figure 6.4, the computational time is different of every starting point and the st-4 which is closest to the optimum solution is fastest in convergence.

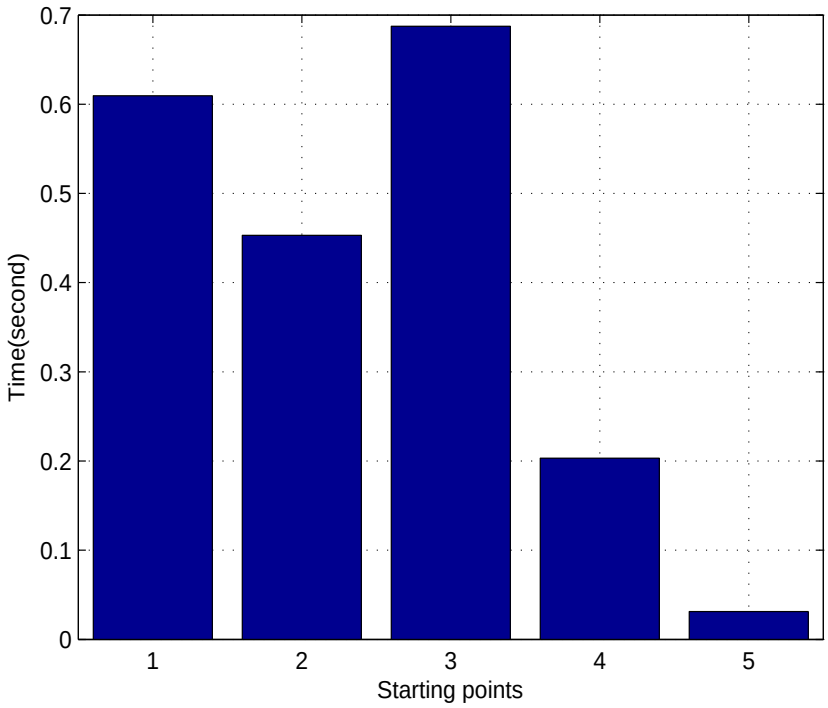

Figure 6.4: Convergence time of each starting point

6.5 Comparison with ANSYS optimisation

This section presents the comparison of optimal results from the presented framework (GA with grillage analysis) with the results from ANSYS (the finite element commercial software).

The testing problem can be stated as follows. The structure is blade stiffened plate made of steel, $E = 200\ GPa$ (see Figure 6.5). The pressure load acting on the plate is equal to 1 MPa. Its dimensions are $L = 1000\ mm,\ B = 1000\ mm$ and the thickness of

base plate = 10 mm. The stiffener is a blade stiffener having H height and T thickness which are assigned as design variables. The grillage representation of the plate has an effective width equal to its stiffener spacing.

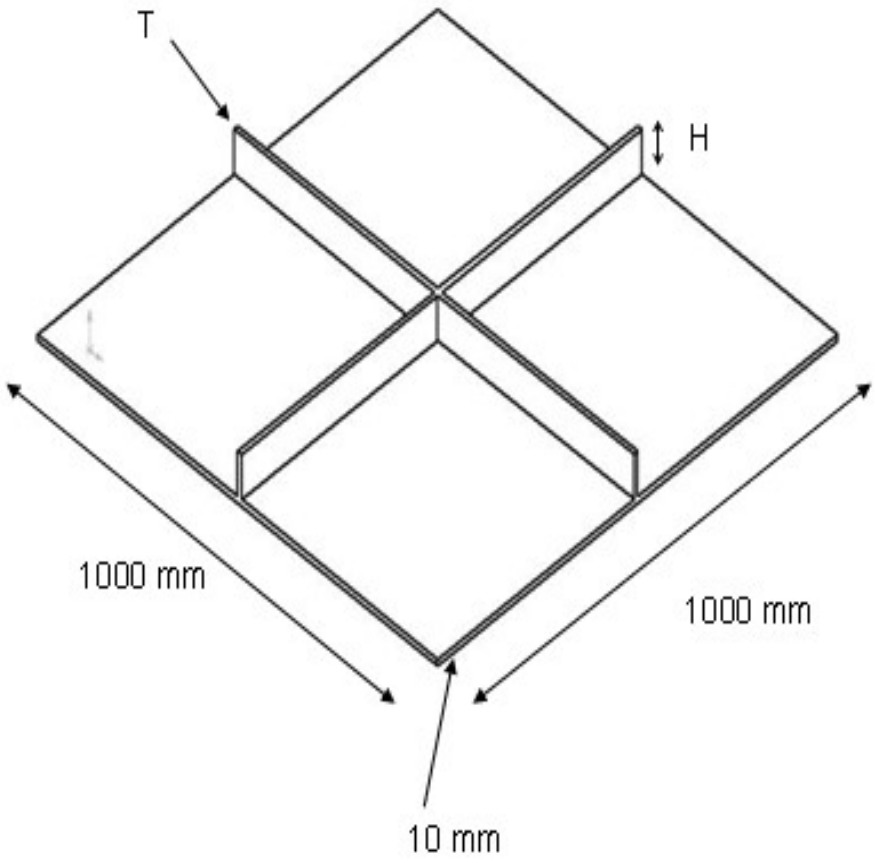

Figure 6.5: The 1×1 blade stiffened plate with its dimensions

The optimisation problem is,

Objective:	Minimise the volume of the plate
Design variables:	1 mm $<$ T $<$ 16 mm
	20 mm $<$ H $<$ 275 mm
Constraint:	0 $<$ deflection $<$ 20 mm

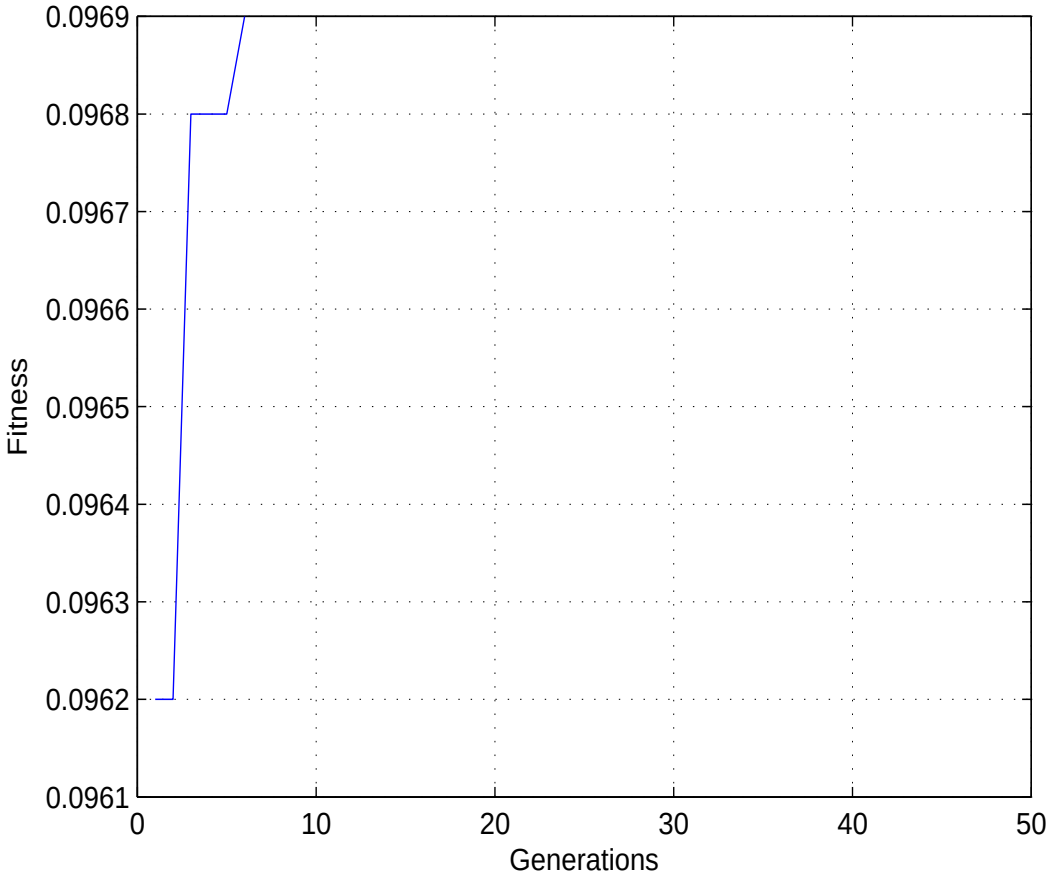

Figure 6.6: The convergence of GA run for 1×1 grillage

The GA used in this problem has chromosome length = 12 bits (8 bits for H and 4 bits for T), population size = 100, crossover probability = 0.8 and mutation probability = 0.1. The GA operators are tournament selection and single point crossover. For this problem, the convergence of GA is presented in Figure 6.6.

Within the ANSYS analysis, the plate with exactly the same shape as the plate in Figure 6.5 (without grillage assumption) is modelled by shell63, 4 node element having six degrees of freedom at each node. The first-order solution method is selected as the optimisation tool. The iteration history of this problem can be seen in Figure 6.7.

The comparison of results from both methods is presented in Table 6.8. It can be concluded that the GA with Grillage analysis provides a volume higher than that of ANSYS, by 0.1164 %. However results can be obtained from the GA with grillage anlysis 376 times quicker than from ANSYS.

Table 6.8: The optimal results of 1×1 blade stiffened plate

	GA with grillage analysis	ANSYS
Stiffener height (H) (mm)	159.0	153.25
Stiffener thickness (T) (mm)	1.0	1.0
Volume (mm^3)	10,318,000	10,306,000
Deflection (mm)	19.89	19.02
Time ($second$)	0.7587	285

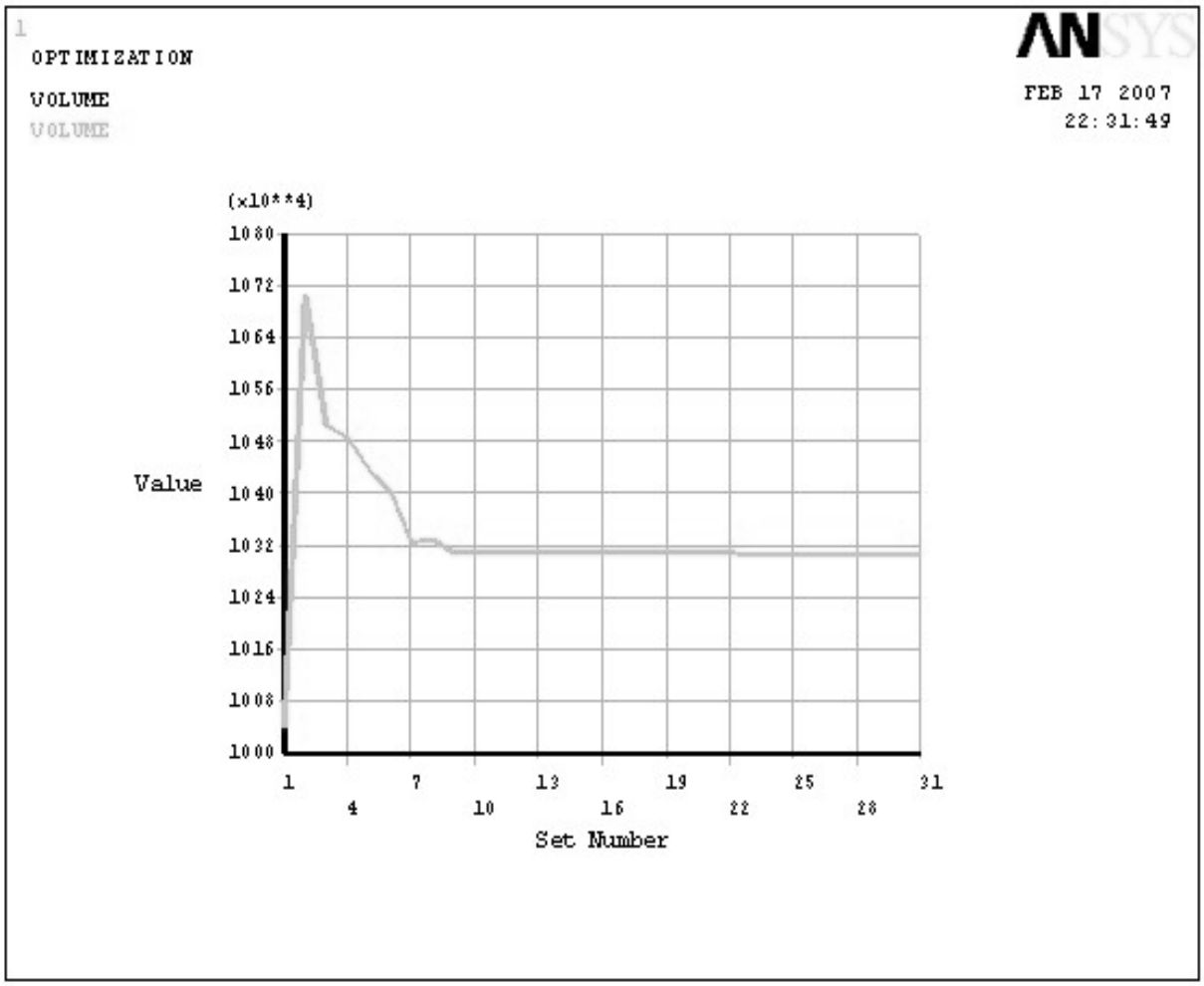

Figure 6.7: The iteration history of ANSYS optimisation

Chapter 7

Applications to stiffened plates

7.1 Introduction

For the next two chapters, the present optimization framework is applied to composite ship structures. Since in the ship structural design process, stiffened plates are considered as the secondary structure and the unstiffened plates are tertiary structures, this chapter is concerned with the design of unidirectional and cross stiffened plates (For the definitions of the parameters of these plate types, see Figure 5.1). All edges of those plates are subjected to a simply supported condition. The pressure load acting on the plates is equal to 0.05 MPa.

For all applications, a symmetric laminate was used. The resin is Epoxy and fibre volume fraction (V_f) is fixed to 0.6. The foam core is Airex ©C70.90 having $E = 84\ MPa, v = 0.32$ and density is 100 kg/m^3. Design variables for the laminate scheme are as follows:

- Number of plies (n) could be 2, 4, 6 or 8.
- Lamina fibre angle (θ) could be 0°, 45°, −45° or 90°. Zero angle means fibres are laid along the x-axis.
- Fibre type for each layer (f) could be E-glass (Eg), High strength carbon (HS), High Modulus carbon (HM) or Ultra High Modulus carbon (UHM). The material

properties of these fibres shown in Table 7.1.

- Areal weight (A_w) (kg/m^2) of fabric for each layer could be 0.25, 0.5, 0.8 or 1.6 for E-glass and 0.2, 0.3, 0.4 or 0.5 for all carbon.

For the stiffened plate, the web height and crown width of the girders and beams are fixed to a quarter of the girder and beam spacing. For all cases, wave numbers (m, n) are equal to one. In addition, the effective width of girders and beams are equal to their spacing since it has a little effect on the solution compared to the height of girders or beams.

Table 7.1: Material properties of a resin and fibres from Smith [105]

	Epoxy	E-glass	HS	HM	UHM
Density ρ (kg/m^3)	1200	2550	1740	2000	2180
Young's modulus E (GPa)	3.0	72	297	520	826
Poission's ratio v	0.37	0.2	-	-	-
Shear modulus G (GPa)	1.09	30	148.5	250	413
Strain failure ϵ^* (%)	5.0	3.0	1.4	0.4	0.3
Tensile strength σ_t^* (GPa)	0.085	2.4	4.1	2.1	2.2
Compressive strength σ_t^* (GPa)	0.130	-	-	-	-
Shear strength τ^* (GPa)	0.0654	-	-	-	-
Cost $(£/kg)$	3.68	1.2	60	300	4320

In considering the strength constraint, the Failure Index (FI) is derived from the maximum stress criterion which is applied to every layer in the laminate at the FI considering positions as shown in Figure 7.1 and Figure 7.2. The maximum stress criterion is selected for all applications because it is simple and suitable for problems having uncomplicated stress results. FI1,FI2 and FI12 denote the failure index in fibre direction, resin direction, and the shear mode (direction one-two), respectively. For the unidirectional stiffened laminated plates with girders only, the following three positions (US1,US2 and US3) shown in Figure 7.1 are considered.

- US1 and US3 are at centre of the plate on the crown element of the girder and on

the base plate element of the girder respectively.

- US2 is at the N.A. of the web element of the middle girder.

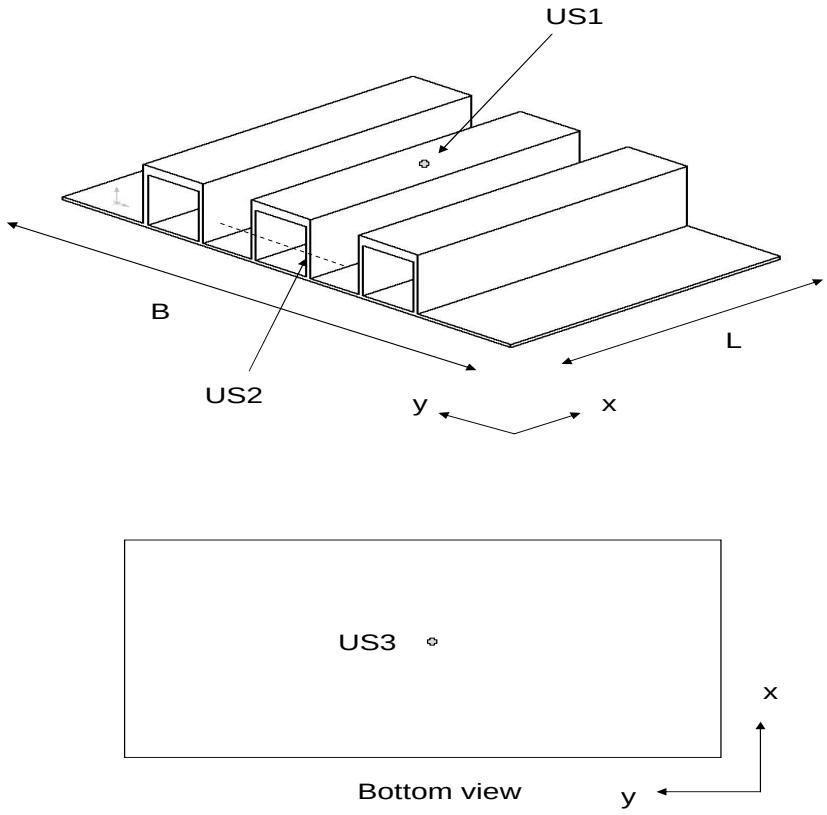

Figure 7.1: Positions at which failure index is considered for unidirectional stiffened plate

For the cross stiffened laminated plates, the following five positions (CS1,CS2,CS3,CS4 and CS5) shown in Figure 7.2 are considered.

- CS1 and CS2 are at the centre of the plate on the crown element of the girder and beam respectively.

- CS3 and CS4 are at the N.A. of the web element of the middle girder and the middle beam, respectively.

- CS5 is at the centre of the plate on the base plate element.

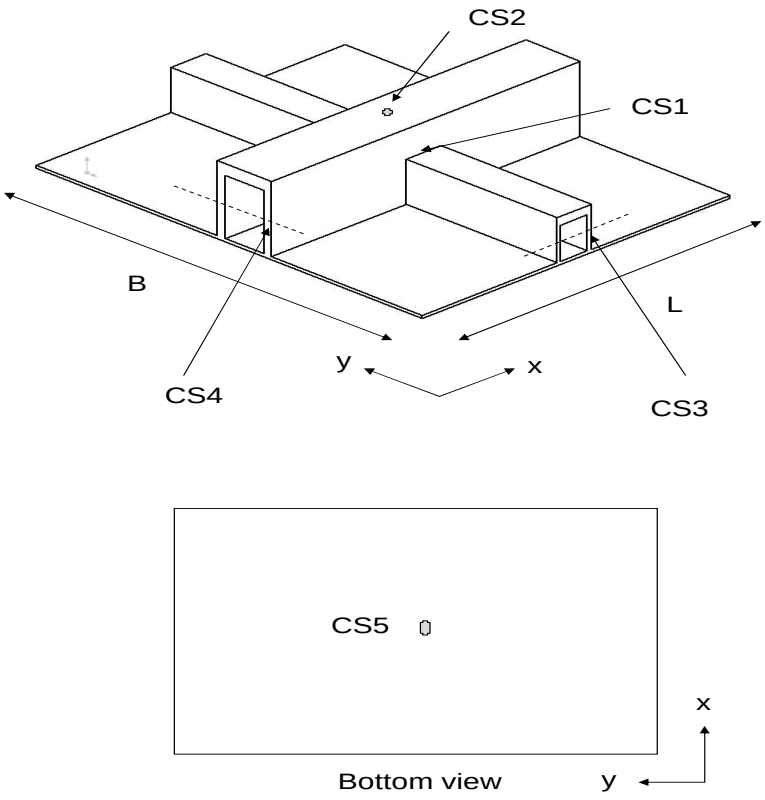

Figure 7.2: Positions at which failure index is considered for cross stiffened plate

7.2 Parametric study of grillage structures

By fixing the number of beams at five, the effect of the number of girders on the maximum deflection of the grillage, made of the same laminate through the structure, can be investigated.

The laminate information is fibre orientation ($[0_{(8)}]_T$), fibre type layup ($[UHM_{(8)}]_T$) and areal weight ($[0.5_{(8)}]_T$). This study has been done for three length to width (L/B)

ratio cases. From Figure 7.3, it can be concluded that the higher the magnitude of (L/B), the lower the effect of the number of girders on the maximum deflection.

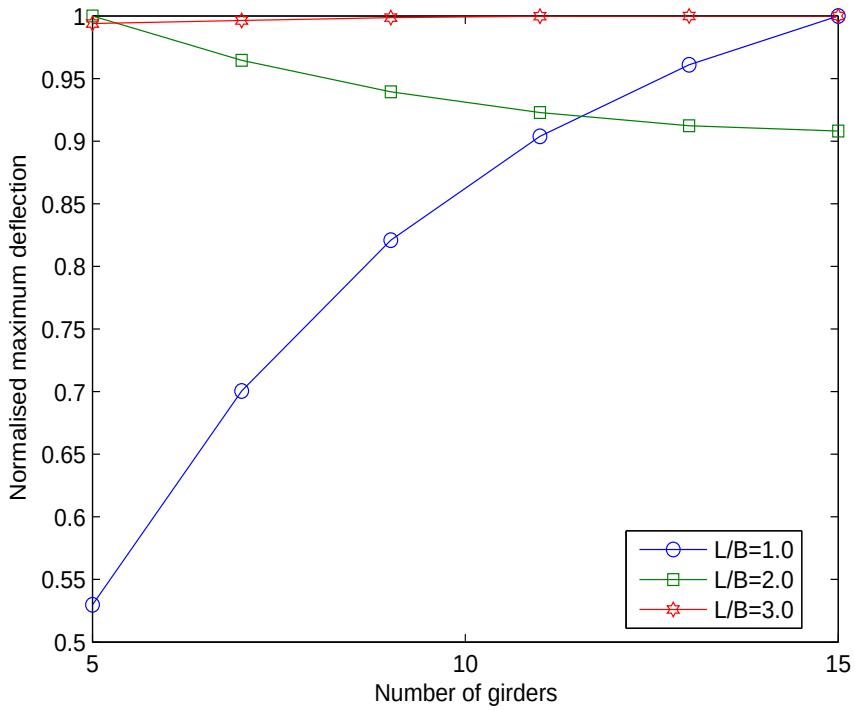

Figure 7.3: Normalised maximum deflection vs. number of girders by fixing number of beams at five for three length-to-width ratio cases

In the study of the effect of the number of girders for a length to width ratio of one, the number of beams was kept constant at five and the same laminate information was used as described above. σ_{gt} and σ_{bt} are the maximum direct stress in the crown element of the middle girder and the middle beam respectively. τ_g and τ_b are the maximum shear stress at the N.A. of the web element of the middle girder and the middle beam respectively.

From Figure 7.4, it can be concluded that the number of girders (g) has little influence on both direct-and shear-stresses on the beams. On the other hand, when g increases, those stresses in the girders are dramatically reduced.

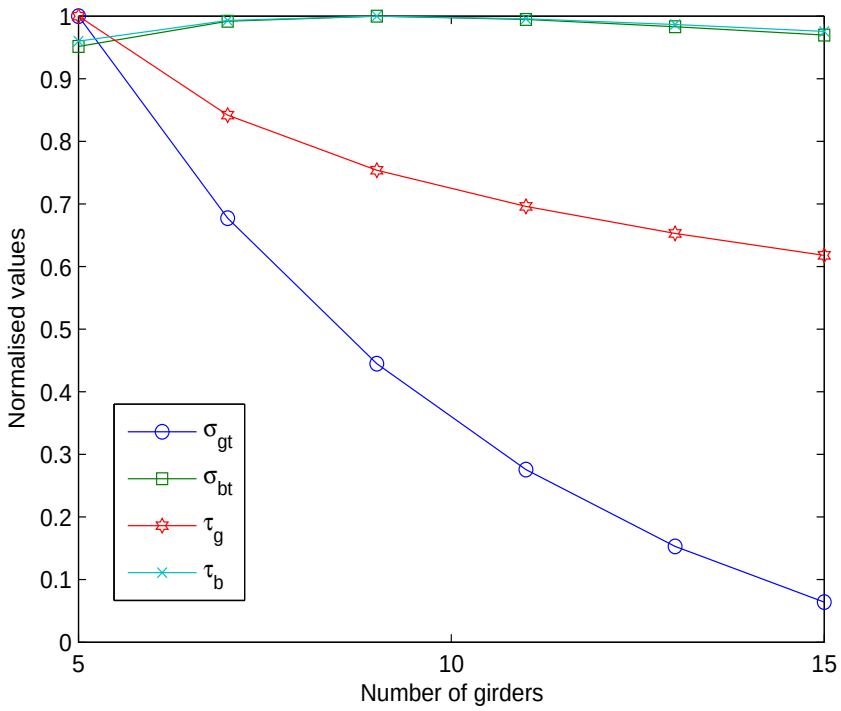

Figure 7.4: Normalised values of direct- and shear- stresses on the crown element of the middle girder and the middle beam vs. number of girders by fixed number of beams at five

To establish the strength constraints or to maximise the strength of the grillage, the maximum stress criterion (see Appendix B) is used in this work and the strength is represented by a Failure Index (FI).

In one lamina, to minimise the magnitude of FI, the stress acting on the lamina should be low, the strength properties of the lamina should be high and fibre angle should be laid properly to support the loads acting on.

To study the effect of fibre angle on the Failure Index (FI) of a lamina, for FI1 and FI2 the lamina is acted upon only by a unit direct stress in the x-axis (σ_x) and for FI12 the lamina is acted upon by a unit shear stress (τ_{xy}). Therefore, $\sigma_x = 1, \sigma_y = 1$ and

$\sigma_{xy} = 1$,. The formulations to evaluate the FI can be written as,

$$FI1 = \frac{\sigma_1}{X_t} \quad ; \quad \sigma_1 = \sigma_x(cos\theta)^2 + \sigma_y(sin\theta)^2 + \sigma_{xy}2(cos\theta sin\theta) \tag{7.1}$$

$$FI2 = \frac{\sigma_2}{Y_t} \quad ; \quad \sigma_2 = \sigma_x(sin\theta)^2 + \sigma_y(cos\theta)^2 - \sigma_{xy}2(cos\theta sin\theta) \tag{7.2}$$

$$FI12 = \frac{\sigma_{12}}{S} \quad ; \quad \sigma_1 = -\sigma_x(cos\theta sin\theta) + \sigma_y(cos\theta sin\theta) + \sigma_{xy}\{(cos\theta)^2 - (sin\theta)^2\} \tag{7.3}$$

All strength properties of the lamina are set to 1.0 which are $X_t = 1, Y_t = 1$ and $S = 1$.

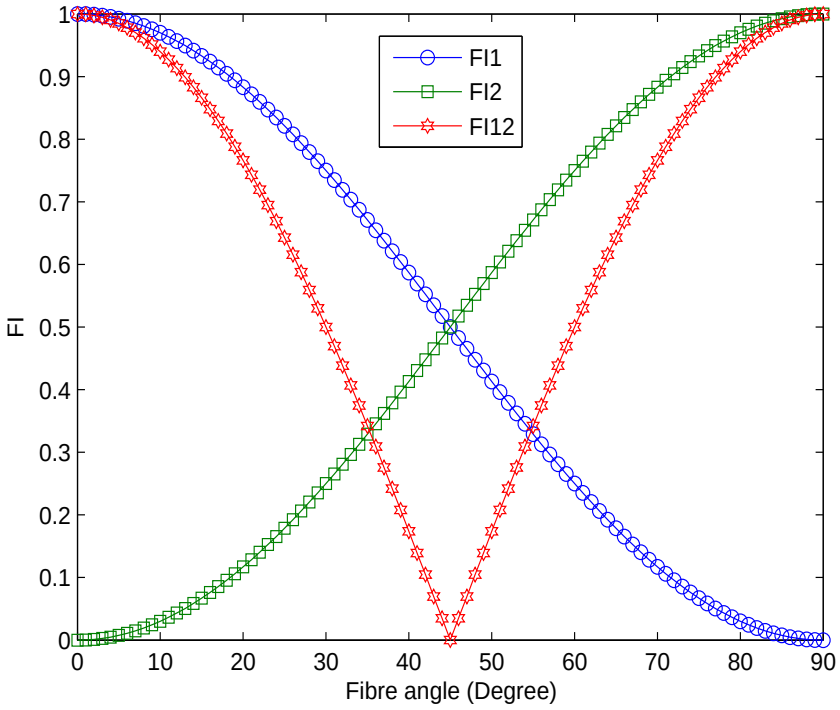

Figure 7.5: The influence of fibre angle on Failure Index (FI) from maximum stress criterion

Fibre angle of the lamina varies from 0° to 90°. Then, the plot of fibre angle against the FI is shown in the Figure 7.5 and the following points can be discussed:

- The FI1 and FI2 reach their maximum values at 0° and 90°, respectively. In a real situation, the strength in the transverse fibre direction is quite low compared to that in the fibre direction. Then if $Y_t < X_t$, FI2 at 90° is higher than FI1 at 0° so that for the lamina subjected to only σ_x, fibre is conveniently laid along the x-direction

to resist the stress.

- For lamina subjected to only shear stress, FI12 reaches the maximum value at 0° and at 90° and its minimum value is obtained at 45°. Hence, to resist the shear stress, the 45° fibre angle is required.

7.3 Unidirectional stiffened plate

7.3.1 Maximise stiffness

For this section, the dimension of the unidirectional tophat stiffened plate subjected to simply supported conditions around its edges is $L = 1000\ mm$ and $B = 4500\ mm$. All symbols representing the plate dimensions are the same as in Figure 5.1. The girders having tophat geometry are laid along the shortest side. Girder spacing (mm) is allowed to be either 281.25, 375, 450 or 750.

Objective:	Minimise deflection at $(x = L/2, y = B/2)$
Design variables:	Girder spacing,
(independent)	θ, f, A_w of lamina for every case
Constraint:	Every structural element has the same layup

The optimal results of the design case of maximising plate stiffness are shown in Table 7.2. It can be seen that the girder spacing takes the highest value and fibres are aligned along the girder direction (along shortest side of the plate). All selected fibres are Ultra High Modulus carbon (UHM) with its maximum areal weight. This maximises the flexural rigidity which provides the lowest central deflection because the deflection is a function of flexural rigidity.

Table 7.2: Minimisation of the central deflection for the unidirectional stiffened laminated plate

Girder spacing (mm)	750
Fibre angle	[0/0/0/0]s
Fibre type	[UHM/UHM/UHM/UHM]s
A_w (kg/m^2)	[0.5/0.5/0.5/0.5]s
δ_{max} (mm)	0.0358

7.3.2 Maximise strength

Objective: There are 3 cases

(1) Minimise FI at position-US1

(2) Minimise FI at position-US2

(3) Minimise FI at position-US3

Design variables: Girder spacing, θ, f, A_w of lamina for every case

Constraint: Every structural element has the same layup for every case

Table 7.3: Minimisation of Failure Index (FI) at three positions on the unidirectional stiffened laminated plate

	Minimise FI at		
	US1	US2	US3
Girder spacing (mm)	750.0	281.25	750.0
Fibre angle	[0/0/0/0]s	[-45/45/45/45]s	[0/0/0/0]s
Fibre type	[Eg/Eg/Eg/Eg]s	[Eg/Eg/Eg/Eg]s	[Eg/Eg/Eg/Eg]s
A_w (kg/m^2)	[1.6/1.6/1.6/1.6]s	[1.6/1.6/1.6/1.6]s	[1.6/1.6/1.6/1.6]s
FI-US1	0.0053	0.1994	0.0053
FI-US2	0.0173	0.0104	0.0173
FI-US3	0.0043	0.1323	0.0043

For the case of maximising plate strength, the optimum results and GA convergence are shown in Table 7.3 and Figure 7.6 respectively. The discussion of those results are as follows. Fibre angle is controlled by the direction of stress. For example, minimising failure index (FI) at the crown and base plate element, the fibre angle is laid along girder

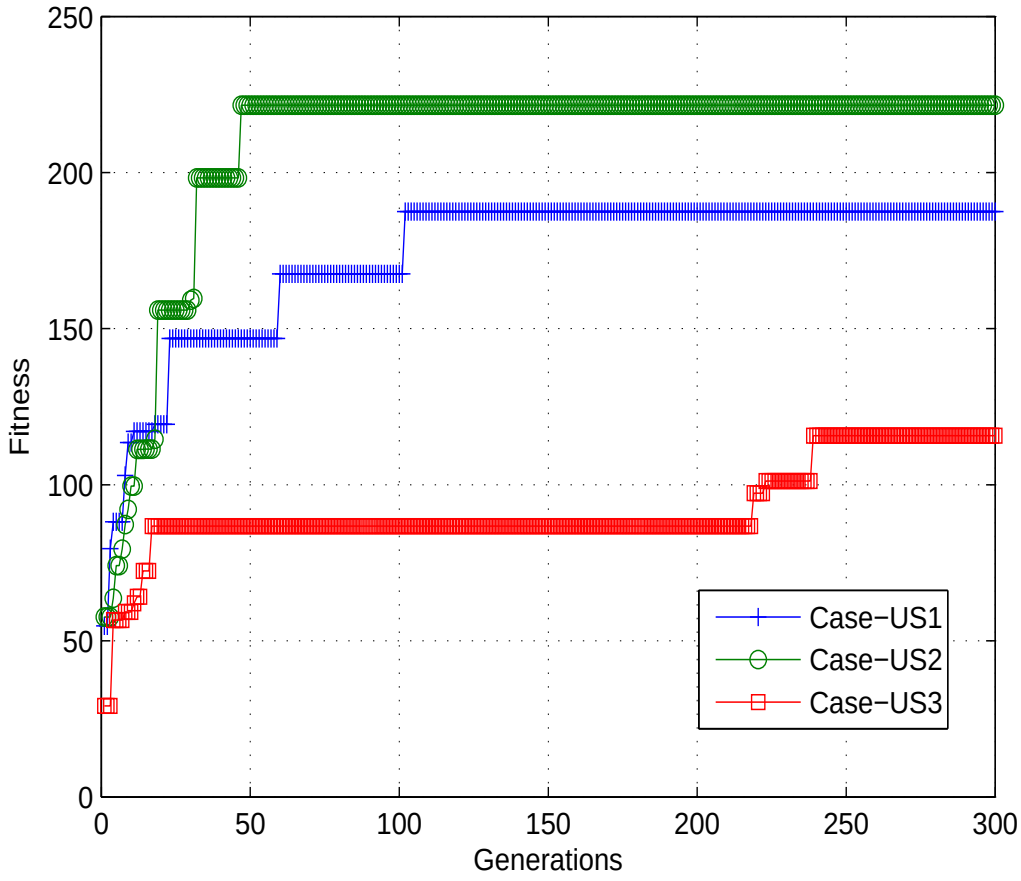

Figure 7.6: Convergence of GA run for maximisation of strength: unidirectional stiffened plates

direction. Maximising strength at webs, fibre angle is 45 or -45 degree. All selected fibres are E-glass with its highest areal weight because this gives high thickness leading to high flexural rigidity and the lower Young's modulus, therefore lower stress is expected and in fact obtained (see Table 7.3) To increase the second moment of area, girder spacing is the upper bond value except the case of maximising strength at web, where it is at the lower bound value because the shorter the web, the lower the shear stress results.

7.3.3 Weight minimisation

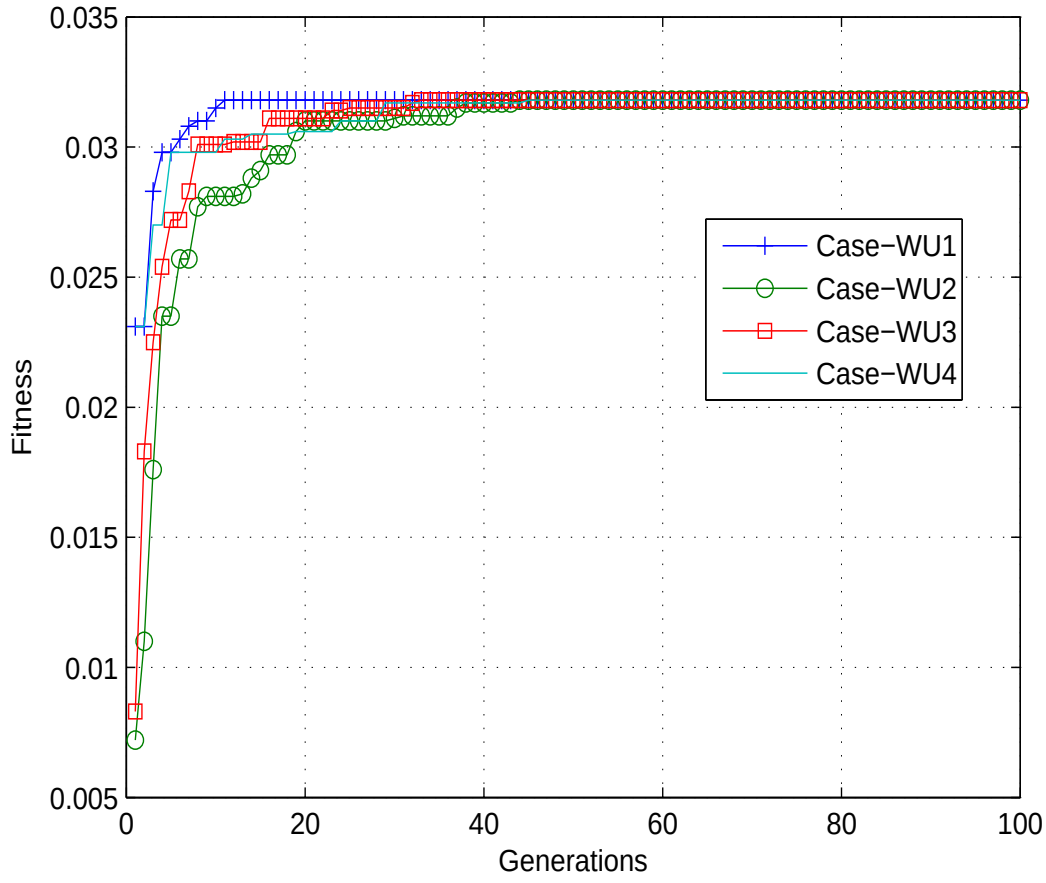

Figure 7.7: Convergence of GA run for weight minimisation: unidirectional stiffened plates

Objective:	Minimise weight of plate with 4 different cases (different set of constraints)	
Design variables:	Girder spacing, θ, f, A_w of base plate, web and crown element	
(independent)	for every case	
Constraints:	(1) Case-WU1:	$\delta_{max} < \infty\ mm, \quad FI_{max} < \infty$
	(2) Case-WU2:	$\delta_{max} < 10\ mm, \quad FI_{max} < 1.0$
	(3) Case-WU3:	$\delta_{max} < 10\ mm, \quad FI_{max} < 0.1$
	(4) Case-WU4:	$\delta_{max} < 1.0\ mm, \quad FI_{max} < 0.1$
Note:	The symbol ,<, means the optimum solutions must provide	
	δ_{max} and FI_{max} less than the given limit	

The case of weight minimisation under the stiffness and strength constraint gives the results shown in Table 7.4, their GA convergence shown in Figure 7.7 and their discussions are as follows. To reduce the weight, the GA has selected unsurprisingly carbon fibre. Fibre angle of zero degree (along girder direction) help the plate to satisfy the stiffness constraint. Although the high strength carbon (HS) has the lowest density, the UHM is selected because the UHM provide the lower thickness. However, HS appear at the crown element when the strength constraint is tightened. In Case-WU3, although the FI-limit is reduced to 10% of Case-WU2 to 0.1, there is much less effect on minimum weight (increase from that of the Case-WU1, 0.11%). Both Case-WU4 and Case-WU3 give the same optimum result. Therefore, reduction of deflection limit has no effect for this application.

Table 7.4: Weight minimisation of unidirectional stiffened laminated plate subjected to stiffness and strength constraints

		Case-WU1	Case-WU2	Case-WU3	Case-WU4
Constraints	$\delta_{max}(mm) <$	∞	10.0	10.0	1.0
	$FI_{max} <$	∞	1.0	0.1	0.1
Girder spacing (mm)		750.0	750.0	750.0	750.0
Base plate	Fibre angle	[-45]s	[0]s	[0]s	[0]s
	Fibre types	[UHM]s	[UHM]s	[UHM]s	[UHM]s
	A_w (kg/m^2)	[0.2]s	[0.2]s	[0.2]s	[0.2]s
Web	Fibre angle	[45]s	[90]s	[90]s	[90]s
	Fibre types	[UHM]s	[UHM]s	[UHM]s	[UHM]s
	A_w (kg/m^2)	[0.2]s	[0.2]s	[0.2]s	[0.2]s
Crown	Fibre angle	[45]s	[0]s	[0]s	[0]s
	Fibre types	[UHM]s	[UHM]s	[HS]s	[HS]s
	A_w (kg/m^2)	[0.2]s	[0.2]s	[0.2]s	[0.2]s
Weight (kg)		31.4187	31.4187	31.4535	31.4535
δ_{max} (mm)		8.8657	1.6547	0.7212	0.7212
FI-US1		1.19808	0.2236	0.0468	0.0468
FI-US2		0.2558	0.0023	0.0345	0.0345
FI-US3		1.1865	0.0166	0.0780	0.0780

7.4 Tophat cross stiffened plate

7.4.1 Maximise stiffness

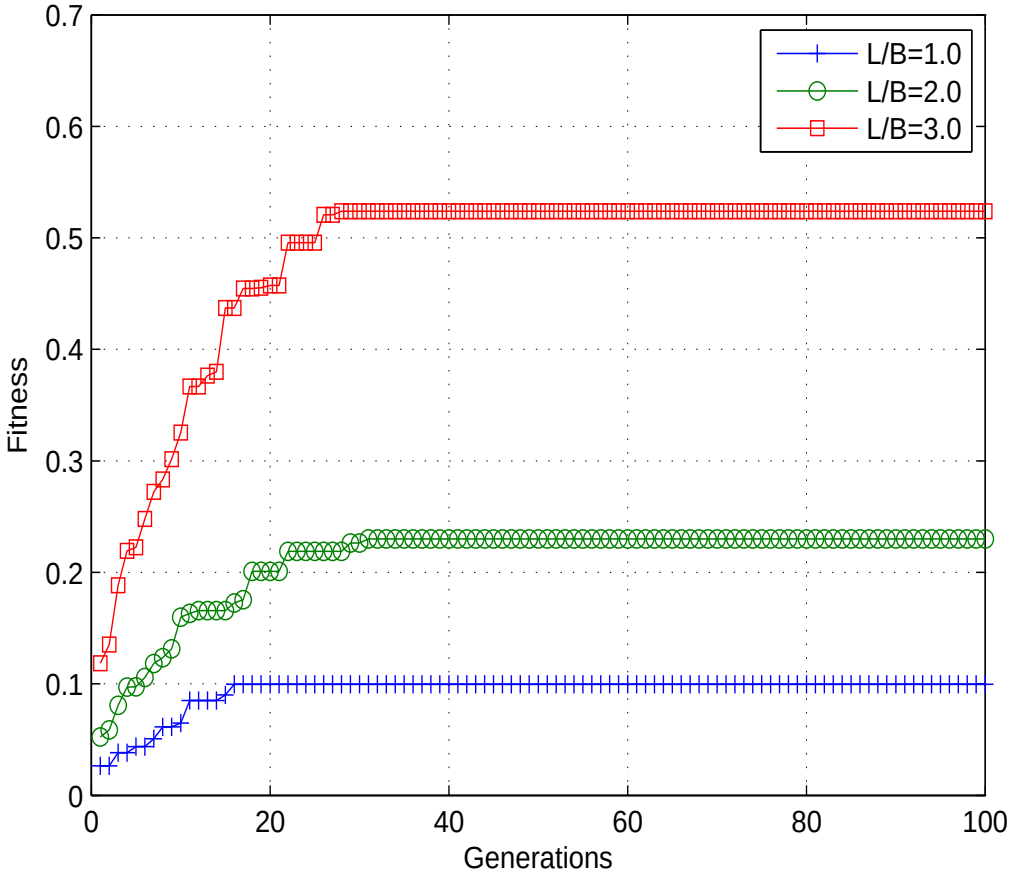

Figure 7.8: Convergence of GA run for maximisation of stiffness: cross stiffened plates

Objective: Minimise deflection at $(L/2, B/2)$

there are three cases

(1) $L/B = 1.0, \quad B = 4500\ mm$

(2) $L/B = 2.0, \quad B = 4500\ mm$

(3) $L/B = 3.0, \quad B = 4500\ mm$

All symbols representing the plate dimensions are the same as in Figure 5.1

Design variables: Girder spacing, beam spacing, θ, f, A_w of lamina for every case

Girder spacing: For all cases, 281.25, 375, 450, 750

Beam spacing: For individual case,

(range in mm) (1) 281.25, 375, 450, 750

(2) 562.25, 750, 900, 1500

(3) 843.75, 1125, 1350, 2250

Constraint: Every structural element has the same layup for every case

Note: All symbols representing the plate dimensions are the same as in Figure 5.1

The optimal results of the design case of maximising plate stiffness are shown in Table 7.5 and their GA convergence is shown in Figure 7.8. Optimum results of this design case are similar to those of the unidirectional stiffened plates. The following notices can be obtained. To maximise the stiffness, Ultra High Modulus carbon (UHM) is selected because of its highest Young modulus. The areal weight of UHM is at its highest value because it provides the highest thickness. Beam spacing is always wider than girder spacing except for the square plate. In this instance, both girder and beam spacing are the upper-bound value because the larger girder or beam, the higher the the second moment of area. By setting all elements to the same layup scheme, fibre angle is all zero degree (lay along stiffener's direction).

Table 7.5: Minimisation of central deflection of cross stiffened laminated plate

	$(L/B) = 1.0$	$(L/B) = 2.0$	$(L/B) = 3.0$
Girder spacing (mm)	750.0	281.25	750.0
Beam spacing (mm)	750.0	1500.0	2250.0
Fibre angle	[0/0/0/0]s	[0/0/0/0]s	[0/0/0/0]s
Fibre type	[UHM/UHM/UHM/UHM]s	[UHM/UHM/UHM/UHM]s	[UHM/UHM/UHM/UHM]s
A_w (kg/m^3)	[0.5/0.5/0.5/0.5]s	[0.5/0.5/0.5/0.5]s	[0.5/0.5/0.5/0.5]s
δ_{max} (mm)	10.0292	4.3475	1.9091

7.4.2 Maximise strength

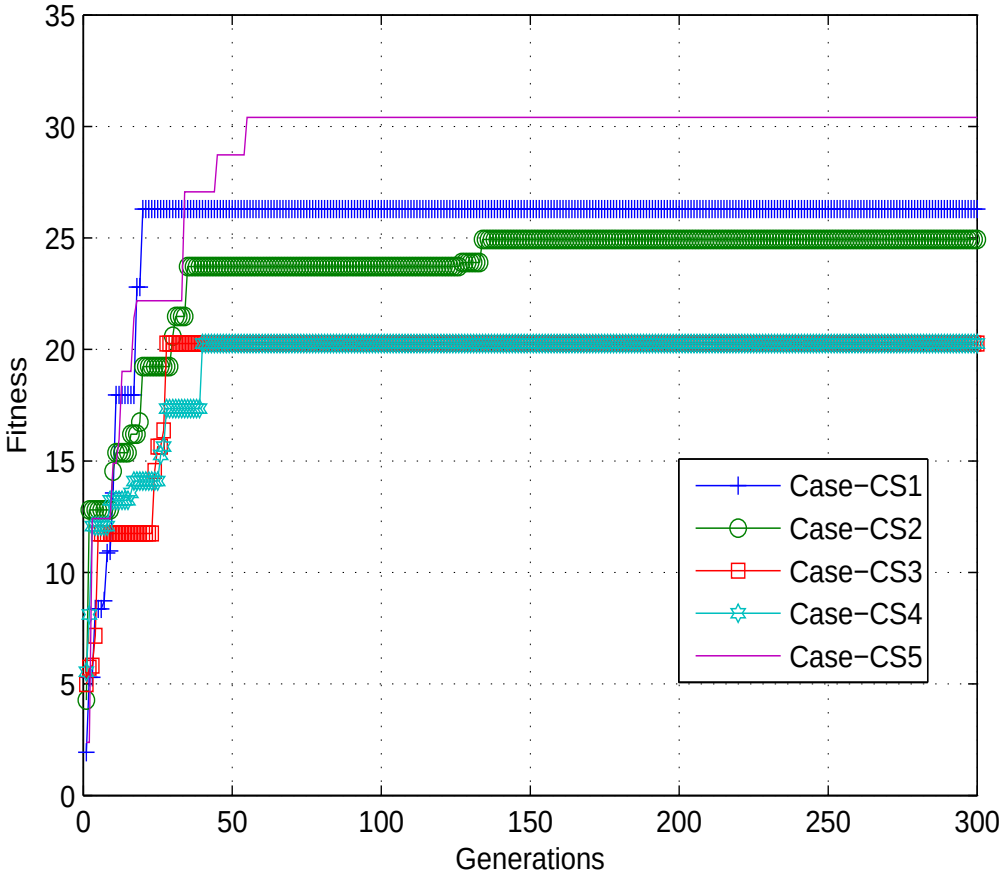

Figure 7.9: Convergence of GA run for maximisation of strength: cross stiffened plates

Plate dimension: $L = 4500\ mm$, $B = 4500\ mm$, all symbols representing plate dimensions are the same as in Figure 5.1

Objective: There are 5 cases

(1) Minimise FI at position-CS1

(2) Minimise FI at position-CS2

(3) Minimise FI at position-CS3

(4) Minimise FI at position-CS4

(5) Minimise FI at position-CS5

Design variables (independent): Girder spacing, beam spacing,
θ, f, A_w of lamina for every case

Girder spacing (range in mm) : For all cases, 281.25,375,450,750

Beam spacing (range in mm) : For all cases, 281.25,375,450,750

Constraint: Every structural element has the same layup for every case

Table 7.6: Minimisation of Failure Index (FI) at five positions on the cross stiffened laminated plate

	Minimise FI at				
	CS1	CS2	CS3	CS4	CS5
Girder spacing (mm)	281.25	750.0	281.25	750.0	281.25
Beam spacing (mm)	750.0	281.25	750.0	281.25	750.0
Fibre angle	$[90_{(8)}]_T$	$[0_{(8)}]_T$	$[-45_{(8)}]_T$	$[-45_{(8)}]_T$	$[90_{(8)}]_T$
Fibre type	$[UHM_{(8)}]_T$	$[HS_{(8)}]_T$	$[Eg_{(8)}]_T$	$[Eg_{(8)}]_T$	$[UHM_{(8)}]_T$
A_w (kg/m^2)	$[0.5_{(8)}]_T$	$[0.5_{(8)}]_T$	$[1.6_{(8)}]_T$	$[1.6_{(8)}]_T$	$[0.5_{(8)}]_T$
FI-CS1	0.0380	0.1234	0.5122	1.3409	0.0380
FI-CS2	0.7348	0.0401	1.3409	0.5122	0.7348
FI-CS3	0.1421	0.6373	0.0493	0.1498	0.1421
FI-CS4	0.1115	0.2395	0.1498	0.0493	0.1115
FI-CS5	0.0329	0.7057	0.7464	0.7464	0.0329

For the case of maximising plate strength, the optimum results and GA convergence are shown in Table 7.6 and Figure 7.9 respectively. From those results, it can be noticed that if the FI at girder is minimised, the girder spacing is the lower bound value. On the other hand, if the FI at beam is minimised, the beam spacing is the lower bound value. Again, 45° fibre angle is used to resist the shear stress on the web of girders and beams. To reduce the magnitude of shear stress, the webs of girder or beam must be shorter.

7.4.3 Weight minimisation

Plate dimension is $L = 6096\ mm$, $B = 2540\ mm$, all symbols representing the plate dimensions are the same as in Figure 5.1

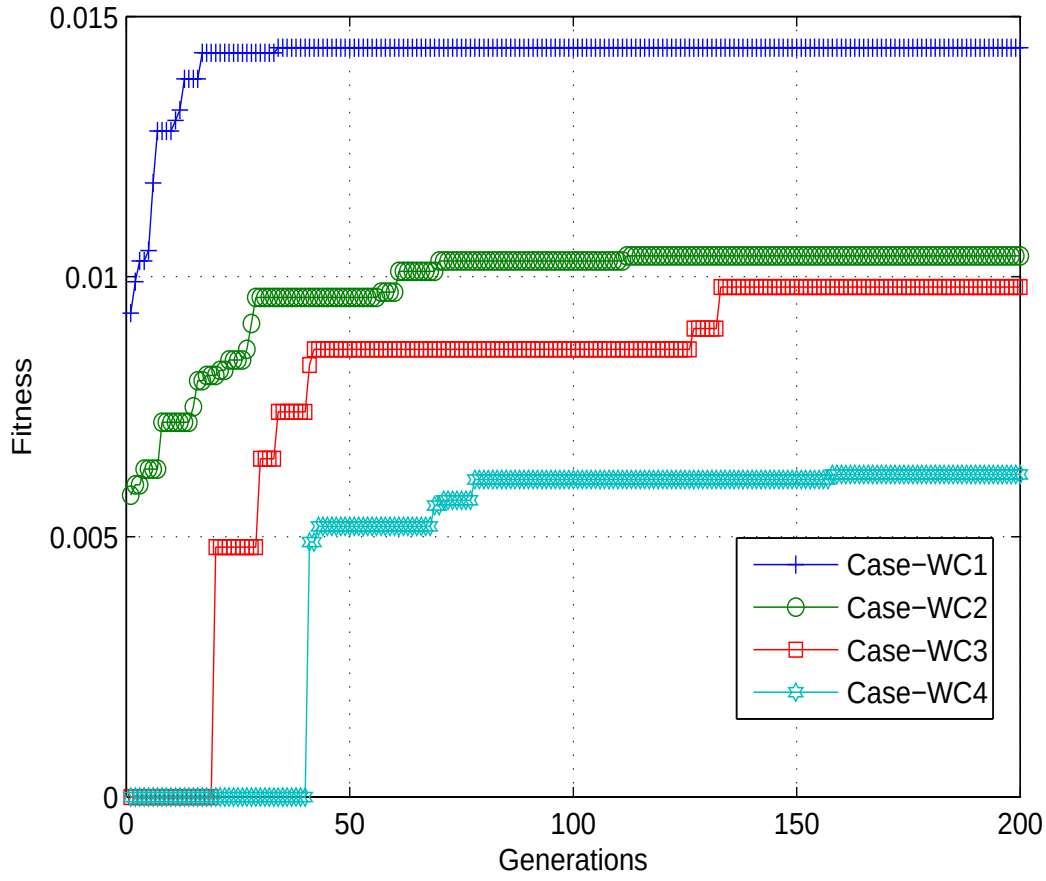

Figure 7.10: Convergence of GA run for weight minimisation: cross stiffened plates

Objective: Minimise weight of plate with 4 different cases (different set of constraints)

Design variables (independent): Girder spacing, beam spacing
θ, f, A_w of lamina of base plate,web and crown element of girder and beam for every case

Girder spacing (range in mm) : For every case, 158.75, 211.67, 254, 423.33

Beam spacing (range in mm) : For every case, 381.0, 508, 609.6, 1016

Constraints: (1) Case-WC1: $\delta_{max} < \infty \; mm \quad FI_{max} < \infty$
(2) Case-WC2: $\delta_{max} < 10 \; mm \quad FI_{max} < 1.0$
(3) Case-WC3: $\delta_{max} < 10 \; mm \quad FI_{max} < 0.1$
(4) Case-WC4: $\delta_{max} < 1.0 \; mm \quad FI_{max} < 0.1$

Note: The symbol ,<, means the optimum solutions must provide δ_{max} and FI_{max} less than the given limit

The GA convergence of this case can be seen in Figure 7.10. From the optimum results presented in Table 7.7 and with consideration of the discussion in section 7.3.3, the following points can be drawn out.

- For Case-WC1, every element contains only the light fibre (UHM) and there are only two layers (lower-bound value of number of layers) for each laminate element.
- With constraints in Case-WC2, the minimum weight increases by 38.32% from Case-WC1 where the limitation of deflection and FI are infinity. The maximum deflection is forced by the constraints to change from 1707.42 mm to 24.96 mm (reduced by 98.54%).
- The stiffness constraint has more influence on the minimum weight than the strength constraint because, when the FI limit is reduced to 10% of Case-WC2, the minimum weight increases by 6.62% from Case-WC2 and when the maximum deflection limit is reduced to 10% of Case-WC3. Keeping FI limit the same as in Case-WC3, the minimum weight increases by 66.82%.

Table 7.7: Weight minimisation of cross stiffened laminated plate under stiffness and strength constraints

		Case-WC1	Case-WC2	Case-WC3	Case-WC4
Constraints	$\delta_{max}(mm) <$	∞	25.40	25.40	2.54
	$FI_{max} <$	∞	1.0	0.1	0.1
Girder spacing (mm)		158.75	158.75	158.75	158.75
Beam spacing (mm)		381.00	609.60	508.00	1016.00
Base plate	Fibre angle	[0]s	[90]s	[90]s	[90]s
	Fibre types	[UHM]s	[UHM]s	[UHM]s	[UHM]s
	A_w (kg/m^2)	[0.2]s	[0.2]s	[0.2]s	[0.2]s
Web of girders	Fibre angle	[0]s	[0]s	[90]s	[90]s
	Fibre types	[UHM]s	[UHM]s	[UHM]s	[UHM]s
	A_w (kg/m^2)	[0.2]s	[0.2]s	[0.2]s	[0.2]s
Crown of girders	Fibre angle	[0]s	[90]s	[90]s	[0]s
	Fibre types	[UHM]s	[HM]s	[UHM]s	[HM]s
	A_w (kg/m^2)	[0.2]s	[0.2]s	[0.2]s	[0.4]s
Web of beams	Fibre angle	[45]s	[90]s	[-45]s	[-45]s
	Fibre types	[UHM]s	[HM]s	[UHM]s	[HS]s
	A_w (kg/m^2)	[0.2]s	[0.2]s	[0.2]s	[0.2]s
Crown of beams	Fibre angle	[-45]s	[45/-45/45]s	[0/0/0]s	[-45/-45/-45/45]s
	Fibre types	[UHM]s	[UHM/HS/HS]s	[Eg/HS/Eg]s	[Eg/HS/Eg/Eg]s
	A_w (kg/m^2)	[0.2]s	[0.2/0.3/0.5]s	[0.8/0.2/1.6]s	[1.6/0.3/1.6/1.6]s
Weight (kg)		69.34	95.91	102.21	160
δ_{max} (mm)		1707.42	24.96	18.42	2.48
FI-CS1		3.1130	0.0298	0.0223	0.0034
FI-CS2		18.8227	0.4219	0.0824	0.0571
FI-CS3		1.2466	0.0063	0.0004	0.0008
FI-CS4		2.5404	0.1191	0.0883	0.0146
FI-CS5		18.5840	0.0314	0.0726	0.0368

Chapter 8

Applications to unstiffened plates

8.1 Introduction

In the previous chapter, the optimisation has been performed for tophat stiffened plates represented by a grillage without stability constraints. In a design process, we need to consider the plate between the stiffeners as well. As one important design criterion in composite ship design is buckling, in this chapter the optimal results are studied through applying buckling resistance as the design objective for a single skin laminated plate. In addition, the stiffness of the plate is also one of the case studies since the stiffness is one of the main problems of composite structures. It is noted that the following application examples use the same definition of design variables as in the Chapter 7 except fibre angle (θ) could be 0° or 90° only.

8.2 Parametric study

The laminate plates used for this study are simply supported around the edges and have dimensions, $L = 1000\ mm$ and $B = 400\ mm$. The pressure acting on the plate when considering the maximum deflection (δ_{max}) was $0.05\ N/mm^2$. The laminate information is fibre orientation ($[90_{(8)}]_T$), fibre type layup ($[Eg_{(8)}]_T$) and areal weight of $[0.25_{(8)}]_T$. The laminate has $0.1634\ mm$ layer thickness (t_k). To study the effect of Young's modulus of

fibre (E_f) and t_k on δ_{max} and on critical buckling load N_{cr} for uniaxial compression, E_f and t_k are increased from 1.0 to 3.0 times their own reference values (E_f of E-glass and $t_k = 0.1634\ mm$). Output values of δ_{max} and N_{cr} are normalised through dividing those values by the maximum values of an individual output set.

From Figure 8.1, when the magnitude of E_f and t_k increase, the result of central deflection decrease. In addition, the layer thickness has more effect on central deflection than Young's modulus of fibre because the central deflection of a laminate plate depends on flexural rigidity which is related to t_k^3 (see Eq. 6.2).

Similar results are found for critical buckling load (N_{cr}). From Figure 8.2, the higher the values of the Young's modulus of fibre and layer thickness, the higher the values of N_{cr} that can be obtained. The thickness has much more influence on N_{cr} than the Young's modulus of fibre because $N_{cr}\ \alpha\ E_f$ and $N_{cr}\ \alpha\ t_k^2$.

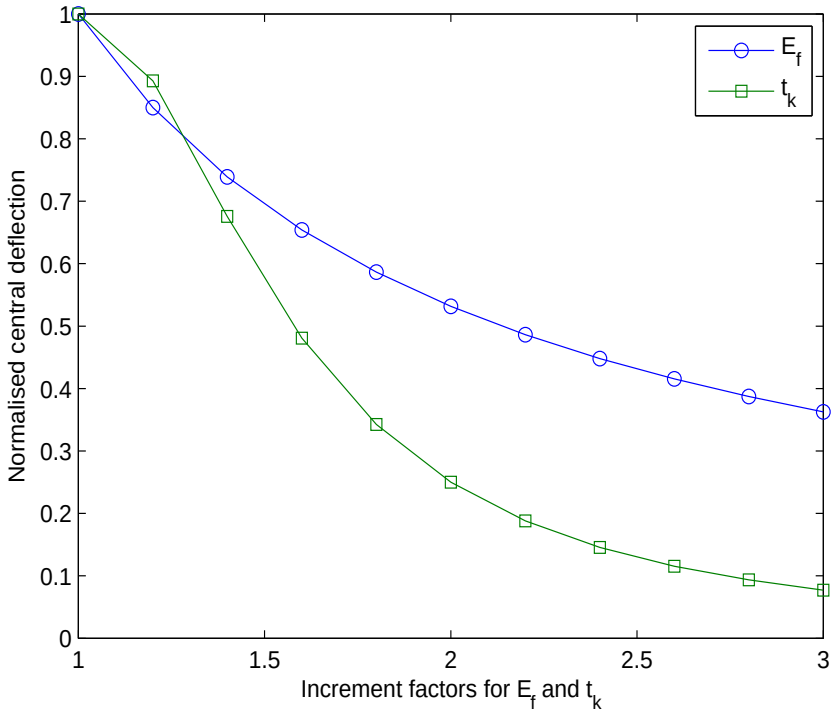

Figure 8.1: The effect of Young's modulus of fibre and layer thickness on central deflection

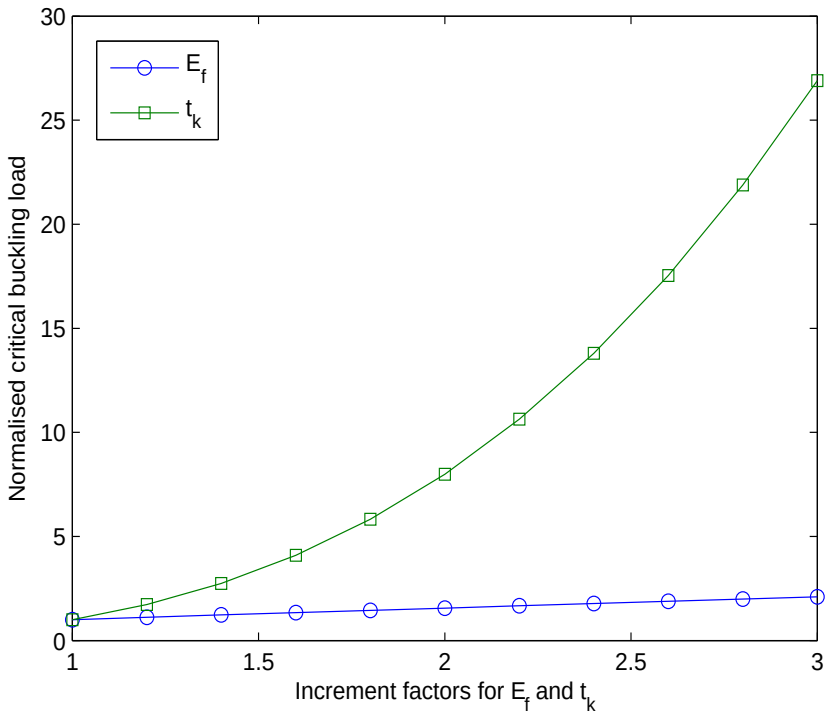

Figure 8.2: The effect of Young's modulus of fibre and layer thickness on critical uniaxial compressive buckling load

8.3 Laminated plate

8.3.1 Maximise stiffness

This section is to present the maximisation of plate stiffness which is represented by the magnitude of the central deflection and to study the optimal results when the number of design variables increase. Plate dimension in reference to Figure 5.3 is $L = 1000\ mm$ and $B = 400\ mm$. The optimisation is performed in the following three cases.

- Case-MD1: design variable is fibre angle in each lamina. Fibre type and its Areal weight (Aw) are fixed to E-glass and 0.5 kg/m^2, respectively.
- Case-MD2: design variables are fibre angle and fibre type in each lamina. Aw is fixed to 0.5 kg/m^2.
- Case-MD3: design variables are fibre angle, fibre type and Aw in each lamina.

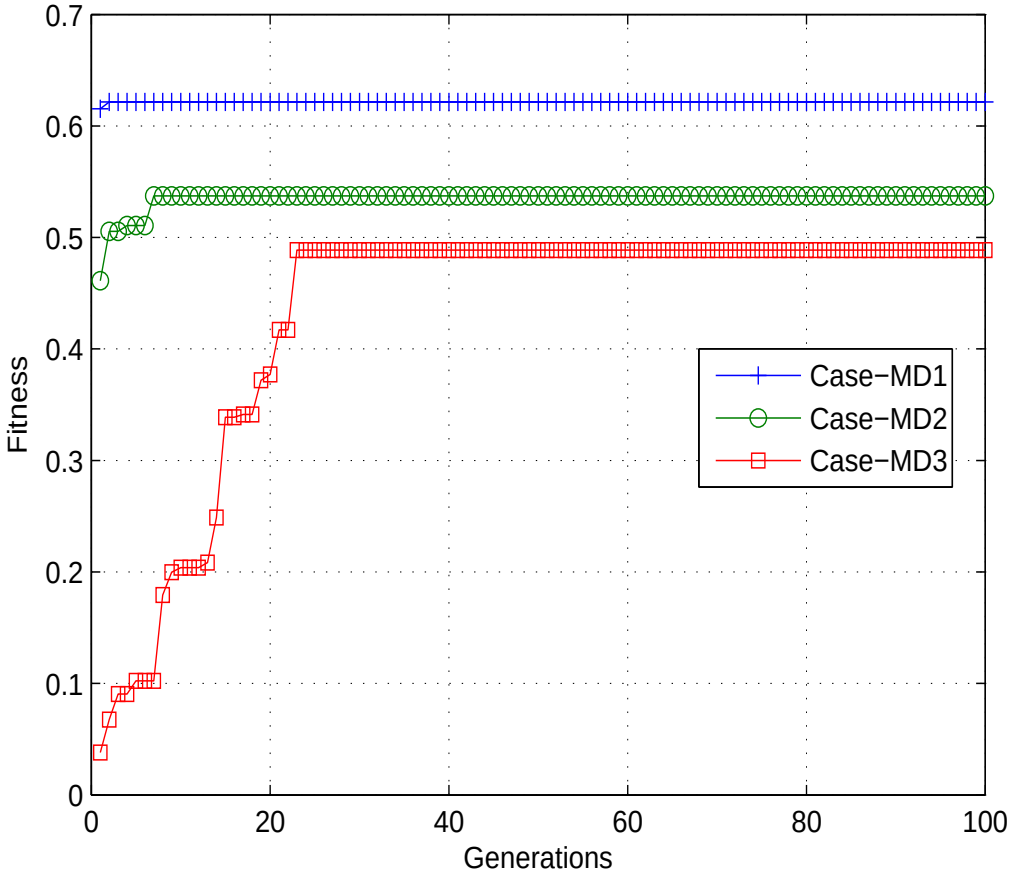

Figure 8.3: Convergence of GA run for maximisation of stiffness: laminated plate

The GA convergence of these optimisations are in Figure 8.3. From Table 8.1, the following points can be made:

- 90° fibre angle (laying along the shortest side of the plate) leads to the minimum result of central deflection because for the rectangular plate, the fibre along its shortest side tends to resist the uniform pressure load.
- When choice of fibre type is assigned as a design variable, fibres having high Young's modulus appear as the optimum result. Especially, for the case-MD2 where Aw is fixed, only carbon is selected for.
- For the case-MD3, the optimum is obtained when Aw is maximised because this gives the highest layer thickness.

- In the case-MD1, the deflection is very high because the plate is very thin and subjected to a high pressure load. After fibre type or/and areal weight become design variables, the deflection is dramatically reduced. This shows a large influence of each design variable on the plate stiffness.

Table 8.1: Minimisation of central deflection for the unstiffened laminated plate

	Case-MD1	Case-MD2	Case-MD3
Fibre angle	[90/90/90/90]s	[90/90/90/90]s	[90/90/90/90]s
Fibre type	-	[UHM/UHM/HS/HM]s	[UHM/Eg/Eg/Eg]s
A_w (kg/m^2)	-	-	[0.5/1.6/1.6/1.6]s
Deflection (mm)	289.63	15.51	4.09

8.3.2 Maximise strength

The plate under simply supported condition around its edges and design cases used in this section are the same as the former section (maximise stiffness). Then, the design cases (MS1, MS2 and MS3) have the same definition as the design cases (MD1, MD2 and MD3). The objective of all cases is to minimise the value of maximum Failure Index (FI_{max}).

Table 8.2: Maximise strength of the unstiffened laminated plate

	Case-MS1	Case-MS2	Case-MS3
Fibre angle	[0/0/0/90]s	[0/0/0/0]s	[0/0/0/90]s
Fibre type	-	[UHM/HS/HS/HS]s	[Eg/Eg/Eg/Eg]s
A_w (kg/m^2)	-	-	[1.6/1.6/1.6/1.6]s
FI_{max}	7.25	2.97	0.71

The optimal results are given in Table 8.2 and their GA convergence in Figure 8.4. The discussion of those results is as follows.

- Each design variable has a large influence on the strength of the plate: FI_{max} of case MS2 and MS3 reduced from that of case MS1 by 59.03 % and 90.21 % respectively.

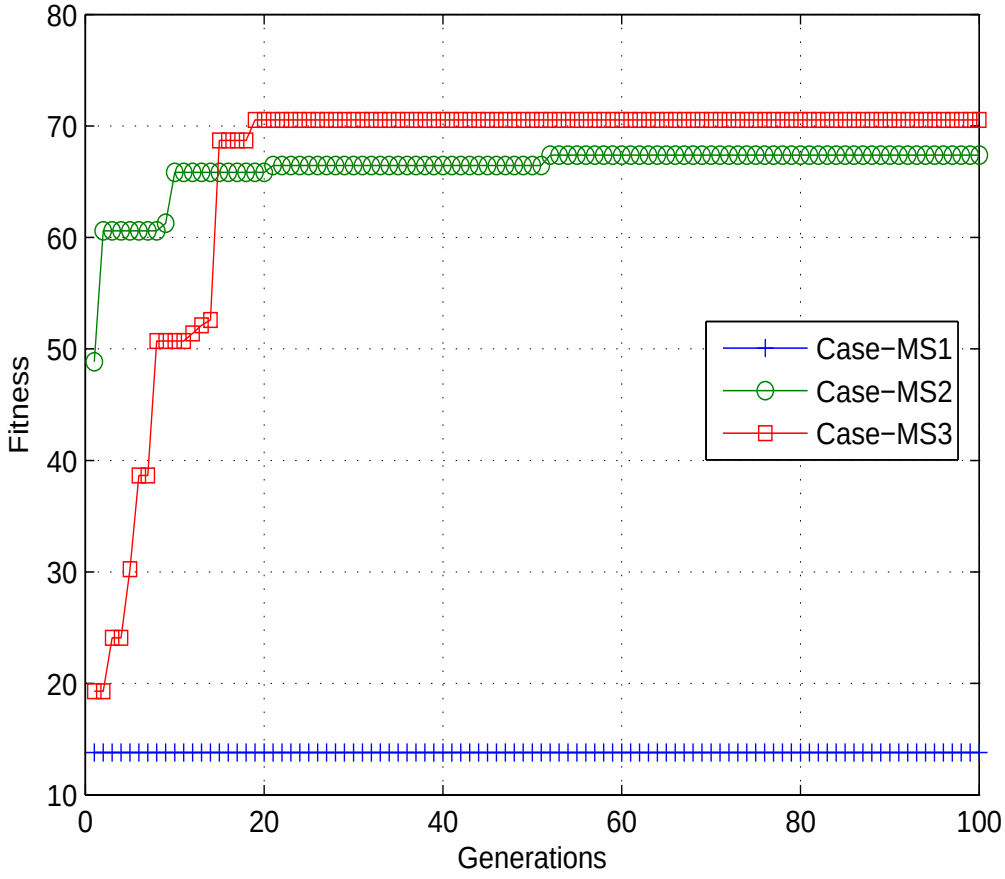

Figure 8.4: Convergence of GA run for maximisation of strength: laminated plate

This means that as the number of design variables increases, the strength of the plate increases.

- To increase the strength of the plate, the fibre angle in most layers is zero degrees because this can reduce the magnitude of Young's modulus along the shortest side of the plate thereby reducing the magnitude of the maximum stress.

- The layer thickness is also significant for the strength of a plate as can be seen from the Case-MS3: E-glass with the highest areal weight is selected.

8.3.3 Maximisation of critical buckling load

The specimen is a square laminated plate with $L = 200\ mm$ and $B = 200\ mm$ as shown in Figure 5.3. The optimisation has been performed for uniaxial and biaxial compression. For each of these load types, there are three cases. Case-MB1, Case-MB2 and Case-MB3 use the same conditions as Case-MD1, Case-MD2 and Case-MD3 respectively. From Table 8.3, it can be concluded that

- The optimum results for layup for both uniaxial and biaxial compression are the same for all cases. The critical buckling load for biaxial compression is half that of uniaxial compression.
- To obtain the maximum critical buckling load for this plate, the laminate should be either a [0/90/90/90]s or [90/0/0/0]s layup in order to provide a high bending stiffness.
- The critical buckling load of the plate is a function of bending stiffness. Hence, a higher fibre modulus leads to a higher critical buckling load. Therefore, the selected fibre layup in Case-MB2 is [UHM/UHM/HS/HM]s.
- For Case-MB3, Areal weight (Aw) is also a design variable. Because layer thickness has an effect on the optimum results (see Figure 8.2), E-glass and its upper-bound Aw is selected for six layers.

Table 8.3: Maximisation of buckling load for the unstiffened laminated plate

Load types		Case-MB1	Case-MB2	Case-MB3
Uniaxial compression	Fibre angle	[0/90/90/90]s [90/0/0/0]s	[0/90/90/90]s [90/0/0/0]s	[0/90/90/90]s [90/0/0/0]s
	Fibre type	-	[UHM/UHM/HS/HM]s	[UHM/Eg/Eg/Eg]s
	A_w (kg/m^2)	-	-	[0.5/1.6/1.6/1.6]s
	N_{cr} (N/mm)	29.92	361.40	1480.01
Biaxial compression	Fibre angle	[0/90/90/90]s [90/0/0/0]s	[0/90/90/90]s [90/0/0/0]s	[0/90/90/90]s [90/0/0/0]s
	Fibre type	-	[UHM/UHM/HS/HM]s	[UHM/Eg/Eg/Eg]s
	A_w (kg/m^2)	-	-	[0.5/1.6/1.6/1.6]s
	N_{cr} (N/mm)	14.96	180.70	740.00

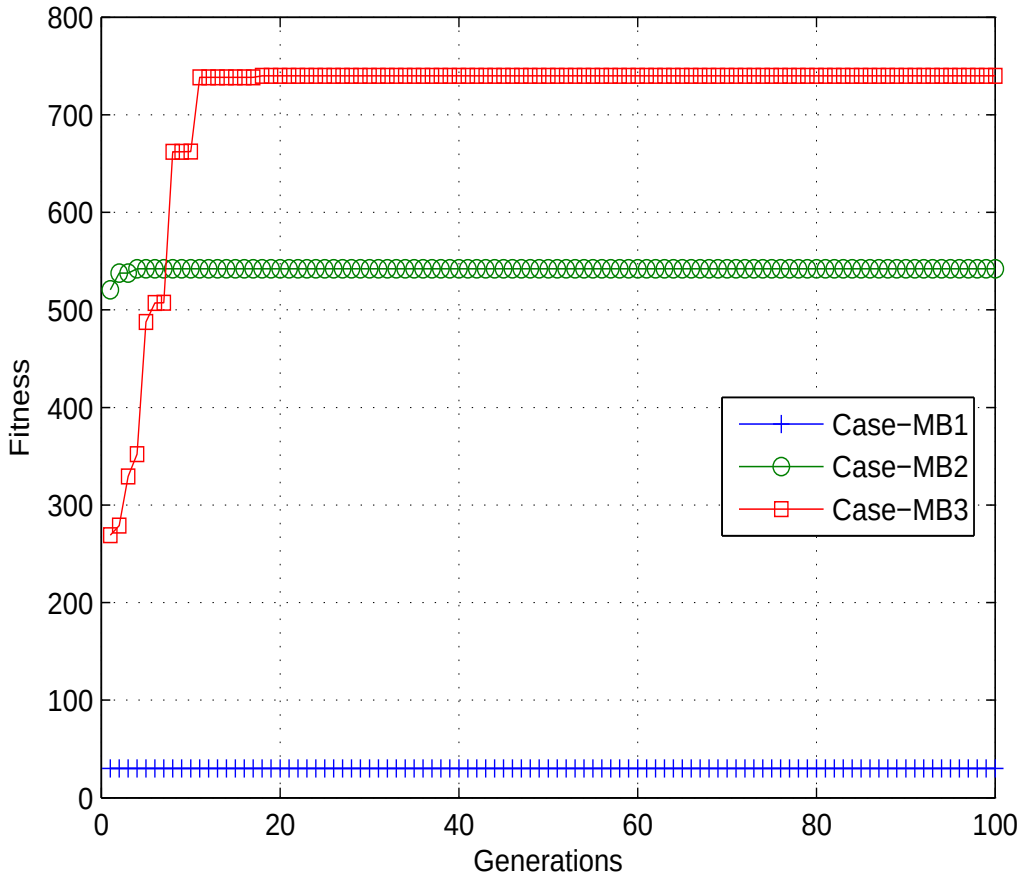

Figure 8.5: Convergence of GA run for maximisation of critical buckling load for uniaxial compression: laminated plate

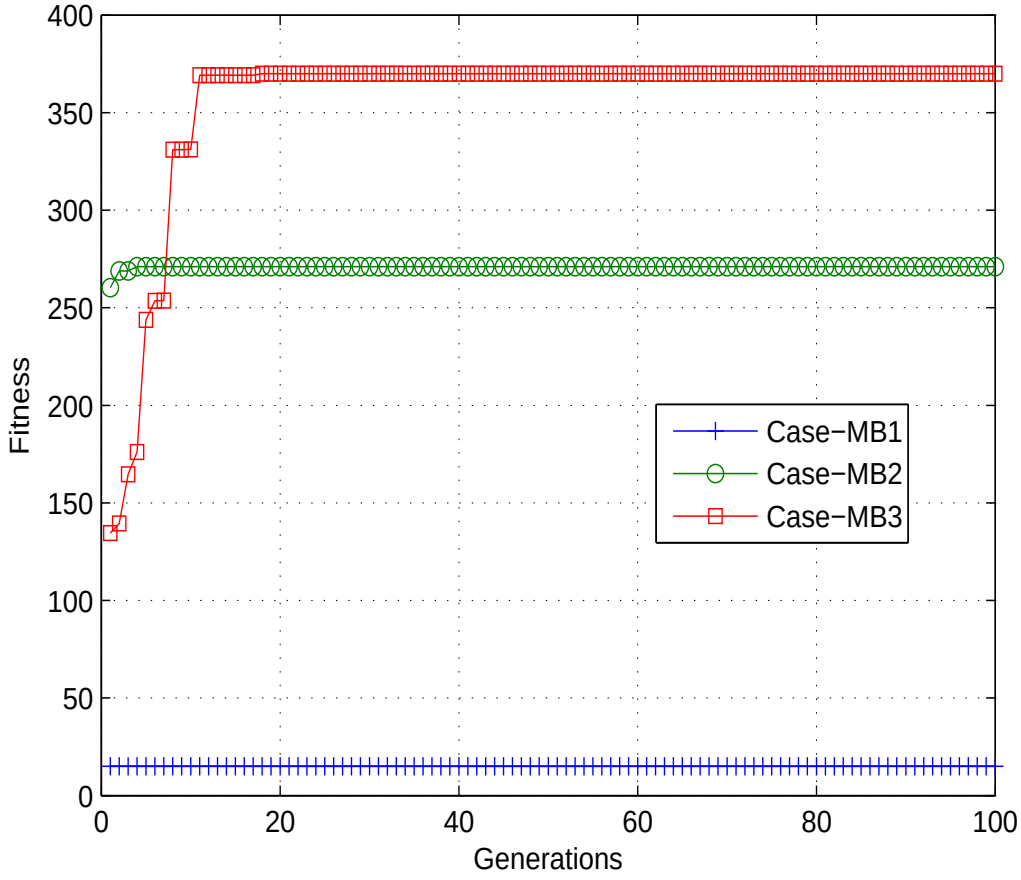

Figure 8.6: Convergence of GA run for maximisation of critical buckling load for biaxial compression: laminated plate

Chapter 9

Conclusion and further work

9.1 Conclusion

The methodology (or optimisation framework), which has been used to design composite ship structures for the initial design stage, was firstly introduced. The framework is unique due to the combination of GA and grillage analysis adapted for composite structure. Moreover, to increase the value of the framework, its capability has been expanded to cover three plate types (unstiffened plate, unidirectional plate and cross stiffened plate). Hence, for a structural analysis of unstiffened laminated plate, Higher order shear deformation theory is selected because it can provide accurate solutions with a favouable computational time compared to the other methods.

The accuracy of optimal results depends on the accuracy of the subroutine program. Hence, the important modules within the developed program have been separately validated. As the adapted grillage analysis is a combination of an analysis of steel grillage and equivalent elastic properties, these two components were individually validated. The steel grillage results of Clarkson (1969) and the equivalent elastic properties calculated by Datoo (1998) were used as reference results. In the case of the structural analysis of unstiffened laminate plates, the results of mechanical behaviour presented by Reddy (1998) have been employed for validation. After connecting all the subroutines together,

the correctness of the optimisation procedures has been proved by using the simple composite optimisation problem (maximisation of centre deflection of unstiffened laminate plate), which already has known optimal solutions. The strength constraint selected for this work was based on the principal maximum stress criterion because this criterion is easy to check correctness and its failure prediction is similar to the other criteria.

The program has been successfully applied to many composite structural optimisation problems; from the problem of small design space with a composite structure having simple geometry (unstiffened laminated plate) to a problem with a large design space with a composite structure having complex geometry (tophat cross stiffened plate).

From the optimal results in the application chapters, the following important points can be concluded:

- As the stiffener spacing is related to the stiffener height, the stiffener spacing is likely to reach its upper-bound value to gain the highest flexural rigidity.
- To reduce the shear stress on web and the direct stress on the crown element, the web height must be shorter and the selected fibre should be of the lower Young's modulus.
- Although the high strength carbon is the lightest fibre considered, the ultra high modulus carbon is selected in weight minimisation design case because it can provide thinner elements.
- The crown element is the most sensitive to stiffness constraint and strength constraints because it is far from the neutral axis of stiffener cross section.
- Increasing the number of design variables has a large effect on the value of objective functions. Therefore, when designing structures, it is important to include a large number of design variables as much as possible.

A list of the main contributions of this research work are summarised as follows:

- A comprehensive review of structural analysis for unstiffened plate and stiffened plate, optimisation method and their application to composite structures.
- Establishing an optimisation framework, which could be applied to composite ship structures.
- An examination of the GA module as a robust global optimisation tool.
- An adaptation of the simplified method (steel grillage analysis) for analysing stiffened laminated plates.
- Applications of the proposed framework to three plate types with many design situations.

9.2 Further work

The framework could be further improved to offer a valuable tool for the design of composite ship structures. Therefore, the following points are suggested as further work.

- The framework could be extended to cover the design of the midship section which could be disassembled as many types of plates. Moreover, it should be used for the other plate types such as curvate plate, plate with hole, stiffened sandwich plate and so on.
- Multi-objective optimisation could be introduced into the framework so that the minimisation of weight and cost, which is important in ship design, is possible.
- Plates with other support conditions (such as clamped all edges, clamped and simply supported, clamped at two-edges and so on) should be considered because in real structures those conditions have not been well defined.
- Since there are various load types acting on ship structure, the framework should be used for plates under various load types such as a combination of uniform pressure load and in-plane load.

- A variety of structural analyses such as vibration, buckling and layer-by-layer stresses should be added for each plate type.
- A real material database based on experiment results should be employed to gain a more realistic solutions.
- Introducing new coding, operators or parallel computing will improve the efficiency of the GA.
- Other optimisation frameworks such as the use of GA, FEA and Artificial Neural Networks (ANNs) should be used in order to confirm the optimal results and to be an option for a designer.
- The adopted grillage analysis may be used to build the structural reliability module.

Appendix A

Composite properties

The following equations from Smith (1990) are used to estimate material properties of composite. The density property of composite (ρ_c) is calculated by:

$$\rho_c = \rho_f V_f + \rho_m V_m \tag{A.1}$$

ρ_f and ρ_m are the densities of fibre and matrix and V_f and V_m are volume fractions of fibre and matrix, respectively.

Formulation for estimating longitudinal Young's modulus (E_1) is:

$$E_1 = E_f V_f + E_m V_m \tag{A.2}$$

E_f and E_m are Young's moduli of fibre and matrix.

Poission's ratio (v_{12}) of unidirectional composite is,

$$v_{12} = v_f V_f + v_m V_m \tag{A.3}$$

v_f and v_m are poission's ratios of fibre and matrix respectively.

The Halpin-Tsai equation for transverse composite modulus (E_2) can be expressed as:

$$\frac{E_2}{E_m} = \frac{1 + \xi\eta V_f}{1 - \eta V_f} \tag{A.4}$$

where,

$$\eta = \frac{(E_f/E_m - 1)}{(E_f/E_m) + \xi} \tag{A.5}$$

The composite in-plane shear modulus (G_{12}) can be evaluated from Eq. A.4 and Eq. A.5 by replacing E_2, E_f and E_m with G_{12}, G_f (shear modulus of fibre) and G_m (shear modulus of matrix). The coefficient ξ, which depends on fibre geometry and the form of loading, is determined empirically: for the usual case of circular section fibres, satisfactory results are obtained taking $\xi = 2$ in the evaluation of E_2 and $\xi = 1$ in evaluating G_{12}.

The following equations are used for estimating the strength properties of the composite. Longitudinal tensile strength (X_t) for most glass reinforced polymer composites ($\epsilon_f^* > \epsilon_m^*$) can be described by Eq. A.6.

$$X_t = E_f V_f \epsilon_f^* \tag{A.6}$$

ϵ_f^* and ϵ_m^* are the strains to failure of fibre and matrix respectively.

For most carbon fibre reinforced plastic composites ($\epsilon_f^* < \epsilon_m^*$), the X_t is expressed as:

$$X_t = (E_f V_f + E_m V_m)\epsilon_f^* \tag{A.7}$$

Here, the compressive tensile strength (X_c) is assumed to be equal to X_t. The transverse tensile strength (Y_t) for glass or carbon fibre reinforced polymer can be estimated from:

$$Y_t = \left(1 - (\sqrt{V_f} - V_f)\left(1 - \frac{E_m}{E_2}\right)\right)\sigma_{tm}^* \tag{A.8}$$

σ_m^* is the matrix tensile strength.

To estimate transverse compressive strength (Y_c), Eq. A.8 can be used by replacing σ_m^* with σ_{cm}^* (the matrix compressive strength). The in-plane shear strength (S) for glass or carbon fibre reinforced polymer can be estimated from:

$$S = \left(1 - (\sqrt{V_f} - V_f)\left(1 - \frac{E_m}{E_2}\right)\right)\tau_m^* \tag{A.9}$$

τ_m^* is the matrix shear strength.

Finally, the areal weight (A_w) of fibre, mass per unit area (kg/mm^2), related to density, ρ_f, (kg/mm^3) of the fibre can provide layer thickness, t ,($mm.$) as the following equation:

$$t = \frac{A_w}{\rho_f V_f} \tag{A.10}$$

Appendix B

Composite failure criteria

In marine structure, for single skin laminates, stiffened plates or unstiffened plates the most common failure mode is buckling instability due to the unavoidable presence of some flexure. In this case, plates always fail firstly at the outer ply. The prediction of the load at which the first ply to fail (First Ply Failure) occurs can be made using a failure criterion. Failure criteria are classified into two groups: independent failure criteria and polynomial failure criteria. The application of the correct failure criteria to predict FPF is dependent on material choice, boundary conditions and loading type.

Independent failure criteria such as maximum stress criterion or maximum strain criterion can identify failure mode but do not include stress or strain interaction effects. For designing FRP marine structures, designers prefer to use maximum stress criteria because laminates typically are aligned with the principal stresses so that stress interaction effects can be neglected. The Failure Index (FI) of this criterion can be presented as follows. It is noted that a laminate has not failed as long as the FI is less than 1.

$$FI_{1t} = \frac{\sigma_{1t}}{X_t}, \quad FI_{1c} = \frac{\sigma_{1c}}{X_c} \tag{B.1}$$

$$FI_{2t} = \frac{\sigma_{2t}}{Y_t}, \quad FI_{2c} = \frac{\sigma_{2c}}{Y_c} \tag{B.2}$$

$$FI_{3t} = \frac{\sigma_{3t}}{Z_t}, \quad FI_{3c} = \frac{\sigma_{3c}}{Z_c} \tag{B.3}$$

$$FI_4 = \frac{\sigma_4}{R}, \qquad FI_5 = \frac{\sigma_5}{S} \tag{B.4}$$

$$FI_6 = \frac{\sigma_6}{T} \tag{B.5}$$

where $\sigma_{i=1,2,3}$ are principal stresses, $\sigma_{i=4,5,6}$ are principal shear stresses and their subscript $_t$ and $_c$ denote to tensile and compressive stresses respectively. X_t and X_c are respectively tensile and compressive lamina normal strength in x-direction. Y_t and Y_c are respectively tensile and compressive lamina normal strength in y-direction. Z_t and Z_c are tensile and compressive lamina normal strength in the z-direction. R is lamina shear strength in yz-direction, S is lamina shear strength in the xz-plane and T is lamina shear strength in the xy-plane.

For more accuracy in failure analysis and more freedom in design, the polynomial failure criteria should be used because they take into account stress interaction effects. Smith (1990) suggested the use of the Azzi-Tsai criterion for particular regions such as machinery seating where complex stress patterns exist. The criterion is developed from von Mises yield criterion, which is accurate for isotropic materials under combined stresses. A more complete description of laminate strength under combined loads is given by the Tsai-Wu criterion. Based on this criterion, ply failure occurs when the Failure Index (FI) exceeds one or ply failure occurs if the following inequality is not satisfied.

$$FI = F_i\sigma_i + F_{ij}\sigma_i\sigma_j < 1 \tag{B.6}$$

where all components such as stresses (σ), F_i and F_{ij} coefficients ($i, j = 1, 2, 3, 4, 5, 6$) refer to the the principal material directions.

$$F_1 = (1/X_t - 1/X_c), \qquad F_2 = (1/Y_t - 1/Y_c), \qquad F_3 = (1/Z_t - 1/Z_c)$$

$$F_{11} = 1/(X_tX_c), \qquad F_{22} = 1/(Y_tY_c), \qquad F_{33} = 1/(Z_tZ_c)$$

$$F_{44} = 1/R^2, \qquad F_{55} = 1/S^2, \qquad F_{66} = 1/T^2$$

$$F_{12} = -1/(2\sqrt{X_tX_cY_tY_c}), \quad F_{13} = -1/(2\sqrt{X_tX_cZ_tZ_c}), \quad F_{12} = -1/(2\sqrt{Y_tY_cZ_tZ_c})$$

References

[1] Alm F. (1983) GRP versus steel in ship construction, Naval Forces, Vol.4, No.5, pp.54-55

[2] Aitharaju V.R. and Averill R.C. (1990) c^0 zig-zag finite element for analysis of laminated composite beams, Journal of Engineering mechanics, Vol.125, pp.323-330

[3] Aksu G. and Ali R. (1976) Free vibration analysis of stiffened plates using finite difference method, Journal of sound and vibration, Vol.48, No.1, pp.15-25

[4] Andrews D. (1981) Creative ship design, Transaction of RINA, Vol. 123, pp. 447-471

[5] Andrews D. (2003) A creative approach to ship architecture, Transaction of RINA, Vol. 145, p.229-252

[6] Balendra T. and Shanmugam N.E.(1985) Free vibration of plated structures by grillage method, Journal of sound and vibration, Vol.99, No.3, pp.333-350

[7] Barboro E.J. and Reddy J.N. (1990) General two-dimensional theory of laminated cylindrical shells, AIAA Journal, Vol .28, pp.545-553

[8] Bazaraa M., Jarvis J. and Sherali H. (1990) Linear programing and network flows, John & Sons, New York

[9] Bedair O.K. (1997) Analysis of stiffened plates under lateral loading using sequential quadratic programming (SQP), Computer & Structures, Vol. 62, pp.63-80.

[10] Bisagni C. and Lanzi L. (2002) Post-buckling optimisation of composite stiffened panels using neural networks, Composite Structures, Vol.58, pp.237-247

[11] Box M.J. (1965) A new method of constrained optimization and a comparison, Computer Journal, Vol.8, pp.42-45

[12] Bruyneel M. and Fleury C. (2002) Composite structures optimization using sequential convex programming, Advances in Engineering Software, Vol.33, pp.697-711

[13] Canadian highway bridge design code (CHBDC) (2000) Ontario Ministry of transportation and communications, Downsview, Ontario, Canada

[14] Carroll C.W. (1961) The created response surface technique for optimizing nonlinear restrained systems, Operation Research, Vol.9, pp. 169-184

[15] Chalmers D.W. (1982) Preliminary structural design of warship, Transaction of RINA, Vol. 124

[16] Chattopadhyay B., Sinha P.K. and Mukhopadhyay M. (1992) Finite element free vibration analysis of eccentrically stiffened composite plates, Journal of reinforced plastics and composites, Vol.11, No.9, pp.1003-1034

[17] Chattopadhyay B, Sinnha P.K. and Mukhopadhyay M. (1993) Finite element analysis of bead-stiffened composite plates under transverse loads, Journal of reinforced plastics and composites, Vol.12, No.1, pp.76-100

[18] Cheung M.S. (1984) Analysis of continuous curved box-girder bridges by the finite strip method' China Civil Engineering Journal, Vol. 17, No. 3, 1984, pp. 1-10

[19] Cheung M.S., Bakht B. and Jaeger L.G. (1982) Analysis of box girder bridges by grillage and orthotropic plate methods, Canadian Journal of Civil Engineering, Vol. 9, no. 4, pp. 595-601

[20] Clarkson J. (1963) Test of flat plated grillages under uniform pressure, Transaction of RINA, Vol.105

[21] Clarkson J. (1965) The elastic analysis of flat grillages, Cambridge University Press, Cambridge.

[22] Costa L., Fernandes L., Figueiredo I., Judice J., Leal R. and Oliveira P. (2004) Multiple- and single-objective approaches to laminate optimization with genetic algorithms, Struct. Multidisc. Optim., Vol.27, pp.55-65

[23] Dang C. and Li M. (2006) A floating-point genetic algorithm for solving the unit commitment problem, European journal of operation research, (article in press)

[24] Datoo M.H. (1991) Mechanics of fibrous composites, Elsevier science publishers Ltd., Essex, England

[25] Dawe D.J., Lam S.S.E. and Azizian Z.G. (1993) Finite strip post-local buckling analysis of composite prismatic plate structures, Computers and Structures, Vol.48, No.6, pp.1011-1023

[26] Dawe D.J. and Peshkam V. (1996) Note on finite strip buckling analysis of composite plate structures, Composite structures, Vol.34, pp.163-168

[27] Deka D.J., Sandeep G., Chakrabory D. and Dutta A. (2005) Multiobjective optimization of laminated composites using finite element method and genetic algorithm, Journal of reinforced plastics and composites, Vol.24, No.3, pp.273-285

[28] Eric Greene Associates Inc. (2001) Marine composites, Second edition, Annapolis, MD21403, USA

[29] Evan H.R., Alinia M.M., Labanti P., and Shanmugam N.E. (1983) Theoretical investigation of the collapse of multi-cellular structures under lateral loading, Journal of constructional steel research, Vol.3, No.2, pp.23-30

[30] Fiacco A.V. and McCormick G.P. (1967) The slacked unconstrained minimization technique for convex programing, SIAM Journal on Applied Mathematics, Vol.15, pp.505-515

[31] Fisher K.W. (1972) Economic optimisation procedures in preliminary ship design, Transactions of RINA, Vol. 114, pp. 293-317.

[32] Frieze P.A., Winkle I.E., Das P.K. and Baird D. (1987) Optimisation of stiffened cylinders in offshore construction, Transaction of RINA, Vol. 129

[33] Gantovnik V.B., G*ü*rdal Z. and Watson L.T. (2002) A genetic algorithm with memory for optimal design of laminated sandwich composite panels, Composite Structures, Vol.58, pp.513-520

[34] Gen M. and Cheng R. (1997) Genetic algorithm and engineering design, John Wiley & Sons, New York.

[35] Goswami S. (1997) Response of composite stiffened shells under stochastic excitation, Journal of reinforced plastics and composites, Vol.16, No.16, pp.1492-1522

[36] Guo M. and Harik I.E. (1996) Free vibration of stiffened composite laminates, Proceeding of engineering mechanics, Vol.2, pp.1163-1166

[37] Harik I.E., Guo M.W. and Madasamy C.M. (1997) Bending of stiffened composite laminates, International SAMPE Technical conference, Vol.29, Composites for Real World, pp.744-750

[38] Hirano Y. (1979) Optimum design of laminated plates under axial compression, AIAA Journal, Vol.17, pp.1017-1019

[39] Horsmon Jr. A.W. and Bernhard B. (2003) Exploiting technology to optimise the design of large composite vessels, Transactions-society of naval architects and marine engineers, Vol.111, pp.309-330

[40] Hosseini-Toudeshky H., Ovesy H.R. and Kharazi M. (2005) The development of an approximate method for the design of based-stiffened composite panels, Thin-walled structures, Vol. 43, no.11, pp.1663-1676

[41] Huffington N.J. Jr. and Blacksburg V.A. (1956) Theoretical determination of rigidity properties of orthogonally stiffened plates, Journal of applied mechanics, Vol.78

[42] Hughes O. (1997) Two first principles structural designs of a fast ferry-all-aluminium ad all-composite, FAST'97 papers, pp.91-98

[43] Jang C.D. , Seo S.I. and Kim S.K. (1996) A study on the optimum structural design of surface effect ships, Marine Structures, Vol.9, pp.519-544

[44] Kang J.H. and Kim C.G. (2005) Minimum-weight design of compressively loaded composite plates and stiffened panels for postbuckling strength by genetic algorithm, Composite Structures, Vol.69, pp.239-246

[45] Kant T. and Swaminathan K. (2002) Analytical solutions for the static analysis of laminated composite and sandwich plates based on higher order refined theory, Composite Structures, Vol.56, pp.329-344

[46] Karr, D.G., Beier K.P. and Rigo P. (2002) A framework for simulation-based design of ship structures, Journal of ship production, Vol.18(1), 33-46

[47] Keane A.J. (1988) A computer based method for hull form concept design: applications to stability analyses, Transaction of RINA, Vol. 130

[48] Kelley J.E.Jr. (1960) The cutting plane method for solving convex programs, Journal of SIAM, Vol.8, pp.703-712

[49] Kim C.W. and Lee J.S. (2005) Optimal design of laminated composite plates for maximum buckling load using genetic algorithm, Proc. IMechE Part C-Journal of mechanical engineering science, Vol. 219, pp.869-878

[50] Kim C.W., Hwang W., Park H.C., and Han K.S. (1997) Stacking sequence optimization of laminated plates, Composite Structures, Vol.39, pp.283-288

[51] Krisek V., Evan H.R., and Ahmad M.K.M. (1990) Shear lag analysis for composite box girder, Journal of Constructional Steel Research, Vol. 16, No. 1, pp. 1-21

[52] Lazaides T.O. (1952) The design and analysis of openwork prestressed concrete beam grillages, Civil Engineering, Vol.47, No. 552

[53] Lee Y.J. and Lin C.C. (2004) Optimised design of composite propeller, Mechanics of advanced materials and structures, Vol.11, pp.17-30

[54] Leung A.Y.T. Junchuan N., Lim C.W., and Song K., (2003) A new unconstrined third-order plate theory for Navier solutions of symmetrically laminated plates, Computers and Structures, Vol.81, pp. 2539-2548

[55] Liu D. and Li X. (1996) An over view of laminate theories based on displacement hypothesis, Journal of composite materials, Vol.30, No.14, pp.1539-1561

[56] Lo K.H., Christensen R.M. and Wu E.M. (1977) A high-order theory of plate deformation-part 1: homogeneous plate, Journal of Applied mechanics, Vol.44, pp.669-676

[57] Loughlan J. (1996) Buckling of composite stiffened box sections subjected to compression and bending, Composite structures, Vol.35, No. 1, pp.101-116

[58] Loughlan J. and Delaunoy J.M. (1993) Buckling of composite stiffened plates with some emphasis on the effects of fiber orientation and on loading configuration, Composite structures, Vol.25, pp.485-494

[59] Loukakis T.A. (1988) A new form of optimization diagrams for preliminary propeller design, Transaction of RINA, Vol. 131

[60] Lu H.C. and Tzeng S.T. (2000) Genetic algorithm approach for designing arbitrary FIR log filters, ISCAS 2000, IEEE international symposium on circuits and systems, May 28-31, Geneva, Switzerland

[61] Maneepan K., Jeong H.K. and Shenoi R.A. (2005) Optimisation of FRP tophat stiffened single skin and monocoque sandwich plates using genetic algorithm, Proceeding of 15^{th} international offshore and polar engineering conference, June 19-24, Seoul, Korea, pp. 513-518

[62] Maneepan K., Shenoi R.A., Jeong H.K. and Blake J.I.R. (2006) Multi-objective optimisation of orthogonally tophat-stiffened composite laminates plates, Proceedings of 25^{th} international conference on offshore mechanics and arctic engineering, June 4-9, 2006, Hamburg, Germany, OMAE2006-92442

[63] Manohar P. K. (1993) Structural Optimization: Status and Promise, American Institute of Aeronautics & Astronautics, Washington

[64] Marsh G. (2001) Composite ship shafts shape up, Reinforced plastics, Vol.45, No.11, pp.32-36

[65] Marsh J.G. and Taylor P. (1990) PC program for orthotropic plate box girder bridges, Australia second national structural engineering conference, Institution of engineering, Australia, pp.224-235

[66] Maisano A.J. (2003) Manufacturing processes of composite materials for a human-powered submarine, Oceans Conference Record (IEEE), Vol.5, pp.2678-2681

[67] Mikami I. and Yonezawa H. (1983) Inelastic buckling of plate girders with transverse stiffeners under bending, Technology reports of Kansai University, No.24, pp.293-307

[68] Mikami I. and Niwa K. (1996) Ultimate compressive strength of orthotrogonally stiffened steel plate, Journal of structural engineering, Vol.122, No.6, pp.674-682

[69] Mindlin R.D. (1951) Influence of rotary inertia and shear on flexural motions of isotropic elastic plates, Journal of applied mechanics, Vol.18, pp.31-38

[70] Moe J. and Svere L. (1968) Cost and weight minization of structures with special emphasis on longitudinal strength members of tankers, Transactions of RINA, Vol. 110, pp. 43-70.

[71] Moh J.S. and Hwu C. (1997) Optimization for buckling of composite sandwich plates, AIAA Journal, Vol.35, No.5, pp.863-868

[72] Mouritz A.P., Gellert E., Burchill P. and Challis K. (2001) Review of advanced composite structures for naval ships and submarines, Composite Structures, Vol.53, pp.21-41

[73] Muc A. and Gurba W. (2001) Genetic algorithms and finite element analysis in optimization of composite structures, Composite Structures, Vol.54, pp.275-281

[74] Mukhopadhyay M. (1989a) Vibration and stability analysis of stiffened plates by semi-analytic finite difference method, Part I: Consideration of bending displacements only, Journal of sound and vibration, Vol.130, No.1, pp.27-39

[75] Mukhopadhyay M. (1989b) Vibration and stability analysis of stiffened plates by semi-analytic finite difference method, Part II: Consideration of bending and axial displacements only, Journal of sound and vibration, Vol.130, No.1, pp.27-39

[76] Nagendra S., Jestin D., Gürdal Z., Haftka R.T. and Watson L.T. (1996) Improved genetic algorithm for the design of stiffened composite panels, Computers & Structures, Vol.58, No.3, pp.543-555

[77] Nelder J.A. and Mead R. (1965) A simplex method for function minimisation, Computer Journal, Vol.7, pp.308-313

[78] Pagano N.J. (1970) Exact solutions for rectangular bidirectional composites and sandwich plates, Journal of Composite Materials, Vol.4, pp.20-34

[79] Park C.H., Lee W.I., Han W.S. and Vautrin A. (2003) Weight minimization of composite laminated plates with multiple constraints, Composite Science and Technology, Vol.63, pp.1015-1026

[80] Park J.H., Hwang J.H., Lee C.S. and Hwang W. (2001) Stacking sequence design of composite laminates for maximum strength using genetic algorithms, Composite Structures, Vol.52, pp.217-231

[81] Papalambros P.Y. and Wide D.J. (1988) Principles of optimal design, Cambridge university press, New York

[82] Pagano N.J. (1969) Exact solutions for composite laminates in cylindrical bending, Journal of composite materials, Vol.3, pp.426-440

[83] Rahul, Chakraborty D., and Dutta A. (2005) Optimization of FRP composites against impact induced failure using island model parallel genetic algorithm, Composites science and technology, Vol.65, pp.2003-2013

[84] Rao S.S. (1978) Optimization: theory and applications, Wiley Eastern, New Delhi

[85] Rao K.P. (2000) Study of the behaviour of laminated composite beam, plate and shell structures using some specifically developed finite elements, Journal of spacecraft technology, Vol.10, No.2, pp.1-13

[86] Razzaq R.J. and El-Zafrany A. (2005) Non-linear stress analysis of composite layered plates and shells using a mesh reduction method, Engineering analysis with boundary elements, Vol.29, No.12, pp.1115-1123

[87] Reddy J.N. (1984) A simple higher-order theory for laminated composite plates, Journal of applied mechanics, Vol.51, pp.745-752

[88] Reddy J.N. (1997) Mechanics of laminated composite plates, CRC Press Inc., London

[89] Riche R.L. and Haftka R.T. (1993) Optimization of laminates stacking sequence for buckling load maximization by genetic algorithm, AIAA Journal, Vol.33, No.5, pp.951-956

[90] Rigo P. (2001) A module-oriented tool for optimum design of stiffened structures-Part I, Marine Structures, Vol.14, pp.611-629

[91] Rigo P. and Fleury C. (2001) Scantling optimization based on convex linearizations and a dual approach-Part II, Marine structures, Vol.14, pp.631-649

[92] Rosen J.B. (1960) The gradient project method of nonlinear programming: Part I-nonlinear constraints, SIAM Journal, Vol. 8, pp.181-217

[93] Rules for Building and Classing High-Speed Craft. (2001), American Bureau of Shipping: New York.

[94] Rules for Classification of High Speed and Light Craft. (1991), Det Norske Veritas: Hovik.

[95] Rules for the Classification of Special Service Craft. (2004), Lloyd's Register of Shipping: London.

[96] Sadek E.A. and Tawfik S.A. (2000) Finite element model for the analysis of stiffened laminated plates, Computers and structures, Vol. 75, pp.369-383

[97] Schmit L.A. and Mehrinfar M. (1982) Multilevel optimum design of structures with fiber-composite stiffened-panel components, AIAA Journal, Vol.20, pp.138-147

[98] Sciuva M.D., Gherlone M. and Lomario D. (2003) Multiconstrained optimization of laminated and sandwich plates using evolutionary algorithms and higher-order plate theories, Composite Structures, Vol.59, pp.149-154

[99] Sen P. (1992) Marine design: the multiple criteria approach, Transactions of RINA, Vol. 134, pp. 261-276.

[100] Shenoi R.A. and Wellicome J.F. (1993a) Composite materials in maritime structures: volume 1 fundamental aspects, Cambridge university press, Cambridge.

[101] Sivakumar K., Iyengar N.G.R. and Deb K. (1998) Optimum design of laminated composite plates with cutouts using a genetic algorithm, Composite Structures, Vol.42, pp.265-279

[102] Smith C.S. (1964) Analysis of grillage structures by the force method, Transaction of RINA, Vol.106

[103] Smith C.S. (1966) Elastic analysis of stiffened plating under lateral loading, Transaction of RINA, Vol.108, pp.113-131

[104] Smith C.S. (1972) Buckling problems in the design of fibreglass-reinforced plastic ships, Journal of ship research, Vol.116, No.3, pp.174-190

[105] Smith C.S. (1990) Design of marine structures in composite materials, Elsevier applied science, London

[106] Smith C.S. and Clarke J.D. (1986) Advances in marine structures, Elsevier applied science, London.

[107] Smith G.K. (1973) A design scheme for ship structures, Transactions of RINA, Vol. 115, pp. 47-66.

[108] Soares C.M.M., Correia V.F., Mateus H. and Herskovits J. (1995) A discrete model for the optimal design of thin composite plate-shell type structures using a two-level approach, Composite Structures, Vol.30, pp.147-157

[109] Soremekun G.,G*ü*rdal Z., Haftka R.T. and Watson L.T. (2001) Composite laminate design optimization by genetic algorithm with generalized elitist selection, Computers and Structures, Vol.79, pp.131-143

[110] Sponberge E.W. (1986) Carbon fibre sailboat hulls: how to optimize the use of an expensive material, Marine Technology, Vol.23, pp.165-174

[111] SP Systems (2006) ,The SP Systems guide to composite, Retrieved January 8, 2006 from website: www.spsystems.com

[112] Tan K.H. and Montage P. (1991) Simple grillage analogy for the analysis of steel sandwich panels with penetrations, Structural engineer, Vol.69, No.15, pp.271-276

[113] Timosheko S.A. and Woinowsky-Krieger S. (1959) Theory of plates and shells, McGRAW-HILL book company, INC., London.

[114] Toledano A. and Murakami H. (1987) A composite plate theory for arbitrary laminate configurations, Journal of applied mechanics, Vol.54, pp.181-189

[115] Tucker J.S. (1979) Glass reinforced plastic submersibles, Trans. NEC Int. Engrs & Shipbuilders, Vol.95, No.2, 1979

[116] Turvey G.J. and Der Avanessian N.G.V. (1985) Elastic large deflection analysis of ring-stiffened circular plates using graded finite differences, NUMETA 85, Numerical methods in engineering: theory and applications, Proceedings of the international conference, Swansea, Wales, pp.875-884

[117] Vendeler G. (1945) Grillage beams in ships and similar structures, Oslo: Grondahl & Son

[118] Walker M., Reiss T. and Adali S. (1997) Optimal design of symmetrically laminated plates for minimum deflection and weight, Composite Structures, Vol.39, pp.337-346

[119] Walker M. and Smith R.E. (2003) A technique for the multiobjective optimisation of laminated composite structures using genetic algorithms and finite element analysis, Composite Structures, Vol.62, pp.123-128

[120] Wang S. and Dawe D.J. (1996) Finite strip large deflection and post-overall-buckling analysis of diaphragm-supported plate structures, Computers and structures, Vol.61, No.1, pp.155-170

[121] Wang X., Oguamanam D.C.D. and Hansen J.S. (2005) Shape optimisation of stiffeners in stiffened composite plates with thermal residual stresses, Structural and multidisciplinary optimisation, Vol.30, No.1, pp.38-42

[122] Wastson D.G.M. (1976) Some ship design methods, Transactions of RINA, Vol. 118, pp. 279-321.

[123] Whitney J.M. (1972) Stress analysis of thick laminated composite and sandwich plates, Journal of composite material, Vol.6, pp.426-440

[124] Whiney J.M. and Pagano N.J. (1970) Shear deformation in heterogeneous anisotropic plates, Transaction of the ASME: Journal of Applied mechanics, Vol.37, No.4, pp.1031-1036

[125] Yoda T. and Atluri S.N. (1992) Postbuckling analysis of stiffened laminated composite panels using a higher-order shear deformation theory, Computational mechanics, Vol.9, No.6, pp.390-404

[126] Yuan W.X. and Dawe D.J. (2004) Free vibration and stability analysis of stiffened sandwich plates, Composite structures, Vol.63, No.1, pp.123-137.